Deborah A. Sivas (CA Bar No. 135446)
Matthew J. Sanders (CA Bar No. 222757)
Sidni M. Frederick (CA Bar Student Cert. No. 00650615)
Catherine H. Rocchi (CA Bar Student Cert. No. 00648085)
ENVIRONMENTAL LAW CLINIC
Mills Legal Clinic at Stanford Law School
559 Nathan Abbott Way
Stanford, California 94305-8610
Telephone: (650) 723-0325
Facsimile: (650) 723-4426
Email: dsivas@stanford.edu
Email: matthewjsanders@stanford.edu

Attorneys for Plaintiff Unite the Parks

René P. Voss (CA Bar No. 255758)
NATURAL RESOURCES LAW
15 Alderney Road
San Anselmo, CA 94960
Phone: (415) 446-9027
Email: renepvoss@gmail.com

Attorney for Plaintiffs Sequoia ForestKeeper
and Earth Island Institute

UNITED STATES DISTRICT COURT

FOR THE EASTERN DISTRICT OF CALIFORNIA

FRESNO DIVISION

UNITE THE PARKS; SEQUOIA FORESTKEEPER; and EARTH ISLAND INSTITUTE,

Plaintiffs,

v.

UNITED STATES FOREST SERVICE, an agency of the U.S. Department of Agriculture; and UNITED STATES FISH AND WILDLIFE SERVICE, an agency of the U.S. Department of the Interior, Defendants.

Date: May 18, 2021
Time: 9:30 am
Courtroom: 5

Case No. 1:21−CV−00518−DAD−HBK

DECLARATION OF DR. JOSEPH WERNE IN SUPPORT OF PLAINTIFFS' MOTION FOR PRELIMINARY INJUNCTION

I, Joseph Werne, declare as follows:

SUMMARY OF QUALIFICATIONS

1. I submit this declaration in support of the Plaintiffs' Motion for Preliminary Injunction in this case regarding Defendants' plans to continue logging and vegetation management activities in the range of the Southern Sierra Nevada Pacific Fisher (SSN fisher) on the Sierra, Sequoia, and Stanislaus National Forests. I have personal knowledge of the matters stated herein and, if called as a witness, would and could competently testify thereto.

2. I am a research scientist with a Ph.D. in Physics (1993) from the University of Chicago. I have a 34-year science career with a primary emphasis on high-resolution numerical modeling and simulation of atmospheric dynamics. I have 78 scientific publications in refereed

journals, book chapters, and conference proceedings. My most-frequently cited works center on two dominant themes: simulation and modeling of buoyant convection (which was my thesis work), and accurate modeling of atmospheric turbulence. Both of these subjects are important for understanding the atmospheric response and feedback to wildland fire. I have co-hosted workshops at the National Center for Atmospheric Research (NCAR) and at the University of Colorado at Boulder on the theory and modeling of atmospheric dynamics. I have presented invited lectures on atmospheric turbulence theory and modeling and high-performance computing across the U.S., in Japan, Italy, England, and elsewhere in Europe. I have served as either the principle investigator or co-investigator on over 20 research and high-performance-computing projects related to atmospheric simulation and modeling. A true and correct copy of my Curriculum Vitae (CV) is attached as Exhibit A.

3. I am currently the co-lead of a working group of assembled experts in wildland-fire theory and modeling. The group's expertise includes fire physics, high-resolution numerical weather-fire simulation, forest ecology, wildlife ecology, and wildfire insurance. The goals of the working group are to: a) integrate and incorporate the current state of the art in each of these disciplines into an improved Wildland-Fire Behavior Assessment tool to aid land-management decision making, and b) apply the results of our wildland-fire-behavior work to improved fire

resilience assessments in California.

4. I serve as the Chief Scientist for Unite the Parks, which is a 501(c)(3) non-profit organization focused on nature preservation, conservation, restoration and advocacy, primarily in the Sierra Nevada and California.

5. I am a lifelong supporter and user of our National Parks and National Monuments, where I frequently camp, hike, climb, and mountain bike, including three times in the Sierra Nevada in 2020. I find my greatest peace, personal clarity, and sense of wonder when outside in nature, especially at night under the stars, far away from city lights. I have plans to return to the Sierra National Forest as soon as this coming summer of 2021.

6. In 2020, I attended the 67th Annual Meeting of the Western Section of The Wildlife Society (2-7 February 2020), which included presentations on the Southern Sierra Nevada Pacific fisher. I also attended the California Fisher Working Group (2 February 2020) and the Southern Sierra Fisher Working Group (3 February 2020) special sessions of The Wildlife Society meeting.

At the special sessions I listened to presentations on the latest studies related to the endangered Southern Sierra Nevada Distinct Population Segment (SSN DPS) of the Pacific fisher.

STATEMENT OF OPINION

Overview

7. Old-growth trees are integral to Pacific fisher survival, and to forest fire safety. Fishers give birth and raise babies inside the cavities of large trees, so they need them for reproduction; and our forests need the fire-resistant microclimates that large trees create. Unfortunately, we are increasingly losing old-growth trees to unnaturally large wildland fires that have become more frequent in recent years. California's 2020 fire season was the most destructive in the state's history, continuing a trend of ever-increasing fire size and severity; and the most comprehensive analysis of wildland-fire data to-date suggests land-management practices may be contributing to the problem.

8. In this declaration, my expertise speaks to atmospheric dynamics and how its incomplete consideration in current fuels-reduction treatments can make our forests less fire resilient, as the best-available science demonstrates. I will describe how current inconsistent treatment of the atmosphere in operational fire models can mislead scientists into believing errant fire-resilience predictions. Until these issues are remedied, current vegetation treatments should be

halted until we better understand their consequences, because claimed increased fire resilience remains unproven. In fact, current practices may be reducing the fire resilience of our forests.

9. Below I provide background information for context related to Pacific fishers and the large trees they need. I describe the primary threat to large trees from fire, namely, crown fires, and I detail how current land-management practices designed to protect large trees from fire can lead to the opposite effect. Finally, I present the latest science, which shows how current fuels reduction practices can make our forests less firesafe, and I show how operational fire models can mislead us into believing vegetation treatments are effective, when they actually are not.

Background

10. The Pacific fisher is a member of the weasel family with quick reflexes, excellent climbing skills, and exceptional fur. It is a midsize forest carnivore that eats small mammals and is eaten by cougars, bobcats, and coyote. Fisher population numbers have been decimated by historic fur trapping and logging of its old-growth forest habitat, and on May 15, 2020 the Distinct Population Segment (DPS) of the Pacific fisher in the Southern Sierra Nevada (SSN) was listed as

endangered by the USFWS (U.S. Fish and Wildlife Service) under the Endangered Species Act.

11. In the forests where Pacific fishers live, fire occurs naturally; and the large trees fishers need for reproduction also help make the forest firesafe. It is well established that large, old-growth trees are able to resist burning because of their thick bark and large-diameter trunks; also, their high canopies create cool microclimate environments that help protect surrounding habitat by blocking the wind, shading the soil, retaining moisture, and significantly lowering surface temperatures (e.g., Binkley et al. 2007, Lesmeister et al. 2019). True and correct copies of the Binkley and Lesmeister papers are attached as Exhibits B and C, respectively. Though they typically number less than 2% of the individual trees in a forest, trees larger than 40 inches in diameter can account for nearly half of a forest's biomass (Lutz et al. 2012). A true and correct copy of this paper is attached as Exhibit D. Unfortunately, for every old-growth tree that remains today, more than seven have already been logged. Compared to historical abundances, only 12% of Sierra Nevada old-growth trees remain (Erman et al. 1996, Vol. II). Therefore, safeguarding our last large trees is critically important for protecting both the fisher's ability to reproduce and the forest's ability to survive wildfire.

Crown Fires Threaten Our Remaining Large Trees

12. Major threats to large trees are overstory crown fires, which occur when treetops ignite during severe burns. Analysis of severe-burn patches in the 2013 Rim Fire found that crown fire disproportionately kills larger trees compared to smaller trees (Lydersen et al. 2016). Removing “ladder fuels” that connect the ground to the overstory is therefore a common-sense practice designed to prevent fires on the forest floor from climbing to the treetops (e.g., PSW GTR-220). Nevertheless, recent research using detailed high-resolution numerical simulations reports that removing ladder fuels can easily increase the likelihood of crown-fire occurrence, despite being designed to reduce it (Banerjee et al. 2020). The reason for this seemingly counter intuitive result involves the important role atmospheric motions play, and it demonstrates how focusing solely on forest fuels can make matters worse, if one neglects to also consider how vegetation treatments can increase the oxygen supply to a fire.

Accurate Fire Modeling Must Include Atmospheric Dynamics

13. Current operational fire models are incomplete, because they attempt to characterize complex fire behavior across a landscape using limited resources. In contrast, detailed

high-resolution numerical fire simulations on high-performance supercomputers do a much better job, but they are too slow and too expensive for operational use. This is because operational models must rapidly obtain and compare a large number of different ignition and vegetation treatment scenarios if they are to be useful. Nevertheless, fast models that produce unrealistic results can have catastrophic consequences for forestland management, and below I discuss two examples that demonstrate serious deficiencies with application of all of the USFS (U.S. Forest Service) operational models, including BehavePlus, FARSITE, FlamMap, FVS-FFE, and FSPro.

14. The first example concerns inadequate handling of the wind resistance associated with ladder fuels. When ladder fuels are removed, the ground-level windspeed and turbulent mixing both increase, leading to faster fire spread and greater oxygen-transport efficiency; this, in turn, results in increased fire intensity. As recent high-resolution numerical fire simulations show (e.g., Banerjee et al. 2020, Atchley et al. 2021), in many cases this aerodynamic effect is more important than the fire-dampening effects of the fuels reduction being evaluated. Nevertheless, comparisons using operational fire models do not predict this result because they ignore

aerodynamic differences between model runs with and without ladder fuels, using the same specified windspeed for both cases. For example, see the USFS tutorial, Jones et al. 2010 at page 15, where a constant 20 mph windspeed is specified. (A true and correct copy of this paper is attached as Exhibit E.) The model results are discussed in detail for varying degrees of ladder-fuel removal (e.g., 0, 10, 20, 25, and 100 percent), but all cases are computed with exactly the same 20 mph windspeed. In reality, increasing levels of fuels reduction will be accompanied by higher windspeeds as the sub-canopy wind drag drops, but this is not considered by Jones et al., and this is typical of operational fire-model use. This mistake is repeated in the next example Jones et al. discuss, where on page 22 they state, “The fire scenario was the same,” meaning the same constant 20 mph windspeed was again used.

15. Two recent studies using high-resolution numerical fire simulations demonstrate just how consequential neglecting canopy wind-drag effects can be, leading to potentially disastrous results if aggressive ladder-fuel removal is applied. One study is by Atchley et al. 2021, sponsored by the USFS (a true and correct copy of which is included as Exhibit F), and the other is by Banerjee et al. 2020 (a true and correct copy of which is included as Exhibit G). In both papers, separate simulations are performed to compare different fuels configurations, and both papers demonstrate that the removal of ladder fuels reduces the sub-canopy wind drag, ultimately

leading to increased fire spread. In other words, they both show how fuels-reduction treatments can increase fire spread, which is the opposite of what the operational model studies predict. Furthermore, the Banerjee et al. 2020 paper goes further and also shows that aggressive ladder fuel removal increases the likelihood of overstory crown fires compared to more modest ladder fuel reductions, which is again opposite to operational model-run predictions.

16. From these results, it is clear that evaluating wildland fire resilience using current USFS operational fire-modeling theory is suspect, especially since operational models fail to properly include all of the important effects associated with specified fuels treatments, especially canopy wind resistance, which both Atchley et al. (2021) and Banerjee et al. (2020) show are extremely important. Until operational fire models are updated to include the latest and best available science, claims of improved fire resilience should be viewed with skepticism, and

treatments should stop until they are carefully validated against more accurate simulation methods. Our forests and the fisher may very-well depend on it.

Missing Fire Physics Can Be More Important than Fuel Load and Severe Weather

17. In addition to the focused process studies like those of Atchley et al. 2021 and

Banerjee et al. 2020, realistic high-resolution numerical fire simulations are also used to study the details of real-world fires. Since the simulations require significant computer time, they are done after the fact, but they are helpful for learning aspects of fire behavior that would be otherwise difficult to determine. For example, Coen et al. 2018, also sponsored by the USFS (a true and correct copy of which is included here as Exhibit H) uses high-resolution simulations to deconstruct the 2014 King Fire, and its authors show that fire-induced winds were primarily responsible for the fire's rapid growth and size. In their study, Coen et al. demonstrate that drought and fuel load were secondary effects compared to fire-induced atmospheric motions, which operational fire-behavior models neglect. Two important conclusions from the study are: 1. "… extreme fires need not arise from extreme fire environment conditions," and 2. "… models used in operations do not capture fire-induced winds and dynamic feedbacks so [they] can underestimate megafire events." In other words, the inability of operational models to simulate plume-driven megafires like the 2014 King Fire is not due to climate change or extreme weather events, but instead because of known missing physics in the operational models.

18. Additional evidence that vegetation treatments may be excluding important fire physics is suggested by the most comprehensive study to-date of wildland-fire data, which was conducted by Bradley et al. (2016), a true and correct copy of which is included as Exhibit I. They analyze satellite data for 1500 fires from 1984 to 2014, affecting 23.5 million acres of forestland. Their results show that the more heavily forestland is managed, the more severely it burns, and the least-managed land (i.e., our National Parks and Wilderness Areas) are the most firesafe (correcting for forest type, topography, and climate variables). Other scientific studies find similar results (e.g., Donato et al., 2006; Thompson et al., 2007; Cruz et al., 2014; Zald and Dunn, 2018). This suggests our land-management activities may be making our forestlands less firesafe, not more.

Long-Term Landscape-Resilience Claims are Unproven, and Sometimes They are Wrong

19. Current vegetation treatments advocated by the USFS were defined in 2009 in technical report PSW-GTR-220, and then later they were clarified in 2012 in PSW-GTR-237. Their efficacy for increased long-term, i.e., 30-year, landscape resilience is therefore not directly proven, since they were not practiced 30 years ago. Hence, claims of long-term resilience are

theoretical, and they are only as credible as the models used to predict them. Given the results of Atchley et al. 2021, Banerjee et al. 2020, Coen et al. 2018, and Bradley et al. 2016, are we willing to bet the Pacific fisher's future on them?

20. Attempts to evaluate these claimed long-term benefits demonstrate that a) they are *not* based on the best available science and b) they exaggerate or mischaracterize the findings in the references used to justify them. In contrast, the most comprehensive scientific study to date examining forestland-fire data demonstrates that land-management practices are producing forestlands that are less firesafe, not more; see paragraphs 13-18. Though this may seem counter intuitive, the reason is straightforward: the fire-behavior theory being used to guide vegetation treatments is incomplete because it does not sufficiently consider atmospheric motions, neither those induced by the fire, nor those induced by the vegetation treatments being analyzed. Until operational fire models are updated to address these deficiencies by including the latest available science, claims of improved long-term landscape resilience remain unproven, and the known harm being done to the Pacific fisher is therefore not justified.

21. Unfortunately, appropriate caution when interpreting operational model results is

not apparent when long-term improvements are asserted by the Services. For example, in its June 12 addendum to its 2020 Programmatic Biological Opinion (2020 PBO), the USFWS justifies anticipated negative impacts to the SSN DPS of the Pacific fisher, and its habitat, including its permitted Incidental Take of twelve individuals, by asserting planned vegetation treatments would "be beneficial for the fisher in the long-term by increased resilience of habitat" (2020 PBO addendum at 6). Similarly, in its February 23, 2021 Amendment to the Programmatic Biological Assessment (2020 PBA), the USFS makes similar claims, stating "Many of the management activities analyzed here and in the May 19, 2020 PBA are designed to reduce fuels and the risk of high-severity fires within the SSNDPS. Management activities that reduce the risk of high-severity

fire confer a long-term benefit to the SSNDPS resilience to fire …." (2020 PBA Amendment at 5- 6, February 23, 2021). Similar claims are repeated throughout the project documents associated with the 45 vegetation-treatment projects approved by USFWS.

Conclusion

22. Recent high-resolution numerical fire simulations demonstrate important deficiencies in the current USFS fire-behavior theory being used to analyze and design vegetation treatments that are known by USFS and USFWS to be harming Pacific fisher habitat. By

omitting atmospheric dynamics and wind-drag effects associated with vegetation treatments, fuels reductions designed to reduce fire intensity and fire spread are undoubtedly producing the opposite effect. Also, poorly designed ladder-fuel removal is likely increasing the incidence of crown-fire events that are killing our last large, old-growth trees.

23. Furthermore, the most comprehensive study to-date of forestland-fire data shows that more heavily managed forestland burns more severely, and the least-managed land (i.e., our National Parks and Wilderness Areas) are the most firesafe (correcting for forest type, topography, and climate variables).

24. Claims of long-term fire resilience are theoretical, and they are only as credible as the operational models being used to predict them. Assertions of long-term landscape resilience should be viewed with skepticism, and given the best-available science, including Atchley et al. 2021, Banerjee et al. 2020, Coen et al. 2018, and Bradley et al. 2016, are we willing to bet the Pacific fisher's future on unproven assertions being made by the Services?

25. Given recent trends in California of ever-increasing fire size and severity, the desire to take decisive action to make things better is understandable. However, if our actions are ill informed by flawed application of operational fire-behavior models that are guiding us to make an already dire situation worse, until we fully understand the consequences of the actions we take, no

action is preferred.

I declare, under penalty of perjury, that the foregoing is true and correct to the best of my knowledge and recollection. Executed on April 4, 2021 in Lafayette, Colorado.

Joseph Werne

References

Atchley, A.L., R. Linn, A. Jonko, C. Hoffman, J.D. Hyman, F. Pimont, C. Sieg, R.S. Middleton, 2021. Effects of fuel spatial distribution on wildland fire behavior. International Journal of Wildland Fire. doi:10.1071/WF20096.

Balch, J.K., B.A. Bradley, J.T. Abatzoglou, R.C. Nagy, E.J. Fusco, A.L. Mahood, 2017. Human started wildfires expand the fire niche across the United States. Proc. Nat'l Accad. Sci. 114(11), pp.2946-2951.

Banerjee, T., W. Heilman, S. Goodrick, J.K. Hiers, and R. Linn, 2020. Effects of canopy midstory management and fuel moisture on wildfire behavior. Nature, Sci Reps 10:17312. https://doi.org/10.1038/s41598-020-74338-9

Bradley, C.M., C.T. Hanson, and D.A. DellaSalla, 2016. Does increased forest protection correspond to higher fire severity in frequent-fire forests of the western USA? Ecosphere 7: article e01492.

Coen, J.L., E.N. Stavros, and J.A. Fites-Kaufman, 2018. Deconstructing the King megafire. Ecological Applications, 28(6), 2018, pp.1565-1580.

Cruz ,M.G., M.E. Alexander, and J.E. Dam, 2014. Using modeled surface and crown fire behavior characteristics to evaluate fuel treatment effectiveness: a caution. Forest Science 60:1000-1004.

Donato, D.C., J.B. Fontaine, J.L. Campbell, W.D. Robinson, J.B. Kauffman, B.E. Law, 2006. Post-Wildfire Logging Hinders Regeneration and Inreases Fire Risk. Science 311 (5759), 352.

Erman, D.C. et al. 1996. Sierra Nevada Ecosystem Project, Final Report to Congress, Vol. II, Assessment and Scientific Basis for Management Options. Wildland Resources Center Report No. 37, ISBN 1-887673-01-6, Center for Water and Wildland Resources, University of California, Davis, CA 627-657.

Jones, J.G., W. Chung, C. Seielstad, J. Sullivan, K. Krueger, 2010. Optimizing spatial and temporal treatments to maintain effective fire and non-fire fuels treatments at landscape scales. Final Report, JFSP Project 06-3-3-14. U.S. Department of Agriculture/U.S. Department of the Interior, Joint Fire Science Program. 33p.

Lutz, J.A., A.J. Larson, M.E. Swanson, J.A. Freund, 2012. Ecological Importance of Large Diameter Trees in a Temperate Mixed-Conifer Forest. PLoS ONE 7(5):e36131.

Lydersen, J.M., B.M. Collins, J.D. Miller, D.L. Fry, S.L. Stephens, 2016. Relating Fire-Caused Change in Forest Structure to Remotely Sensed Estimates of Fire Severity. Fire Ecology, 12(3), pp.99-116.

PSW-GTR-220: North, M., P. Stine, K. O'Hara, W. Zielinski, S. Stephens, 2009. An Ecosystem Management Strategy for Sierran Mixed-Conifer Forests. USDA, FS General Technical Report.

PSW-GTR-237: North, M., ed. 2012, Managing Sierra Nevada Forests. USDA, FS, General Technical Report.

Thompson, J.R., T.A. Spies, and L.M. Ganio, 2007. Reburn severity in managed and unmanaged vegetation in a large wildfire. Proc. Nat'l Academy of Sciences, 104(25).

USFS. 2021. Amendment to the Programmatic Biological Assessment for the Southern Sierra Nevada DPS of Pacific fisher. U.S. Forest Service, Pacific Southwest Region, Vallejo, CA, 23 February 2021.

USFWS. 2020. Batch 1 Appendage to the Programmatic Biological Opinion on the Proposed U.S. Forest service Management Programs for the Endangered Southern Sierra Nevada Distinct Population Segment of the Fisher. U.S. Fish and Wildlife Service, Sacramento Fish and Wildlife Office, Sacramento, CA, 12 June 2020.

Zald, H.S.J. and C.J. Dunn. 2018. Sever fire weather and intensive forest management increase fire severity in a multi-ownership landscape. Ecological Apps, 28(4), doi:10.1002/eap.1710.

EXHIBIT A

Curriculum Vitae: JOSEPH WERNE

Institutional Address:
NorthWest Research Associates
3380 Mitchell Lane, Boulder, CO 80301, 303-415-9701 x207, werne@nwra.com

Education:
Old Dominion University
B.S. (summa), Physics (1987)
B.S. (summa), Mech. Eng'g & Mechanics (1987)
The University of Chicago, Ph.D., Physics (1993)

Positions Held:
1985-

87 Engineering Co-op, Reactor Plant Planning Yard, Newport News Shipbuilding
1987-89 Teaching Assistant, Physics Department, The University of Chicago
1989-92 Research Assistant, Department of Astronomy and Astrophysics, The University of
Chicago 1992-94 Postdoctoral Fellow, Advanced Study Program, National Center for Atmospheric
Research 1994-95 Visiting Scientist, National Center for Atmospheric Research
1995-96 Research Associate, Joint Institute for Laboratory Astrophysics & Laboratory for Atmospheric and Space Physics, Univ. of Colorado
1997-01 Research Scientist, NorthWest Research Associates
2001-08 Assistant Division Manager, NorthWest Research Associates
2006-18 Vice President, NorthWest Research Associates
1998- Affiliated Faculty, Department of Applied Mathematics, Univ. of Colorado
2001- Senior Research Scientist, NorthWest Research Associates
2003- Director on the Board, NorthWest Research Associates

Professional Societies:
American Physical Society
American Astronomical Society

Professional Activities:
Presentations: Gordon Conference on Modeling in Solar Terrestrial Physics (1990); Gordon Conference on Solar Plasma and MHD Processes (1991); Army High Performance Computing Research Center, Workshop on Visualization and Statistical Analysis in Hard Turbulence (1992); The James Franck Institute, The University of Chicago, Turbulence Meeting (1993); Pittsburgh Supercomputing Center, Supercomputing Techniques: Parallel Processing/Cray T3D (1994); Woods Hole Oceanographic Institution Summer Program in Geophysical Fluid Dynamics (1995); NCAR Geophysical and Astrophysical Convection (1995); American Physical Society 43th, 44th, 46th, 47th, 48th, 58th, 60th & 66th Annual Meetings of the Division of Fluid Dynamics (1990-91, 1993-95, 2005, 2007, 2013); University of California 12th Annual Conference in Nonlinear Science (1996); National Center for Supercomputing Applications, Parallel Computing Workshop; SGI Origin (1997); DoD HPCMO User Group Conference (1998, 1999, 2000, 2001, 2002, 2003, 2004, 2005, 2006, 2007, 2008, 2009, 2010, 2011); Global Grid Forum 2 and 3, Washington, D.C. (2001) and Frascati, Italy (2001); EUROMECH Workshop 428 "Transport by coherent structures in environmental and geophysical flows," Torino, Italy (2001); Department of Energy, Environmental Meterology Program, "Vertical Transport and Mixing," Salt Lake City (2001, 2002); Center for Turbulence Research, "30 Years of Dynamic Modeling," Stanford University (2002); Invited Speaker, Center for Nonlinear Studies, Los Alamos National Laboratory (2003); Invited Speaker, "Helio- and Asteroseismology: Towards a Golden Future," Yale University, New Haven, Connecticut (2004); "Turbulence and Waves," Lighthill Institute of Mathematical Sciences, London, UK (2004); Visiting Scientist Colloquium, NASA Langley Research Center (2005); Invited Speaker, "Turbulent Mixing and Beyond," Trieste, Italy (2007); Co-organizer, NCAR 2008 Theme of the Year Workshop "Petascale Computing: Its Impact on Geophysical Modeling and Simulation" (2008). Invited Speaker, 20th DoD HPCMO User Group Conference, Schaumburg, IL (2010); Invited Speaker, "Turbulent Mixing and Beyond TMB-2011," Trieste, Italy (2011); Invited Speaker, Fundamental Aspects of Geophysical Turbulence II (2015); VIII International Symposium on Stratified Flows (2016); Invited Speaker, "McWilliams Symposium" National Center for Atmospheric Research, Boulder, CO (2016).

Software: Principle Architect & Author, *Practical Supercomputing Toolkit*, used by the Department of Defense (DoD) High Performance Computing and Modernization Program (HPCMP) to define a uniform command-line interface that streamlines use of disparate supercomputer platforms, high-speed networks, and archival data storage systems at all of the DoD HPC centers: https://pstoolkit.nwra.com. Principle Architect & Author, *Werne-NWRA Triple Code*, a highly accurate pseudo-spectral fluid dynamics solver designed to run efficiently on modern massively parallel supercomputer platforms: https://cora.nwra.com/~werne/triple/.

Teaching: Instructor, Summer MCAT Program, The University of Chicago, Biological Sciences Division and the Pritzker School of Medicine (1989-92). Principal Lecturer, NCAR 2008 Summer School: Geophysical Turbulence. Instructor, University of Colorado at Boulder 2009 Supercomputing Workshop, Fluid Instabilities, Waves, and Turbulence, as part of Professor Juri Toomre's ASTR/ATOC 5410 Graduate Course

Awards: A.D. Morgan Scholarship (1986-87); Faculty Award in Mechanical Engineering and Mechanics (1987); Outstanding Senior Award in Physics (1987); Gregor Wentzel Prize for Excellence as Graduate Student Tutor (1988).

Societies: Phi Kappa Phi; Pi Tau Sigma; Tau Beta Pi.

General Fields of Investigation:
Theoretical and numerical turbulence process, dynamics, and transport mechanisms in geophysical and astrophysical applications, including both stable and unstable stratification. Specific research areas include high-Rayleigh-number convection, penetrative convection, rotating convection, stratified sheer turbulence, gravity-wave breaking, wave-wave interactions, multi scale shear and wave dynamics, magnetohydrodynamic instability and turbulence processes, and optimal-perturbation theory. Applications have included ocean- and atmosphere-dynamics modeling, aircraft-wakes evolution and ground interactions, plasma dynamics for space-weather applications, solar-interior modeling, helioseismic analysis of the solar interior, and Bayesian hierarchical turbulence-process modeling in the troposphere and stratosphere. A primary emphasis has been on efficient and accurate spectral numerical methods, large-scale and high-performance computing, and massively parallel computing on a wide range of architectures, starting with the Cray XMP and YMP vector machines, the modestly parallel Cray C90, and then larger scale and massively parallel platforms, including the Cray T3D, T3E, XT3, XT4, XT5, XE6, XC40; IBM SP, P4+, P5+, P6; SGI O2k, O3k, Altix; Compaq SC40/45.

Business Development:
Developed, analyzed, and helped implement the 2000 NWRA Business Model, which encourages Research Scientists to become Principal-Investigator (PI) Partners in a successful research-science company. This model is novel, maximizes PI compensation, minimizes corporate taxes, has proven to be an invaluable recruiting tool for NWRA, and has worked successfully since 2000.

Publications:

1. *Design of a Mars Oxygen Processor*: Ash, R., J. Werne and M. B. Haywood 1989, in *The Case for Mars III* edited by C. Stoker, AAS Science and Technology Series, **75**, 479-487.
2. *Numerical Simluatins of Soft and Hard Turbulence: Preliminary Results for Two-Dimensional Convection*: DeLuca, E. E., J. Werne, R. Rosner, and F. Cattaneo 1990, Phys. Rev. Letters, **64(20)**, 2370-3.
3. *The Development of Hard-Turbulent Convection in Two Dimensions: Numerical Evidence*: Werne, J., E. E. DeLuca, R. Rosner and F. Cattaneo 1991, Phys. Rev. Letters, **67(25)**, 3519.
4. *The Structure of Hard-Turbulent Convection in Two Dimensions: Numerical Evidence*: Werne, J. 1993, Phys. Rev. E, **48**, 1020.
5. *Plume Model for the Boundary-Layer Dynamics in Hard Turbulence* : Werne, J. 1994, Phys. Rev. E, **49**, 4072. 6. *Incompressibility and No-Slip Boundaries in the Chebyshev-Tau Approximation: Correction to Kleiser and Schumann's Influence-Matrix Solution*: Werne, J. 1995, J. Comput. Phys., **120**, 260.
7. *Penetrative Convection in Rapidly Rotating Flows: Preliminary Results from Numerical Simulation*: Julien, K., S. Legg, J. McWilliams, and J. Werne 1996, Dyn. Atmos. Oceans, **24**, 237.
8. *Turbulent Rotating Rayleigh-Benard Convection with Comments on 2/7*: Werne, J. 1995, Woods Hole Oceanog. Inst. Tech. Rept. WHOI-95-27.
9. *Hard turbulence in rotating Rayleigh-Benard convection*: Julien, K., S. Legg, J. McWilliams, and J. Werne 1996, Phys. Rev. E, **53**, 5557R.
10. *Rapidly Rotating Turbulent Rayleigh-Benard Convection*: Julien, K., S. Legg, J. McWilliams and J. Werne 1996, J. Fluid Mech., **322**, 243.
11. *Dynamics and Scaling in Quasi Two-Dimneionsal Turbulent Convection*: Bizon, C., A. A. Predtechensky, J. Werne, K. Julien, W. D. McCormick, J. B. Swift and H. Swinney 1997, Physica A., **239**, 204.
12. *Plume Dynamics in Quasi 2D Turbulent Convection*: Bizon, C., J. Werne, A. A. Predtechensky, K. Julien, W. D. McCormick, J. B. Swift and H. L. Swinney 1997, Chaos, **7**, 1.
13. *Turbulent convection: what has rotation taught us?*: Werne, J. 2000 in *Geophysical and Astrophysical Convection*, Eds. P. A. Fox and R. M. Kerr. Gordon and Breach Science Publishers, 221. 14. *The effects of rotation on the global dynamics of turbulent convection*: Julien, K., J. Werne, S. Legg and J. McWilliams 1997 in *SCORe'96: Solar Convection and Oscillations and their Relationship*. Eds. J. Christensen-Dalsgaasrd and F. P. Pijpers. Kluwer Academic Publ., 227-230.
15. *The effect of rotation on convective overshoot*: Julien, K., J. Werne, S. Legg and J. McWilliams 1996, in *SCORe'96: Solar Convection and Oscillations and their Relationships*. Eds. J. Christensen-Dalsgaasrd and F. P. Pijpers. Kluwer Academic Publ., 231-234.
16. *Comment on "There is no Error in the Kleiser-Schumann Influence-Matrix Method"*: Werne, J. 1998, J. Comput. Phys. **141**, 88.

17. *Turbulence in Stratified and Shear Fluids: T3E Simulations*: Werne, J. and D. C. Fritts 1998, 8th DoD HPC User Group Conference, Houston, TX.

18. *2-D Convection in Tall, Narrow Containers: Implications for Theories of Heat Transport in Hard Turbulence*: Werne, J. 1996, (in preparation).

19. *High Rayleigh number convective transport: testing theories by modifying boundary conditions*: Brummell, N., K. Julien, and J. Werne 1996, (in preparation).

20. *Plumes in rotating convection: Part 1. Ensemble statistics and dynamical balances*: Julien, K., S. Legg, J. McWilliams, and J. Werne 1999, J. Fluid Mech. **391**, 151-187.

21. *Statistical Analysis of the Influence of Rotation in Rayleigh-Benard Convection*: Julien, K., S. Legg, J. McWilliams, and J. Werne 1996, (in preparation).

22. *On the linear stability of Hele-Shaw Convection*: Julien, K. and J. Werne 1996, Int. J. Heat and Mass Transfer, (to be submitted).

23. *A new class of equations for rotationally constrained flows*: Julien, K., E. Knobloch and J. Werne 1998, Theoret. and Comput. Fluid Dynamics, **11**, 251-261.

24. *Reduced Equations for Rotationally Constrained Convection*: Julien, K., E. Knobloch and J. Werne 1999, In the International Symposium on Turbulence and Shear Flow Phenomena, v.1, pp. 101-106, Begel House.

25. *A Reduced Description for Rapidly Rotating Turbulent Convection*: Julien, K., E. Knobloch and J. Werne 1998, In Advances in Turbulence VII, Eds U. Frisch, pp. 472-482, Klumer Academic Publishers.

26. *Dynamics of counter-rotating vortex pairs in stratified and sheared environments*: Garten, J. F., S. Arendt, D. C. Fritts and J. Werne 1998, J. Fluid Mech. **361**, 189-236.

27. *Anisotropy in Stratified Shear Turbulence*: Werne, J. and D. C. Fritts 1999, 9th DoD HPC User Group Conference, Monterey, CA.

28. *Stratified shear turbulence: Evolution and statistics*: Werne, J. and D. C. Fritts 1999, Geophys. Res. Letters **26**, 439. 29. *Turbulence-induced fluctuations in ionization and application to PMSE*: Hill, R. J., D. Gibson-Wilde, J. Werne and D. C. Fritts 1999, Earth Planets Space, **51**, 499.

30. *Structure Functions in Stratified Shear Turbulence*: Werne, J. and D. C. Fritts 2000, 10th DoD HPC User Group Conference, Albuquerque, NM.

31. *Turbulence Dynamics and Mixing due to Gravity Waves in the Lower and Middle Atmosphere*: Fritts, D. C. and J. Werne 2000, in *Atmospheric Science across the Stratopause*, Geophysical Monograph 123, American Geophys. Union, 143-159. 32. *Hierarchical Data Structuring: an MPP I/O How-to*: Werne, J., P. Adams and D. Sanders 2000, Scientific Computing at NPACI, June 14, Volume 4 Issue 12.

33. *Linear scaling during production runs: conquering the I/O bottleneck*: Werne, J., P. Adams and D. Sanders 2000, in *ARSC CRAY T3E Users' Group Newsletter* **193**, April 14, eds. T. Baring & G. Robinson.

34. *Numerical modeling of turbulent zero momentum late wakes in density stratified fluids*: Gourlay, M. J., S.C. Arendt, D.C. Fritts, and J. Werne 2000, 10th DoD HPC User Group Conference, June 5-9, Albuquerque, NM.

35. *Numerical modeling of turbulent non-zero momentum late wakes in density stratified fluids*: Gourlay, M. J., S.C. Arendt, D.C. Fritts, and J. Werne 2000, Fifth International Sypmosium on Stratified Flows, July 10-13, Vancouver, Canada. 36. *Numerical modeling of initially turbulent wakes with net momentum*: Gourlay, M. J., S.C. Arendt, D.C. Fritts, and J. Werne 2001, Phys. Fluids **13**, 3783.

37. *Numerical simulation of late wakes in stratified and sheard flows*: Fritts, D., M. Gourlay, W. Orlando, C. Meyer, J. Werne, and T. Lund 2003, 13th DoD HPC User Group Conference, DOI:10.1109/DODUGC.2001.1253394

38. *Direct numerical simulation of VHF radar measurements of turbulence in the mesosphere*: Gibson-Wilde, D., J. Werne, D. C. Fritts and R. J. Hill 2000, Radio Science **35**, 783.

39. *Anisotropy in a stratified shear layer*: Werne, J. and D. C. Fritts 2001, Physics and Chemistry of the Earth, **26**, 263. 40. *Direct numerical simulations of the Crow instability and subsequent vortex reconnection in a stratified fluid*: Garten, J. F., J. Werne, D. C. Fritts, and S. Arendt 2001, J. Fluid Mech. **426**, 1.

41. *Wave-breaking and shear turbulence simulations in support of the Airborne Laser*: Werne, J., C. Bizon, C. Meyer, and D. C. Fritts 2001, 11th DoD HPC User Group Conference, June, Biloxi, MS.

42. *Vertical transport by convection plumes: Modificiation by rotation*: Legg, S., K. Julien, J. McWilliams, and J. Werne 2001, Phys. Chem. of the Earth, B, 26 (4), 259-262.

43. *The Effects of Ambient Stratification on the Crow Instability and Subsequent Vortex Reconnection*: Garten, J. F., J. Werne, D. C. Fritts and S. Arendt 1999 in *European Series in Applied and Industrial Mathematics,* ESAIM Proceedings, Third International Workshop on Vortex Flow and Related Numerical Methods, Vol 7 Eds: A. Giovannini, G. H. Cottet, Y. Gagnon, A. Ghoniem, E. Meiburg. 44. *Application of turbulence simulations to the meesosphere*: Gibson-Wilde, D., J. Werne, D. C. Fritts, and R. Hill 2000, Proc. MST 9 Radar Workshop, Toulouse, France.

45. *A new dynamical subgrid model for the planetary surface layer. I. The model and a priori tests*: Dubrulle, B., J.-P. Laval, P. P. Sullivan and J. Werne 2002, J. Atmos. Sci. **59**, 857.

46. *Entrainment-zone restratification and flow structures in stratified shear turbulence*: Pettersson-Reif, B.A., J. Werne, \O. Andreassen, C. Meyer, M. Davis-Mansour 2002, Studying Turbulence Using Numerical Simulation Databases -IX, Proceedings of the 2002 Summer Program, Center for Turbulence Research, ed. P. Bradshaw, 245-256.

47. *Layering accompanying turbulence generation due to shear instability and gravity wave breaking*: Fritts, D.C., C. Bizon, J.A. Werne, and C.K. Meyer 2003, J. Geophys. Res. **108**, D8, 8452, doi:10.1029/2002JD002406.

48. *The Need for Control Experiments in Local Helioseismology*: Werne, J., A. Birch, and K. Julien 2004, SOHO 14/GONG 2004, Helio- and Asteroseismology: Towards a Golden Future, New Haven, CT., Es. D. Danesy, European Space Agency SP-559. 49. *Visualization of the Energy-Containing Turbulent Scales*: Helgeland, A., \O. Andreassen, A. Ommundsen, B.A. Pettersson-Reif, J. Werne, T. Gaarder 2004, 2004 IEEE Symposium on Volume Visualization and Graphics (VV'04) 103-109., DOI:10.1109/SVVG.2004.15

50. *Persistence of a Kelvin-Helmholtz instability complex in the upper troposphere*: M.C. Kelley, C.Y. Chen, R.R. Beland, R. Woodman, J.L. Chau, and J. Werne 2005, J. Geophys. Res. **110**, D14, 106, doi:10.1029/2004JD005345. 51. *CAP Phase II Simulations for the Air Force HEL-JTO Project: Atmospheric Turbulence Simulations on NAVO's 3000-Processor IBM P4+ and ARL's 2000-Processor Intel Xeon EM64T Cluster*: Werne, J., T. Lund, B.A. Pettersson-Reif, P. Sullivan, and D.C. Fritts 2005, 15th DoD HPC User Group Conference, June, Nashville, TN., DOI:10.1109/DODUGC.2005.16 52. *Characterization of high altitude turbulence for Air Force platforms*: Ruggiero, F.H., J. Werne, T.S. Lund, D.C. Fritts, K. Wan, L. Wang, A. Mahalov, and B. Nichols 2005, 15th DoD HPC User Group Conference, June, Nashville, TN. 53. *Generalized quasi-geostrophy for spatially anisotropic rotationally constrained flows*: K. Julien, E. Knobloch, R. Milliff & J. Werne 2006, J. Fluid Mech., **555**, 233-274.

54. *Mean and variable forcing of the middle atmosphere by gravity waves*: Fritts, D.C., S.L. Vadas, K. Wan, and J. Werne 2006, J. Atmos. Solar-Terres. Phys., **68**, 247-265.

55. *Characterization of High Altitude Turbulence for Air Force Platforms*: Ruggiero, F.H., J. Werne, A. Mahalov, B. Nichols, and D.E. Wroblewski 2006, 16th DoD HPC User Group Conference, June, Denver, CO.

56. *Numerical simulation of an asymptotically reduced system for rotationally constrained convection*: Sprague, M., K. Julien, E. Knobloch, and J. Werne 2006, J. Fluid Mech., **551**, 141-174.

57. *Characterization of High Altitude Turbulence for Air Force Platforms*: Ruggiero, F.H., A. Mahalov, B. Nichols, J. Werne, and D.E. Wroblewski 2007, 17th DoD HPC User Group Conference, June, Pittsburgh, PA., DOI:10.1109/HPCMP-UGC.2007.15 58. *High-Resolution Simulations and Atmospheric Turbulence Forecating*: Werne, J., D.C. Fritts, L. Wang, T. Lund, and K. Wan 2008, 18th DoD HPC User Group Conference, July, Seattle, WA.

59. *Gravity Wave Instability Dynamics at High Reynolds Numbers. Part II: Turbulence Evolution, Structure, and Anisotropy*: D.C. Fritts, L. Wang, J. Werne, T. Lund, and K. Wan 2009, J. Atmos. Sci., DOI:10.1175/2008JAS2727.1

60. *Gravity wave instability dynamics at high Reynolds numbers, 1: Wave field evolution at large amplitudes and high frequencies*: Fritts, D.C., L. Wang, J. Werne, T. Lund, and K. Wan 2009, J. Atmos. Sci. **66**, 1126-1148, doi:10.1175/2008JAS2726.1. 61. *Gravity wave instability dynamics at high Reynolds numbers, 2: Turbulence evolution, structure, and anisotropy*: Fritts, D.C., L. Wang, J. Werne, T. Lund, and K. Wan 2009, J. Atmos. Sci. **66**1149-1171, doi:10.1175/2008JAS2727.1. 62. *High-Resolution Simulations of Internal Gravity-Wave Fine Structure Interactions and Implications for Atmospheric Turbulence Forecasting*: Werne, J., Fritts, D.C., L. Wang, T. Lund and K. Wan 2009, 19th DoD HPC User Group Conference, 15-19 June, San Diego, CA, DOI: 10.1109/HPCMP-UGC.2009.43

63. *Gravity wave fine-structure interactions: A reservoir of small-scale and large-scale turbulence energy*: Fritts, D.C., L. Wang and J. Werne 2009, Geophys. Res. Lett. **36**, L19805, doi:10.1029/2009GL039501.

64. *Numerical simulation of the linking of Kelvin-Helmholtz instabilities at adjacent shear layers*: Fritts, D.C., B. Laughman, J. Werne, D. Simkhada and M.J. Taylor 2009, J. Geophys., Res. (to be submitted).

65. *Numerical simulation of bore generation and morphology in thermal and Doppler ducts*: Laughman, B., D.C. Fritts, and J. Werne 2009, Ann. Geophys., SpreadFEx special issue, **27**, 511-523.

66. *Atmospheric Turbulence Forecasts for Air Force and Missile Defense Applications*: Werne, J., D.C. Fritts, L. Wang, T. Lund, and K. Wan 2010, Invited Paper, 20th DoD HPC User Group Conference, 14-17 June, Schaumburg, IL, DOI:10.1109/HPCMP UGC.2010.75

67. *Temperature and velocity structure functions in the upper troposhere and lower stratosphere from aircraft measurements (invited)*: Wroblewski, D.E., J. Werne, O. Cote, J. Hacker, and R. Dobosy 2010, J. Geophys. Res., DOI:10.1029/2010JD014618 68. *Comparisons of predicted bore evolutions by the Benjamin-Davis-Ono and Navier-Stokes equations for idealized mesopause thermal ducts*: Laughman, B., D.C. Fritts, and J. Werne 2011, J. Geophys., Res., DOI:10.1029/2010JD014409 69. *Computation of clear-air radar backscatter from numerical simulations of turbulence: 1. Numerical methods and evaluation biases*: Franke, P.M., S. Mahmoud, K. Raizada, K. Wan, D.C. Fritts, T. Lund, and J. Werne 2011, J. Geophys. Res., DOI:10.1029/2011JD015895

70. *Computation of clear-air radar backscatter from numerical simulations of turbulence: 2. Backscatter moments throughout the lifecycle of a Kelvin-Helmholtz instability*: Fritt, D.C., P.M. Franke, K. Wan, T. Lund and J. Werne 2011, J. Geophys. Res., DOI:10.1029/2010JD014618

71. *Interpretation of apparent simultaneous occurrences of Kelvin-Helmholtz instability in two airglow layers: Observations*: Simkhada, D., B. Laughman, D.C. Fritts, J. Werne, and A. Liu 2013, J. Geophys., Res. (submitted).

72. *Kelvin-Helmholtz instability in two airglow layers: Observations*: Simkhada, D., B. Laughman, D.C. Fritts, J. Werne, and A. Liu 2013, J. Geophys., Res. (submitted).

73. *Modeling the implications of Kelvin-Helmholtz instability dynamics for airglow observations*: Fritts, D.C., K. Wan, J. Werne, T. Lund, J.H. Hecht 2014, J. Geophys. Res. Atmos., 119, 8858-8871. doi:10.1002/2014JD021737.

74. *Gravity Wave-Fine Structure Interactions. Part I: Influences of Fine Structure Form and Orientation on Flow Evolution and Instability*: Fritts, D.C., L. Wang, and J.A. Werne 2013, J. Atmos. Sci. 70:12, 3710-3734, DOI:10.1175/JAS-D-13-055.1 75. *Coupled small scale mesospheric dynamics in a dual shear environment over Hawaii II: Modeling and interpretation*: Laughman, B., D.C. Fritts, J. Werne, D.B. Simkhada, M.J. Taylor, and A.Z. Liu 2013, J. Geophys. Res. (submitted). 76. *Quantifying Kelvin-Helmholtz Instability Dynamics Observed in Noctilucent Clouds: 2. Modeling and Interpretation of Observations*: Fritts, D.C., G. Baumgarten, K. Wan, J. Werne, T. Lund 2014, J. Geophys. Res., 119, 9359-9375, doi:10.1002/2014JD021833

77. *Numerial Modeling of Multiscale Dynamics at a High Reynolds Number: Instabilities, Turbulence, and an Assessment of Ozmidov and Thorpe Scales*: Fritts, D.C., L. Wang, M.A. Geller, D.A. Lawrence, J. Werne, B.B. Balsley 2016, J. Atmos. Sci., 73(2), 555-578, doi:10.1175/JAS-D-14-0343.1

78. *Fine Structure, Instabilities, and Turbulence in the Lower Atmosphere: High-Resolution in Situ Slant-Path Measurements with the DataHawk UAV and Comparisons with Numerical Modeling*Balsley, B.B., D.A. Lawrence, D.C. Fritts, L. Wang, K. Wan, J. Werne, 2018, J. Atmos. and Oceanic Tech., 35(3), 619-642, doi:10.1175/JTECH-D-16-0037.1

EXHIBIT B

Binkley, D., T. Sisk, C. Chambers, J. Springer, and W. Block. 2007. The role of old-growth forests in frequent-fire landscapes. *Ecology and Society* **12**(2): 18. [online] URL: http://www.ecologyandsociety.org/vol12/iss2/art18/

Synthesis, part of a Special Feature on The Conservation and Restoration of Old Growth in Frequent-fire Forests of the American West

The Role of Old-growth Forests in Frequent-fire Landscapes

Daniel Binkley [1], *Tom Sisk* [2,3], *Carol Chambers* [4], *Judy Springer* [5], and *William Block* [6]

ABSTRACT. Classic ecological concepts and forestry language regarding old growth are not well suited to frequent-fire landscapes. In frequent-fire, old-growth landscapes, there is a symbiotic relationship between the trees, the understory graminoids, and fire that results in a healthy ecosystem. Patches of old growth interspersed with younger growth and open, grassy areas provide a wide variety of habitats for animals, and have a higher level of biodiversity. Fire suppression is detrimental to these forests, and eventually destroys all old growth. The reintroduction of fire into degraded frequent-fire, old-growth forests, accompanied by appropriate thinning, can restore a balance to these ecosystems. Several areas require further research and study: 1) the ability of the understory to respond to restoration treatments, 2) the rate of ecosystem recovery following wildfires whose level of severity is beyond the historic or natural range of variation, 3) the effects of climate change, and 4) the role of the microbial community. In addition, it is important to recognize that much of our knowledge about these old-growth systems comes from a few frequent-fire forest types.

Key Words: *ecological processes; evolutionary adaptations; historic range of variation (HRV); human values; knowledge gaps; resilience; understory vegetation*

INTRODUCTION

Traditional forestry took decades to understand the unique features of frequent-fire forests. Early foresters in the Southwest were very concerned about the near-absence of young trees in forests dominated by older, widely spaced ponderosa pine (*Pinus ponderosa*) trees, and they realized that frequent fires prevented the development of closed canopy, high-wood-producing forests. A young Aldo Leopold (1920) wrote:

> *...the prevention of light burning during the past 10 years... has brought in growth on large areas where reproduction was hitherto largely lacking. Actual counts show that the 1919 seedling crop runs as high as 100 000 per acre. It does not require any very elaborate argument to show that these tiny trees, averaging only 2 inches high, would be completely destroyed by even a light ground fire.*

Leopold did not yet have the insight to understand the profound consequences of 100 000 seedlings per acre, although he later came to see the more subtle argument that fire prevention thwarted the processes necessary for the long-term health of the forest ecosystem.

Frequent fires challenge the survival of new tree seedlings and strongly shape the long-term development of all the components of a forest. Young trees often establish in clumps, as a legacy of patchy fuels and fire behavior; and this structural legacy may last for centuries. Gaps between clumps may result from a combination of competition with grasses and shrubs, from uneven distribution of seeds, and also the pattern of fire that interacts with the pattern of soils, vegetation, and fine fuels. The intimate mixture of shady clumps of trees and small open meadows provides a local-scale diversity that would be found only at much larger scales in landscapes without frequent fire. Indeed, some classic vocabulary in forestry is not well suited for frequent-fire forests. As noted by Kaufmann et al. in this issue, old-growth characteristics in dry, frequent-fire forests are remarkably different from the old-growth images developed in wetter areas. Even the concept of the forest “stand” as a part of a forest landscape with relatively uniform conditions and somewhat distinct boundaries may not be suitable for frequent-fire forests (Long and Smith 2000). The important details about the spatial arrangement of trees in the landscape relate to the clumping of trees into small groups, and to clusters of these groups, rather than to extensive, uniform areas of similar-size trees stretching across hundreds or thousands of hectares (Fig. 1).

The frequent recurrence of fires reinforces a spatial heterogeneity, promoting a forest with high, small scale variety in plant species composition, animal habitat, and ecological processes. This pattern of local variety is a key defining feature of old-growth forests in frequent-fire landscapes. In this chapter, we consider some of the crucial ecological roles that might depend partially on the spatial arrangements of trees, and those that relate to the fully developed old-growth conditions.

EVOLUTIONARY ADAPTATIONS TO FIRE

The adaptations of large trees to surviving fire are fundamental in the ecology of old-growth forests in frequent-fire landscapes. Depending on the species, trees in these forests have developed a number of characteristics to withstand and survive fire. Although fire typically kills small conifers with thin bark by overheating or destroying the cambium layer (van Mantgem and Schwartz 2003), most coniferous tree species in the mature state have thick, insulating bark that is relatively nonflammable, long needles, self-pruning lower branches, and deep roots. Giant sequoia (*Sequoiadendron giganteum*) also experiences rapid growth that raises canopies off the ground quickly, as well as latent buds and serotinous cones (Stephenson 1999). Jeffrey pine (*Pinus jeffreyi*) develops buds with thick scales that help withstand heat. Sugar pine (*Pinus lambertiana*) has thick, fire-resistant bark and an open canopy that retards the spread of fire through the canopy. Gray pine (*Pinus sabiniana*) has thick bark and is self pruning. Arizona pine (*Pinus arizonica*) has insulated buds, a high capacity to recover from crown scorch and an open crown. Ponderosa pine has thick bud scales; tight needle bunches that enclose and protect the meristems, then open into a loose arrangement that does not favor combustion or propagation of flames; high foliar moisture; and a deep rooting habit. The foliage and buds are also usually elevated away from the flame zone. With its high foliar moisture content, ponderosa pine can withstand extensive scorching as long as the buds and twigs, which tolerate higher temperatures than needles, are not badly scorched.

USING PAST CONDITIONS AS A GUIDE

Historic range of variability (HRV) or natural range of variability are interchangeable terms along with natural variability, historical variation, and natural range of variability. These terms suggest that past conditions and processes can be used as guidance for managing present-day ecosystems, and that disturbance (and resultant variety) is a vital attribute of nearly every ecosystem (Landres et al. 1999). The HRV approach is just a first step in pondering possible future forests and landscapes, because it is difficult to deduce details about HRV (especially across large areas and long times), and because future climate conditions may not track historical trends. Because of changes in fire regimes, particularly caused by grazing and fire suppression, many frequent-fire forests now function well outside the HRV (see Moore et al. 1999, Veblen et al. 2000, Allen et al. 2002, Arno and Fiedler 2005, Zier and Baker 2006). For

---

[1]Colorado Forest Restoration Institute, [2]Northern Arizona University, Environmental Sciences, [3]ForestERA, [4]Northern Arizona University, School of Forestry, [5]Ecological Restoration Institute, [6]U.S. Forest Service Rocky Mountain Research Station

example, Sierra Nevada forests currently are undergoing fire-free periods that are much longer than at any time in the past two centuries (Keeley and Stephenson 2000).

Determining the Historic Structure and Function of Old-growth Forests

Almost all of the frequent-fire landscapes of the western United States have changed dramatically as a result of livestock grazing, timber harvesting, and fire suppression. Given the near absence of fully functioning, old-growth forests in frequent-fire landscapes, scientists have to use a variety of approaches to determine the structure and processes that characterize these forests (Swetnam et al. 1999, Egan and Howell 2001, Friederici 2003). Historical journals, photographs, and records provide information from some forests on the number and sizes of trees before major changes in land use, and the most detailed records even provide information on other features, such as downed logs and bunchgrass locations (Moore et al. 2004). In the absence of historical records, detailed characterizations

Fig. 1. A cartoon description of the key features of old-growth forests in frequent-fire landscapes (left), in contrast to younger forests lacking fire (right).

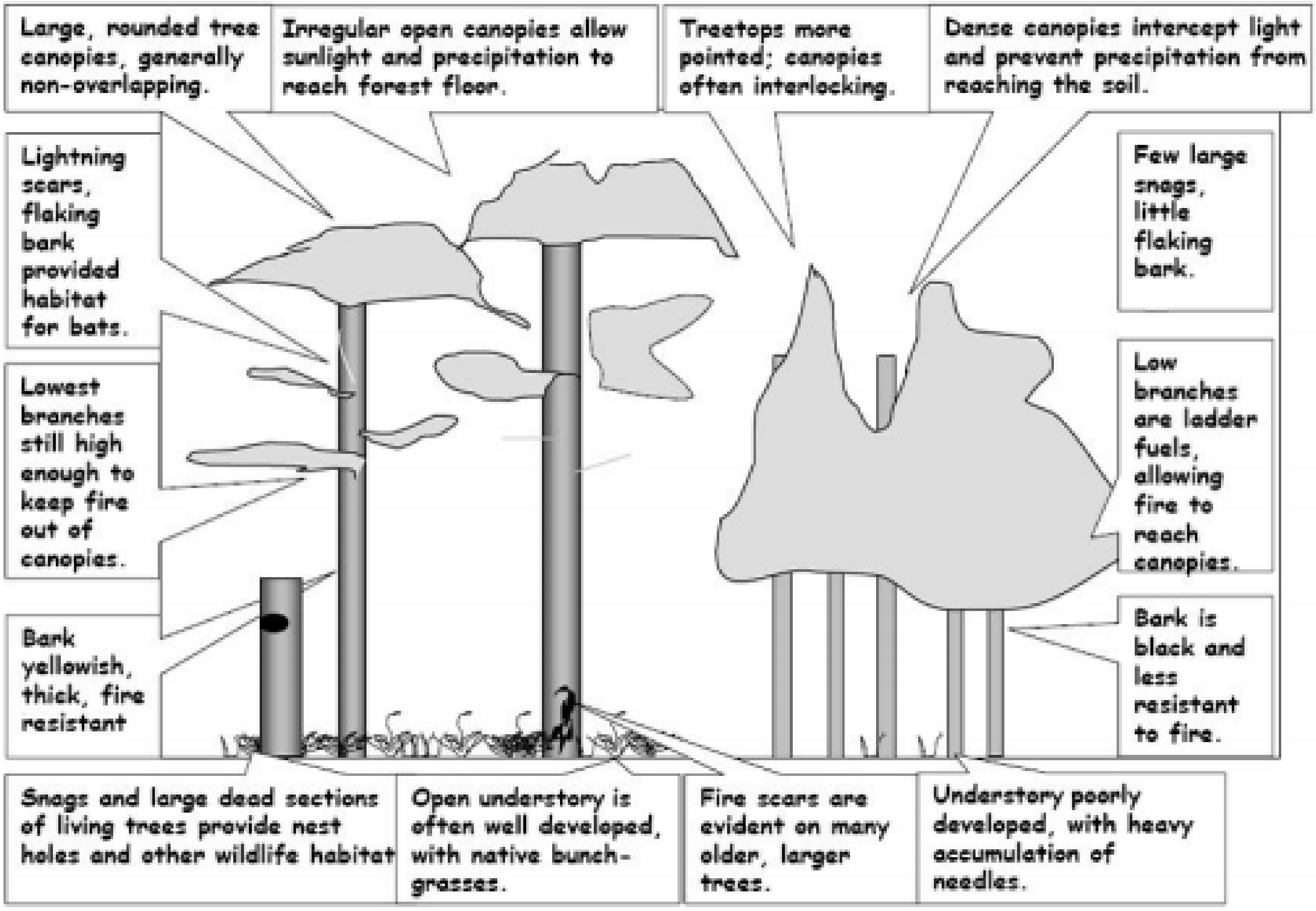

of tree ages, stump ages, and other field evidence can provide solid descriptions of previous conditions. A very few sites, such as the Powell Plateau in the Grand Canyon and some regions of northern Mexico, may have experienced so little change in land use and fire regimes that contemporary measurements are possible (Fulé et al. 2005). Some of the most detailed insights about the structure and function of old-growth forests come from intensive experiments that have reestablished historic forest structure. These treatments include harvesting (and removing) the excessive young trees, retaining most old trees, and reintroducing fire at intervals that match the frequency of historical fires (Bailey and Covington 2002, Fulé et al. 2002, 2006). Forest restoration treatments may not redevelop historical old-growth conditions perfectly for a variety of reasons: 1) the seedbanks of native species may be depleted after decades without fire, 2) exotic species may invade, and 3) the animal communities may not be the same as in past centuries.

We know that historic frequent-fire, old-growth forests were not all alike. For example, Moore and her colleagues (2004), after studying a set of 11 research plots established in the early 1900s in Arizona and New Mexico, found that basal area ranged from 9 to 27 m^2/ha, with an average of 15 m^2/ha. By the end of the century, basal area had doubled on average, although some sites had changed little and others had tripled. Similarly, Arno et al. (1995), using dendrochronological reconstructions of six old-growth ponderosa–Douglas-fir (*Pseudotsuga menziesii*) stands in Montana, found basal densities in 1900 ranging from 15 to 35 m^2/ha. The variety of old-growth forest structures probably varied with environmental factors that influence tree establishment, growth, and mortality, including the interacting effects of fires. We also know that the return intervals for fires were longer for most of the ponderosa pine forests in eastern Montana (Morgan et al. 2002) and the Front Range of Colorado—and modestly longer for forests in western Montana (Arno 1980), eastern Oregon (Youngblood et al. 2004), and eastern Washington (Everett et al. 2000)—than for similar forests in Arizona and New Mexico. However, we don't know how this difference in fire regime led to differences in stand structure and function (for example, see Kaufmann et al. 2006)

PROCESSES

The most essential process in the development of old-growth conditions is time. Frequent-fire forests occur under relatively dry conditions, and the lack of abundant water limits the growth rates of trees. Forests with slow-growing trees take 100–200 years to begin to show the full spectrum of old-growth structure and processes.

However, time alone is not sufficient to encourage old growth in frequent-fire forests. Fundamental to the development of old-growth conditions is the interaction of forest processes with repeated fires. In the absence of repeated fire, tree density tends to remain high, and the fuel structure develops to the point where a very intense fire kills most of the trees. As a result, old-growth conditions are never reached.

Frequent surface fires allow larger trees to persist, limit the success of new trees, and foster the spatial pattern of open meadows mixed with tree clumps. Surface fires that recur every few years or decades kill most of the small trees that managed to establish during years with favorable precipitation and seed crops. The trees that survive the fires experience less competition for light and soil moisture, leading to higher rates of individual growth, thicker bark, and higher canopy base heights—all of which makes these trees more resistant to subsequent surface fires. The grasses, forbs, and shrubs that thrive between clumps of trees are typically burned by surface fires, but these plants often resprout from surviving roots or reseed.

Without the recurring cultivation of the forest by fire, old-growth conditions may not develop. Fire suppression allows tree seedlings to recruit in large numbers, forming denser stands. Wildfire spreads more easily into the canopies of smaller trees with low branches, and from smaller trees into the crowns of previously fire-resistant old trees. With abundant small trees established among the more scattered old growth, fire may spread rapidly across large areas, with high mortality in all age and size classes.

Productivity, Hydrology, and Nutrient Cycling

One of the most distinctive features of frequent-fire, old-growth forests is the major contribution that the understory vegetation (grasses, forbs, shrubs) makes to ecosystem diversity and productivity. In the absence of fire, the density of overstory trees increases, which reduces the diversity of understory vegetation 10–30% (Fig. 2, Laughlin and Grace 2006). This relationship between the density of trees and understory diversity is further influenced by the number of years between fires (the fire return interval). For example, a ponderosa pine forest on the Kaibab Plateau that burned in the past 10 years might have 35 species in the understory, compared with 28 species after 70 years without a fire, and 22 species after 120 years without a fire (Laughlin et al. 2005).

Restoration treatments reduce tree density and lower the total growth of trees in a forest, but increase the growth of residual (retained) trees and the biomass and productivity of the understory. In Montana, understory plant diversity declined the first year after a thinning and burning restoration treatment in a ponderosa pine–Douglas-fir forest, but increased significantly 2 years after treatment (Metlen and Fiedler 2006). Experiments around northern Arizona typically show understory biomass and growth increases of more than two-fold in response to thinning and prescribed burning (Fig. 3; Abella 2004, Gildar et al. 2004, Moore et al. 2004). Restoration treatments appear to have little effect on the total productivity of the forests, but they shift how the growth is allocated between the overstory and understory. A restoration experiment at Fort Valley near Flagstaff, Arizona showed that total production did not change, but the proportion accounted for by the understory rose from 10% to

Fig. 2. The richness of understory plant species declines with increasing density of overstory pine trees, on the Kaibab Plateau in northern Arizona (after Laughlin and Grace 2006). Typical historic conditions would have had about 35 species per 0.1-ha plot, but with changing land use and fire regimes, the most common species richness has declined to 25 to 30 species per 0.1-ha plot.

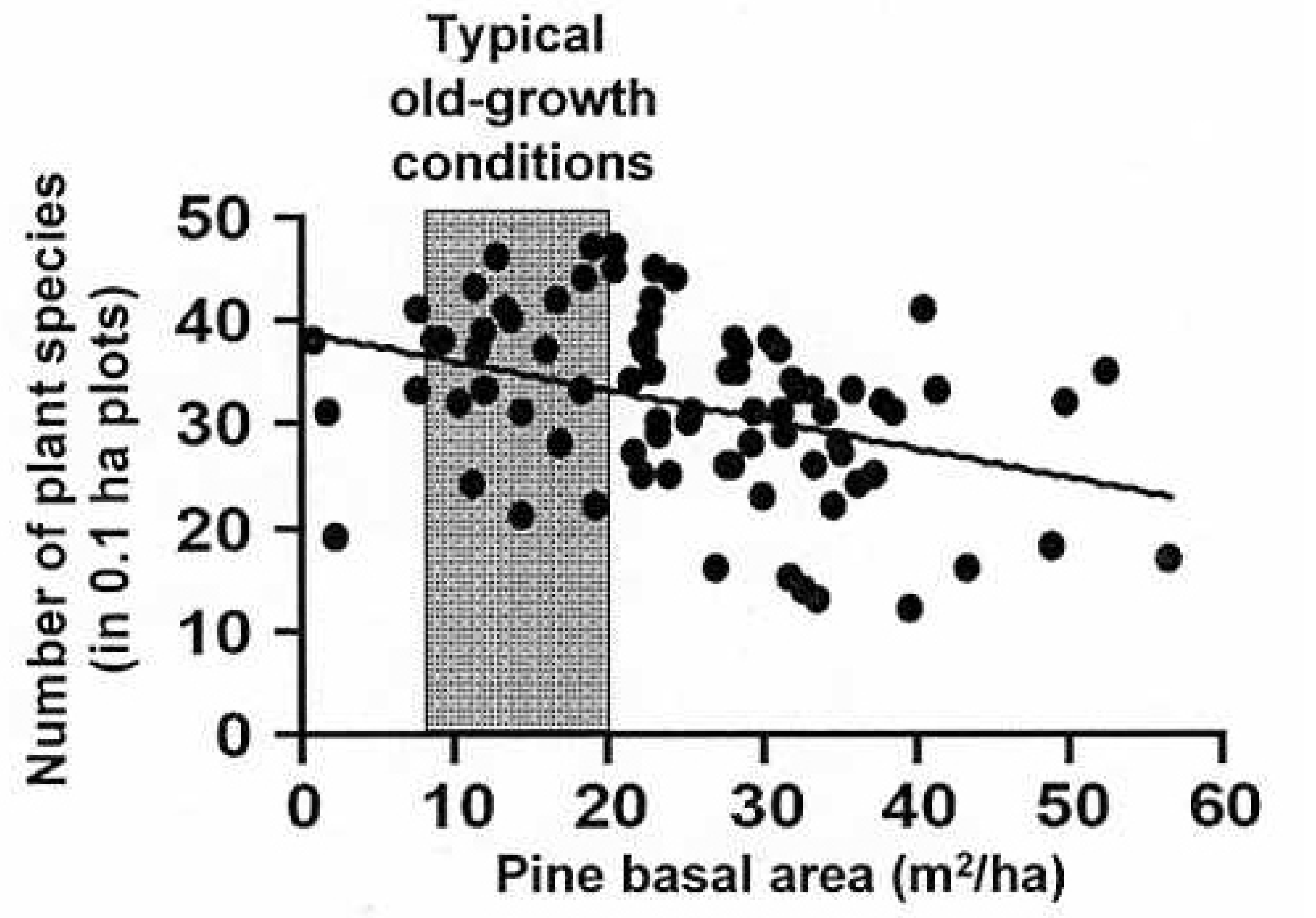

about 25%. The benefit of restoration treatments also differs among plant types. For example, the restoration responses at Fort Valley were greater for grasses than forbs (Moore et al. 2006), greater for leguminous forbs than other types, and greater for C_3 grasses (e.g., bottlebrush squirreltail (*Elymus elymoides* subsp. *elymoides*)) than C_4 grasses (e.g., mountain muhly (*Muhlenbergia montana*)). All of these trends might differ in response to major or minor differences in restoration prescriptions, site history, and current weather.

The higher productivity of understory plants in old growth (and restored) forests in frequent-fire landscapes results in part from the low canopy leaf area of the overstory trees. Tree canopies cover less than half of the ground area (and commonly as little as 25%). Despite this patchy distribution of trees, the total amount of leaves in the tree canopy on 1 ha would still provide 2 or 3 ha of leaf surface area to intercept light. Forests in landscapes with higher supplies of water commonly have canopy surface areas of 4 to 6 ha displayed for each hectare of ground area.

Fig. 3. Understory biomass and growth were much higher in forests with restoration treatments than in control forests (from summary of Abella 2004, Gildar et al. 2004, Moore et al. 2006). The greatest proportional increases occur when the biomass in the unrestored forests is particularly low.

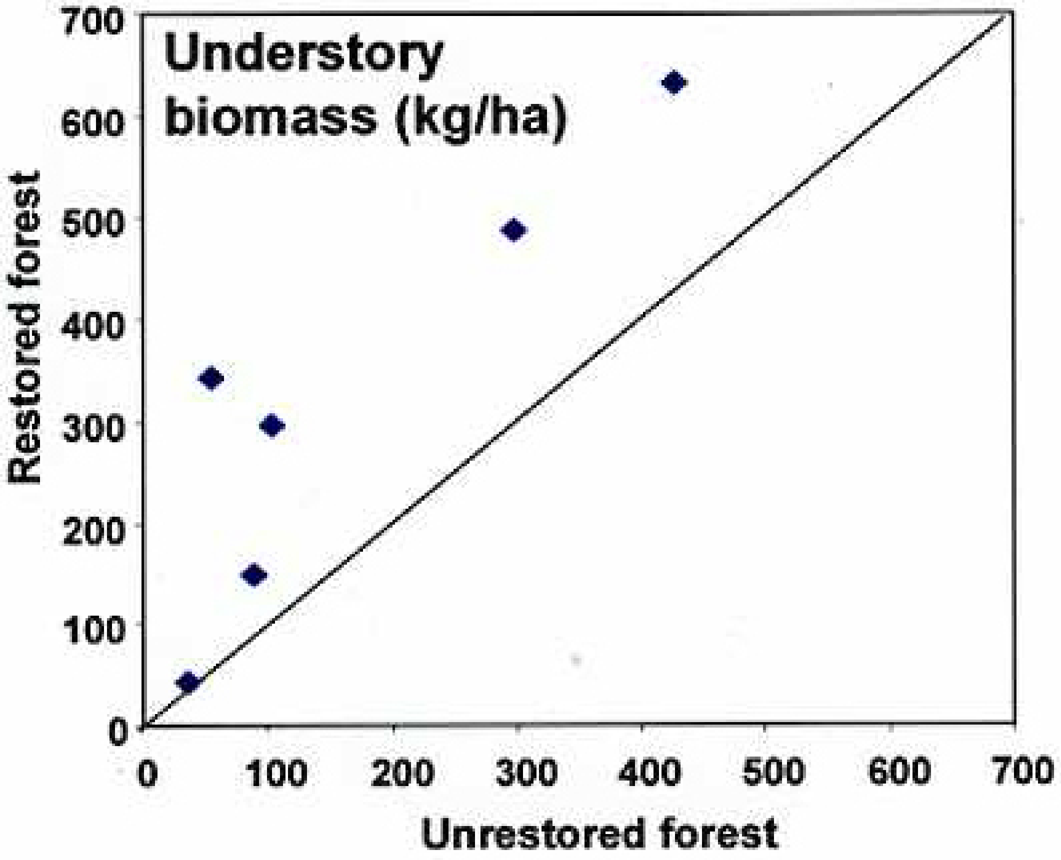

The amount of tree leaf area in a forest may have important effects on the supply of water in the soil that is available for both trees and understory vegetation. Precipitation falling on tree canopies may be intercepted, accumulating briefly on the needles before evaporating back to the atmosphere, never reaching the soil. Forests with high leaf area not only lose more precipitation from this interception loss, but they also have higher rates of water use by trees, with lower amounts of soil water available for use by understory plants. In wetter landscapes, changes in the amount of tree leaf area influence the amount of water reaching streams. For example, reducing tree cover in higher-elevation forests in the Rocky Mountains commonly increases stream flow by 15 to 30% (MacDonald and Stednick 2003). The amount of water flowing in streams in frequent-fire landscapes depends less on the density and size of trees (and canopies) than in wetter areas, because drier conditions mean that water not used by trees will be used by understory plants. Restoring old-growth structure to forests in frequent-fire landscapes may lead to increased streamflow during wet periods and, perhaps, to some recharge of subsurface aquifers.

Forest restoration treatments generally improve the water status of large trees, reducing water stress, and increasing the volume of resin in stems (Wallin et al. 2004, Zausen et al. 2005). Improved water status may enhance the overall vigor of trees, leading to lower rates of mortality from bark beetles and other insects and diseases.

Nutrient cycles in forests are influenced directly by fire, including losses (such as nitrogen converted to gas as biomass is consumed) and probably short term increases in availability of some nutrients (including nitrogen). In the longer run, differences between old-growth and non-old-growth conditions may derive from the indirect effects of changes in vegetation composition than from the direct, cumulative effects of fires (Hart et al. 2005a).

EVOLUTION AND ADAPTATION

The biotic processes in forests develop from interactions between genes, organisms, and environmental factors. The genetics of a forest include those of trees, understory plants, wildlife, and the unimaginably diverse organisms in the soil. Although the interactions among genes, organisms, and environmental factors in a ponderosa pine forest are beyond the scope of this article (and indeed, beyond human comprehension!), we provide a few examples to illustrate the complexity and resilience of this system.

Bark Beetles

Bark beetles are an important, natural component of many conifer ecosystems. Bark beetles (and their fungal symbionts) routinely kill small numbers of pine trees and, occasionally, extremely high beetle populations lead to massive pine mortality across very large areas. A number of factors—drought, lightning strikes, root pathogens, large fire scars, severe defoliation, tree senescence, excessive competition—make an individual old tree or stand more susceptible to bark beetle outbreaks. Recent thinning may also contribute to increased wind turbulence in a stand, leading to root damage and, perhaps, making individual trees susceptible to attack (Christiansen et al. 1987).

Coniferous trees have developed two main mechanisms to counter beetle attacks. First, they have a system of resin ducts in the phloem and xylem that can pitch-out invading beetles. Second, they have developed a hypersensitive reaction to invasion by microorganisms (including fungi, bacteria, and viruses) that enter the tree along with the beetles. A necrotic area, impregnated with resinous and phenolic compounds that prevent beetle gallery construction and fungal proliferation, then forms around the point of infection. This wound resin is highly toxic to beetle eggs and larvae and also inhibits fungal growth (Christiansen et al. 1987).

The ability of a large, old tree to resist an attack depends on its genetic makeup and physiological status (Franceschi et al. 2005). Independent of age, ponderosa pine trees grow slowly when stressed by competition. However, because most old trees are large in size and stature, they may have higher maintenance respiration demands because of the amount of living, non-photosynthetic tissue they maintain compared with younger trees (Skov et al. 2004). Another factor that may limit photosynthetic rate is that these large trees also tend to have more branch junctions and a longer root-leaf hydraulic path length that may decrease hydraulic conductance (Skov et al. 2004). Together, these factors may all contribute to slow growth of old ponderosa pine trees.

Bark beetles are only one of many potential threats to ponderosa pine trees, and the susceptibility to each threat differs among trees. For example, ponderosa pine trees may be attacked by bark beetles and infected by dwarf mistletoe (*Arceuthobium* spp.), but the success of each of these varies among individual ponderosa pines (Fig. 4). Trees that appear susceptible to beetles appear to be resistant to dwarf mistletoe, and vice versa. The continued survival, growth, and seed production of individual pine trees may depend in part on the local prevalence of parasites, which depends in turn on the local genotypes of pines and local environmental conditions.

Abert's Squirrels

Abert's squirrels (*Sciurus aberti*) are also highly dependent on ponderosa pine trees. Ponderosa pines provide them with places to live, nest, rest, and hide from predators as well as food in the form of bark, buds, flowers, and seeds (Hoffmeister 1986). Squirrels choose individual trees based on the (heritable) chemistry of tree phloem. As a result, different populations of Abert's squirrels are adapted to different populations of ponderosa pine (Snyder 1992, 1993; Snyder and Linhart 1994).

Fig. 4. Some ponderosa pine trees were heavily attacked by bark beetles, some heavily infected by dwarf mistletoe parasites, and some were unaffected—but no trees were heavily attacked by both bark beetles and dwarf mistletoe (after Linhart et al. 1994).

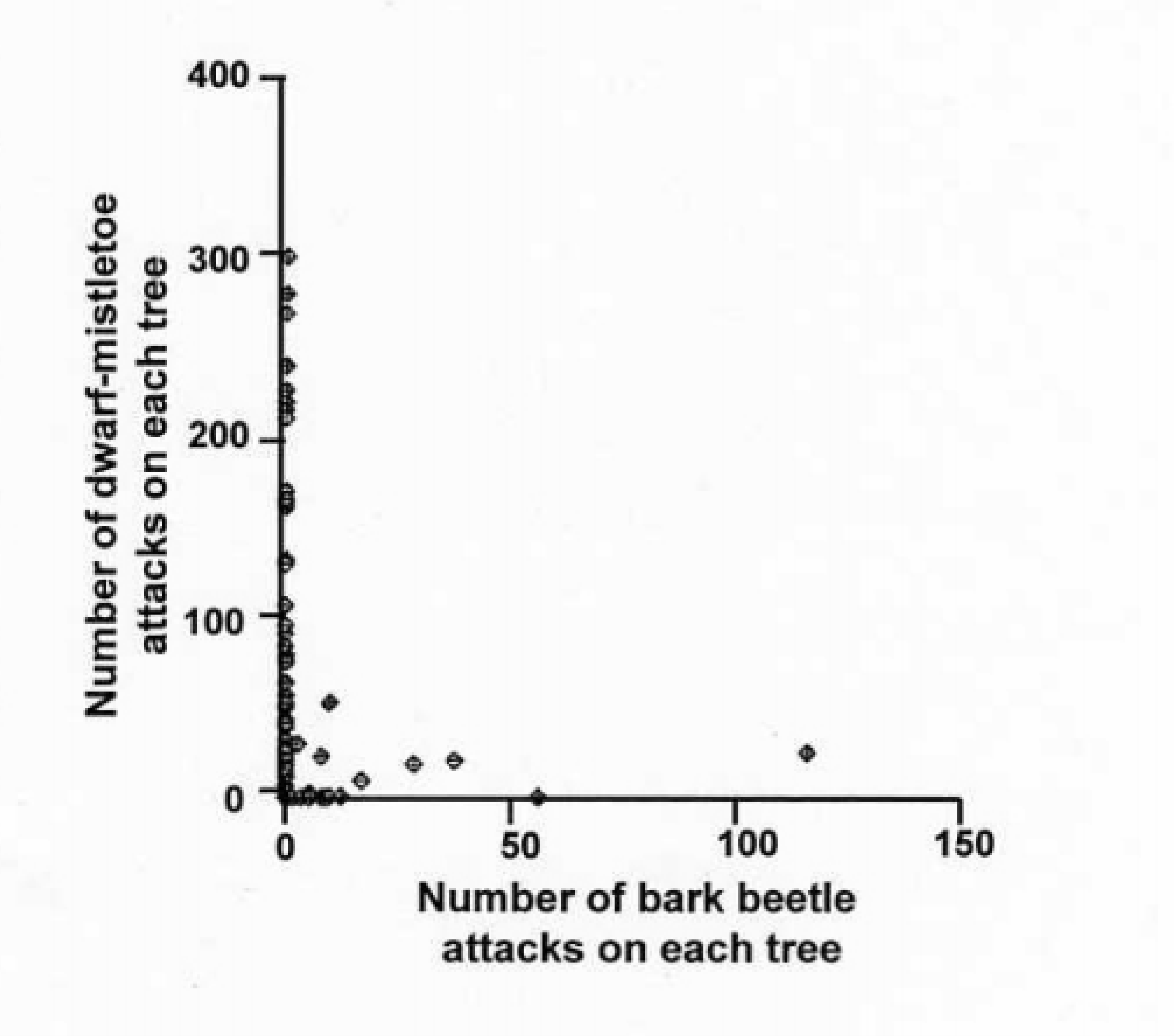

Yet another ecological interaction connects ponderosa pines and Abert's squirrels. Squirrels eat mycorrhizal fungi and help disperse it through their fecal pellets. Mycorrhizal fungi are very important to plant productivity, so if the fungi were rare, then squirrels could, perhaps, enhance forest productivity (Vireday 1982, Kotter and Farentinos 1984a, b).

Mooney and Linhart (2006) have recently developed an even more interwoven story about pines, growth, birds, ants, spiders, aphids, wasps, and dwarf mistletoe.

Genetics and Old Trees

The genotypes of pine trees are influenced by both selective pressures (Abert's squirrels, beetles, and dwarf mistletoes), and by the flow of genes in the neighborhood. The genes of paternal trees flood the local landscape as pollen drifts on the wind, but maternal genes disperse only as far as seeds can fall from a tree or be carried by animals (Latta et al. 1998). Old trees may be particularly important in a forest, as they have (by definition) survived centuries of changing environmental and biotic challenges. The presence of these trees in a landscape is critical for contributing both seeds and pollen to later generations of trees.

Resilience and Fire at the Landscape Scale

Just as individual trees have mechanisms that make them resistant to bark beetles and fire, a healthy, functioning forest will exhibit resilience on a large scale. Persistence, resilience, and resistance are all terms applied to the stability of an ecosystem (Holling 1973, Gunderson et al. 1995, Gunderson and Holling 2002). Ecosystem fragility is the opposite of stability and is expediently defined as "...the degree of change in species abundances and in species composition, following disturbance" (Nilsson and Grelsson 1995). Frequent-fire forests are highly stable in the long term, as long as fire is maintained in the system. However, they may be considered fragile in the short term following a fire. Moreover, many of these forests are now considered fragile in the long term, particularly following the catastrophic fires that result from long periods of fire suppression.

OLD-GROWTH FOREST COMPOSITION

Although processes are the driving forces behind any ecosystem, those processes are reflected and supported by the composition of the ecosystem, that is by the living and non-living entities that exist in the ecosystem. Old-growth forests, by definition, have old trees, but the presence of old trees is just the beginning of a description of the composition of an old-growth forest. The frequent return of fires provides the opportunity for a great range of plants, animals, and microbes to coexist in the same landscape.

Plant Composition and Structure

In frequent-fire landscapes, the diversity of plant species in the forest understory is much greater than the diversity of overstory species. Moreover, frequent fires strongly influence the composition of understory plant communities. The most striking feature of old-growth patches of ponderosa pine may be the towering "yellow-bellies"—the large diameter giants with the yellowish, fire-resistant bark. However, these forests are characterized as much by the understory that develops in the diverse range of habitat conditions: near clumps of big trees, in small openings between clumps, and in the open meadows between groups of large trees. Native perennial graminoids, including several species of fescue (*Festuca* spp.) and sedges (*Carex* spp.), dropseed (*Blepharoneuron tricholepsis*, *Sporobolus* spp.), Indian ricegrass (*Oryzopsis* spp.), and galleta (*Pleuraphis* spp.), as well as grazing-tolerant squirreltail and western wheatgrass (*Pascopyrum smithii*) and the ubiquitous grama grasses (*Bouteloua* spp.), form diverse understory communities that account for a large portion (more than half) of the net annual primary production in many old-growth ponderosa pine stands (Moore et al. 2004).

In addition to the native grasses, many annual and perennial forbs occur, usually as subdominants or rare components of the understory plant community. Native penstemon (*Penstemon* spp.), evening primrose (*Oenothera* spp.), and low growing sages (*Artemesia* spp.) are complemented by diverse composites that flower throughout the growing season. Fire-resilient or -adapted shrubs, such as kinnikinnick (*Arctostaphylos uva-ursi*) and serviceberry (*Amelanchier* spp.) in the Inland Northwest, and cliffrose (*Purshia* spp.) and ceanothus in the Southwest, are characteristic of open-growing, old-growth pine forests. In many Southwest locations, Gambel oak (*Quercus gambelii*), which can be found from a low-growing shrub to subdominant tree, is the second most abundant woody plant.

This heterogeneity in species composition and structural types is characteristic of most types of old-growth forests that develop in frequent-fire landscapes. Large overstory trees typically occur in scattered clumps of several to several dozen individuals sometimes in a dense matrix of younger trees, and other times intermixed with grassland openings of several acres. In terms of species composition, structural diversity, and ecological function, such old-growth forests contrast sharply with the dense stands that commonly develop when fires are suppressed. For example, Gambel oak and ceanothus are common shrubs in most Southwest ponderosa pine forests, but they typically are more common, and individual plants are larger and more developed, in open forests dominated by large pines. This diversity in the woody plant community has far-reaching implications, in part because these species support insect communities that are more diverse and abundant than those found in pure stands of ponderosa pine. Insect abundance, in turn, influences bird and bat populations, pollination rates, and the amount of wildlife forage. In this way, the composition and structural attributes of the ponderosa pine trees set the template for a potentially diverse plant community whose composition and function vary widely.

Animal Communities

Wildlife species respond in a host of ways to the structure of forests, and to boundaries between forests with different structures. Old-growth forests provide habitat for many wildlife species, but the critical habitat characteristics vary tremendously among species in both time and space. Some species are year-round residents, and others use old-growth forests only for breeding, wintering, or migration. Similarly, some species (e.g., pygmy nuthatch (*Sitta pygmaea*)) rely on specific old-growth structural components, such as large trees, whereas others (e. g., Abert's squirrel) need the structure of a whole patch of old-growth trees to facilitate their movements and provide food. Some species (e.g., northern goshawk (*Accipiter gentilis*)) require old growth forest conditions within an entire landscape matrix that contains non-old-growth forests to meet all their ecological needs.

Starting at the small end of the scale, standing dead trees (snags) and partially dead trees (living snags) are an important part of a living forest ecosystem (Waskiewicz 2003, Chambers and Mast 2005). Dozens of species of birds and bats rely on living and dead trees for habitat, and many of these species in turn may influence the success (or failure) of other organisms (e.g., defoliating caterpillars). Resource managers are commonly required to provide a minimum number of snags, but more recent insights have indicated snags alone may not be the key to providing habitat for species such as bats, nuthatches, and bluebirds because the longevity and number of dead snags is limited in frequent-fire forest. For instance, Saab et al. (2006) tested prescribed fire on more than 130 plots in the southwestern United States, and found an average loss of 35% of the downed wood and half of the standing snags (Saab et al. 2006). Boucher et al. (2000) pointed out that snags may not last long in frequent-fire forests because surface fires either ignite snags or topple them by burning the roots. The best long-term habitat may be provided by living snags, which are live trees with large dead limbs or tops. These living snags often develop after lightning strikes, beetle infestations, pathogen attack, or a combination of these factors.

Moving up to the scale of patches or stands, forest structure influences survival and population persistence of a variety of wildlife species. Very uniform spacing of trees, which is the typical result of traditional silvicultural thinning treatments, degrades habitats for Abert's squirrels (Dodd et al. 2003). Information on characteristics and sizes of patches needed by the squirrel and the spatial arrangement of these patches are necessary parts of silvicultural prescriptions that ensure viable populations of these squirrels. Similar silvicultural and management decisions are required for other old-growth-dependent species, including spotted owls (*Strix occidentalis*).

At the scale of entire landscapes, old-growth forests will likely be part of a landscape mosaic that includes forests that lack old-growth characteristics. These non-old-growth habitats (ranging from meadows to dense young stands to maturing second growth stands) might support some aspect of an animal species' needs. For example, northern goshawks are habitat generalists and their populations are often limited by the availability of food, which causes them to move between different habitat types. Reynolds et al. (1992) developed a landscape model of goshawk habitat that identifies a landscape-scale mosaic of six vegetation structural stages, which provide habitat for a suite of northern goshawk prey species. These vegetation structural stages range from grass-forb regeneration conditions to old-growth forest. Although northern goshawks need old-growth forests, particularly for nesting, they also benefit from a diverse mosaic across the landscape.

There are also symbiotic, co-evoluntionary relationships that animals have throughout old-growth forests. As noted in the discussion above about Abert's squirrels, there is almost no limit to the nature of interactions in forests, and we are far from having a clear understanding of which interactions have major, cascading effects. Some wildlife species are considered keystone species in that other species depend on them to provide necessary conditions. For example, populations of hairy woodpeckers (*Picoides villosus*) increase after fire, just as populations of beetles increase (Covert Bratland et al. 2006). In ponderosa pine forests in the Southwest, half of the species that nest in tree cavities cannot excavate cavities (secondary cavity nesting species), so hairy woodpeckers may be critical in supporting a diversity of animals. The feedback cycle turns yet again because, without fires, the population of hairy woodpeckers may be low, reducing the habitat opportunities for other species, further changing the complex forest ecosystem.

Management activities that move a forest away from old-growth conditions change the opportunities for many species. For example, Szaro and Balda (1979) compared four treatments with an uncut control plot that had some characteristics of old-growth forests. Pygmy nuthatches, red-faced warblers (*Cardellina rubrifrons*), hermit thrushes (*Catharus guttatus*), cordilleran flycatchers (*Empidonax occidentalis*), and violet-green swallows (*Tachycineta thalassina*) lost habitat with treatments that moved the forests away from old-growth forest conditions.

Grazing alters herbaceous plant composition and structure, affecting habitat for species such as Mogollon voles (*Microtus mogollonensis*) (Chambers and Doucett 2008). Using a stable-isotope approach, these scientists found that herbivorous voles rely on grass and herbs for food, and that C_3 plants (e.g., yarrow (*Achillea millefolium*), lupine (*Lupinus* spp.), fescue, mulleins (*Verbascum* spp.), snakeweed (*Gutierrezia* spp.)) were a more important food source than C_4 plants (e.g., species of muhly (*Muhlenbergia* spp.) and grama grasses). Excessive ungulate grazing and introduction of invasive plant species that lead to changes in plant species composition or reductions in C_3 plants in montane grasslands and forests would reduce habitat quality for Mogollon voles. Mogollon voles are also important food for the threatened Mexican spotted owl (*Strix occidentalis lucida*) (Ward 2001). Recent research indicates that vole populations are reduced in pine–oak forests as the result of past logging and grazing practices (Block et al. 2005).

As noted throughout this special issue, the loss of old-growth structure in frequent-fire landscapes commonly leads to uncharacteristically severe wildfires, which, in turn, benefit some animal species and harm others. Bock and Block (2005), for instance, compared the bird communities in unburned and moderately and severely burned forests. Three years after the fires, the unburned forest had 31 species in the breeding season and 26 in the non-breeding season. Both levels of burn intensity increased the diversity of birds, with more than 40 species of breeding birds and 33 species of non-breeders. Species groups that increased in response to fire included woodpeckers, flycatchers, and thrushes.

Restoration treatments that move forests toward old-growth structure and composition appear to be effective in restoring bird habitat. Germaine and Germaine (2002) found that the fledgling rate (i.e., number of young to leave the nest) for western bluebirds (*Sialia mexicana*) in restored stands was 1.6 times greater than in dense, untreated stands. Converse et al. (2006a, b) evaluated effects of fuel reduction treatments on small mammals and found that total biomass and population sizes of small mammals generally increased following thinning and fire. The most thorough assessments of post restoration animal responses come from landscape scale treatments near Mt. Trumball in the Grand Canyon–Parashant National Monument in northern Arizona (Covington et al. 2005). Various aspects of wildlife habitat and populations were examined for up to 9 years, and demonstrated that restoring old growth forest structure generally favored species or had much lower negative effects than stand replacing fire. Mule deer (*Odocoileus hemionus*) tended to use restored portions of the landscape at night, although they used restored and control areas about equally during the day. Abert's squirrel populations declined in response to the lower density of pine trees, but the squirrels did continue living in trees in the restored areas. Breeding pairs of northern goshawks were found in control and restored areas, and fledglings were successful in both forest types. The densities of butterflies doubled in restored areas.

Microbial Communities

Given that microbial interactions and processes are the foundation of much of the forest ecosystem, surprisingly little is known about the differences in microbial communities between old-growth forests and post-fire-cessation forests. The two microbial communities that we know the most about are wood decaying fungi and mycorrhizal fungi.

A number of wood-decaying fungi infect primarily old trees, roots, and large branches. Several species of wood-decaying fungi found in unmanaged older forests are rare in younger stands (Romme et al. 1992). Aging trees tend to become increasingly vulnerable to wood-decaying fungi because fungi can enter through dead branch stubs, knots, broken tops, fire scars, and wounds such as those caused by bark beetles or woodpeckers (Farris et al. 2004). In addition to the vital role these pathogens play in the carbon cycle and in recycling nutrients for plants, they also create valuable habitat for numerous wildlife species (Marcot 2002).

Mycorrhizal fungi form symbiotic associations with tree roots, providing water and nutrients to roots in exchange for sugar. Experiments by various researchers have shown that fire may substantially affect these fungal associations, particularly near the soil surface. For example, a study by Pattinson et al. (1999) that simulated the effect of fire showed a decline in numbers of mycorrhizal propagules and a reduction in the hyphal network (the tiny, networked strands of fungus). Korb et al. (2003) found a rapid increase in arbuscular mycorrhizae following restoration treatments in northern Arizona, whereas Smith et al. (2005) reported a short-term reduction in ectomycorrhizal fungi (EMF) following prescribed fire in Oregon.

Researchers have also studied the effects of seasonal burning on the mycorrhizal community. Smith et al. (2004) detected that fall burning in dry ponderosa pine stands significantly reduced duff depth, live root biomass, and EMF species richness compared with spring burning. The probability of mature tree mortality was also greater after fall burning. Meyer et al. (2005) found that burning reduced litter depth and log volume as well as the frequency, biomass, and species richness of mycorrhizal truffles in an area of the Sierra Nevada. The authors posit that decaying woody debris forms an important reservoir of moisture and nutrients, especially in dry forests, for fruiting fungi. It also appears that mycorrhizal fungi are more likely to survive when the duff layer is thin or moist.

Hart et al. (2005a) report that repeated burning (every 2 years during a 20-year period) reduced fine root length, fine root biomass, and mycorrhizal root biomass, as well as the amount of nitrogen and phosphorous stored in the belowground pools. The authors speculate that the change in these pools most likely occurred during the first few prescribed burns when the fuel loads and fire intensities would have been highest. Their results suggest that such frequent burning may have negative long-term effects on belowground biomass pools and nutrient cycling. They also postulate that these negative effects may be avoided by mechanically removing some of the accumulated fuel before prescribed burning.

Despite these descriptive studies and experiments, we essentially know very little about the critical changes that may (or may not) follow the loss of old-growth characteristics in a forest. A recent study (Hart et al. 2005b) found that a fire following a long, fire-free period reduced the diversity of the bacterial community by more than half, yet more than doubled the diversity of the fungal community. We do not know if these dramatic changes have important cascading effects in the forest.

HUMAN VALUES

Although this is covered in more depth by other authors in this special issue, we also want to say that old-growth forests in frequent-fire landscapes provide a host of human values that go beyond the list of species present, or economic and ecological functions. For instance, old-growth forests carry a legacy of information from earlier times. They can tell us a great deal about how climates have varied in past epochs, and how the forests (and fires) responded. Without the information held in tree rings, we would not know how the landscapes of the southwestern United States were influenced by patterns of El Niño/Southern Oscillation precipitation (Grissino-Mayer and Swetnam 2000) or to what degree the rise and fall of dryland civilizations related (or not) to climate (Dean 1988). We also recognize that many people see an inherent beauty in old-growth forests (Huckaby et al. 2003), and find personal sustenance from these “wilderness” or wild landscapes.

KNOWLEDGE GAPS

All forests are complicated ecosystems, making the potential list of gaps in our knowledge almost unbounded. Nevertheless, we can identify several key areas where studies and experiments are needed to fill major gaps that hinder restoration efforts of old growth in the frequent-fire forests of the American West.

Ability of Understory Vegetation to Respond to Restoration Treatments

How well can we recover the historical understory (and related animal habitat features) that characterized old-growth conditions? The absence of fire for a century has been coupled in many forests with a host of other land-use impacts, including intensive livestock grazing and logging. Long-term plots from northern Arizona have shown not only declines in total understory production and species diversity, but also shifts among vegetation types (such as greater losses of C_4 grasses than C_3 grasses). How well can the understory recover its former productivity and species composition in response to thinning or thinning plus fire? Does the season and/ or frequency of burning have an effect on the understory? Will adding native seed from nearby areas be critical? How did use by Native Americans affect the understory of pre-European-settlement, old-growth forest understories? More experiments across a variety of landscape conditions are needed to answer these and other questions related to understory vegetation.

Ability of Frequent-fire Forests to Recover Following Catastrophic Wildfires

How does ecosystem recovery progress after severe wildfires that exceed the historical range of fire behavior in frequent-fire landscapes? We expect that recovery will be slow, but will recovery eventually occur or will the forests be converted to other vegetation types (grasslands or shrublands)? What restoration treatments would be most effective for recovering natural forest composition, structure, and function after large, severe fires? Which treatments can move forests toward old-growth conditions and also reduce risks of severe fires?

Ability to Extrapolate Knowledge of Certain Forests to Other Places and Forest Types

Much of our knowledge about old-growth conditions in frequent-fire landscapes comes from a very limited range of forest types, and detailed information comes from an even more restricted set of intensive study sites. How representative are the ponderosa pine landscapes of northern Arizona for ponderosa pine in other areas? How different are dry mixed-conifer forests from ponderosa pine forests, and how do they vary with landscape position locally and throughout the West? We have a good general understanding the key questions and the important processes, but restoration of old growth conditions in any local forest will depend on locally appropriate details.

The Uncertainty of Climate Change and its Effects on Forested Ecosystems

Climates have changed dramatically in the past 10 000 years, and the 21st century will likely differ from the 19th century. What do we need to know to foster old-growth forest conditions under various climate scenarios? If managers can only afford to restore a portion of a landscape (which is almost always the case), should restoration focus on lower-elevation sites (with the risk that climate changes would shift the ecotone upward)? This knowledge gap will probably not be filled by data collection or experimentation, but the potential effects of climate change need to be kept in mind.

Responses to this article can be read online at:
http://www.ecologyandsociety.org/vol12/iss2/art18/responses/

LITERATURE CITED

Abella, S. R. 2004. Tree thinning and prescribed burning effects on ground flora in Arizona ponderosa pine forests: a review. *Journal of the Arizona-Nevada Academy of Science* **36**:68–76.

Allen, C. D., M. Savage, D. A. Falk, K. F. Suckling, T. W. Swetnam, T. Schulke, P. B. Stacey, P. Morgan, M. Hoffman, and J. T. Klingel. 2002. Ecological restoration of southwestern ponderosa pine ecosystems: a broad perspective. *Ecological Applications* **12**:1418–1433.

Arno, S. F. 1980. Forest fire history in the northern Rockies. *Journal of Forestry* **78**:460–465.

Arno, S. F., and C. E. Fiedler. 2005. *Mimicking nature's fire: restoring fire-prone forests in the West.* Island Press, Washington, D.C., USA.

Arno, S. F., J. Scott, and M. Hartwell. 1995. *Age class structure of old growth ponderosa pine/ Douglas-fir stands and its relationship to fire history.* U.S. Forest Service Research Paper **481**.

Bailey, J. D., and W. W. Covington. 2002. Evaluating ponderosa pine regeneration rates following ecological restoration treatments in northern Arizona, USA. *Forest Ecology and Management* **155**:271–278.

Block, W. M., J. L. Ganey, P. E. Scott, and R. King. 2005. Prey ecology of Mexican spotted owls in pine-oak forests of northern Arizona. *Journal of Wildlife Management* **69**:618–629.

Bock, C. E., and W. M. Block. 2005. Response of birds to fire in the American southwest. Pages 1093– 1099 *in* C. J. Ralph and T. D. Rich, editors. *Bird conservation implementation and integration in the Americas: Proceedings of the third international Partners in Flight conference. Volume 2.* U.S. Forest Service General Technical Report **PSW-GTR-191**.

Boucher, P. F., W. M. Block, G. V. Benavidez, and L. W. Wiebe. 2000. Implementing the expanded prescribed fire program on the Gila National Forest, New Mexico: implications for snag management. *Proceedings of the Tall Timbers Fire Ecology Conference* **21**:104–113.

Chambers, C. L., and R. R. Doucett. 2008. Diet of the Mogollon vole as indicated by stable isotope analysis (13 C and 15 N). *Western North American Naturalist* (In press).

Chambers, C. L., and J. N. Mast. 2005. Ponderosa pine snag dynamics and cavity excavation following wildfire in northern Arizona. *Forest Ecology and Management* **216**:227–240.

Christiansen, E., R. H. Waring, and A. A. Berryman. 1987. Resistance of conifers to bark beetle attack: searching for general relationships. *Forest Ecology and Management* **22**:89–106.

Converse, S. J., W. M. Block, and D. C. White. 2006a. Small mammal population and habitat responses to forest thinning and prescribed fire.

Forest Ecology and Management **228**:263–273.

Converse, S. J., G. C. White, and W. M. Block. 2006b. Small mammal response to thinning and wildfire in ponderosa pine-dominated forests of the southwestern USA. *Journal of Wildlife Management* **70**(6):1711–1722.

Covert-Bratland, K. A., W. M. Block, and T. Theimer. 2006. Hairy woodpecker winter ecology in ponderosa pine forests representing different ages since wildfire. *Journal of Wildlife Management* **70** (5):1379–1392.

Covington, W. W., D. Vosick, and K. A. Lowe. 2005. *Southwest fire initiative final report.* Submitted to the Bureau of Land Management by the Ecological Restoration Institute, Flagstaff, Arizona, USA.

Dean, J. S. 1988. Dendrochronology and paleoenvironmental reconstruction on the Colorado Plateaus. Pages 119–167 *in* G.J. Gumerman, editor. *The Anasazi in a changing environment.* School of American Research Book, Cambridge University Press, New York, New York, USA.

Dodd, N. L., J. S. States, and S. S. Rosenstock. 2003. Tassel-eared squirrel population, habitat condition, and dietary relationships in north-central Arizona. *Journal of Wildlife Management* **67**:622– 633.

Egan, D. and E. A. Howell, editors. 2001. *The historical ecology handbook: a restorationist's guide to reference ecosystems.* Island Press, Washington, D.C., USA.

Everett, R. L., R. Schellhaas, D. Keenum, D. Spurbeck, and P. Ohlson. 2000. Fire history in the ponderosa pine/Douglas-fir forests on the east slope of the Washington Cascades. *Fire Ecology and Management* **129**:207–225.

Farris, K. L., M. J. Huss, and S. Zack. 2004. The role of foraging woodpeckers in the decomposition of ponderosa pine snags. *The Condor* **106**:50–59.

Franceschi, V. R., P. Krokene, E. Christiansen, and T. Krekling. 2005. Anatomical and chemical defenses of conifer bark against bark beetles and other pests. *The New Phytologist* **167**:353–376.

Friederici, P., editor. 2003. *Ecological restoration of southwestern ponderosa pine forests.* Island Press, Washington, D.C., USA.

Fulé, P. Z., W. W. Covington, H. B. Smith, J. D. Springer, T. A. Heinlein, K. D. Huisinga, and M. M. Moore. 2002. Comparing ecological restoration alternatives at Grand Canyon, Arizona. *Forest Ecology and Management* **170**:19–41.

Fulé, P. Z., W. W. Covington, M. T. Stoddard, and D. Bertolette. 2006. Minimal impact restoration treatments have limited effects on forest structure and fuels at Grand Canyon, USA. *Restoration Ecology* **14**(3):357–368.

Fulé, P. Z., J. Villanueva-Díaz, and M. Ramos Gómez. 2005. Fire regime in a conservation reserve in Chihuahua, Mexico. *Canadian Journal of Forest Research* **35**:320–330.

Germaine, H. L., and S. S. Germaine. 2002. Forest restoration treatment effects on the nesting success of western bluebirds. *Restoration Ecology* **10**:362– 367.

Gildar, C. N., P. Z. Fulé, and W. W. Covington. 2004. Plant community variability in ponderosa pine forest has implications for reference conditions. *Natural Areas Journal* **24**(2):101–111.

Grissino-Mayer, H. D., and T. W. Swetnam. 2000. Century-scale climate forcing of fire regimes in the American Southwest. *Holocene* **10**:213–220.

Gunderson, L., and C. S. Holling, editors. 2002. *Panarchy: understanding transformations in human and natural systems.* Island Press, Washington, D. C, USA.

Gunderson, L., C. S. Holling, and S. Light, editors. 1995. *Barriers and bridges to the renewal of ecosystems and institutions.* Columbia University Press, New York, New York, USA.

Hart, S. C., A. T. Classen, and R. J. Wright. 2005a. Long-term interval burning alters fine root and mycorrhizal dynamics in a ponderosa pine forest. *Journal of Applied Ecology* **42**:752–761.

Hart, S. C., T. H. DeLuca, G. S. Newman, M. D. MacKenzie, and S. I. Boyle. 2005b. Post-fire vegetative dynamics as drivers of microbial community structure and function in forest soils. *Forest Ecology and Management* **220**:166–184.

Hoffmeister, D. F. 1986. *Mammals of Arizona.* University of Arizona Press and Arizona Game and Fish Department, Tucson and Phoenix, Arizona, USA.

Holling, C. S. 1973. Resilience and stability of ecological systems. *Annual Review of Ecology and Systematics* **4**:1–23.

Huckaby, L. S., M. R. Kaufmann, P. J. Fornwalt, J. M. Stoker, and C. Dennis. 2003. Identification and ecology of old ponderosa pine trees in the Colorado Front Range. U.S. Forest Service General Technical Report **RMRS-GTR-110**.

Kaufmann, M. R., T. T. Veblen, and W. H. Romme. 2006. *Historical fire regimes in ponderosa pine forests of the Colorado Front Range, and recommendations for ecological restoration and fuels management.* Colorado Forest Restoration Institute, Colorado State University, and The Nature Conservancy, Fort Collins, Colorado, USA.

Keeley, J. E., and N. L. Stephenson. 2000. Restoring natural fire regimes to the Sierra Nevada in an era of global change. Pages 255–265 *in* D. N. Cole, S. F. McCool, W. T. Borrie, and J. O'Loughlin, compilers. *Wilderness science in a time of change conference–Volume 5: Wilderness ecosystems, threats, and management.* U.S. Forest Service Proceedings **RMRS-P-15-VOL-5**.

Korb, J. E., N. C. Johnson, and W. W. Covington. 2003. Arbuscular mycorrhizal propagule densities respond rapidly to ponderosa pine restoration treatments. *Journal of Applied Ecology* **40**:101– 110.

Kotter, M. M., and R. C. Farentinos. 1984a. Formation of ponderosa pine ectomychorrhizae after inoculation with feces of tassel-eared squirrels. *Mycologia* **76**:758–760.

———. 1984b. Tassel-eared squirrels as spore dispersal agents of hypogeous mycorrhizal fungi. *Journal of Mammalogy* **65**:684–667.

Landres, P. B., P. M. Morgan, and F. J. Swanson. 1999. Overview of the use of natural variability concepts in managing ecological systems. *Ecological Applications* **9**(4):1179–1188.

Latta, R. G., Y. B. Linhart, D. Fleck, and M. Elliot. 1998. Direct and indirect estimates of seed versus pollen movement within a population of ponderosa pine. *Evolution* **52**:61–67.

Laughlin, D. C., J. D. Bakker, and P. Z. Fulé. 2005. Understory plant community structure in lower montane and subalpine forests, Grand Canyon National Park, USA. *Journal of Biogeography* **32**:2083–2102.

Laughlin, D. C., and J. B. Grace. 2006. A multivariate model of plant species richness in forested systems: old-growth montane forests with a long history of fire. *Oikos* **114**:60–70.

Leopold, A. 1920. Piute forestry vs. forest fire prevention. *Southwestern Magazine* **2**:12–13. (Reprinted as: Paiute forestry. 1990. Pages 139–142 *in* D.E. Brown and N.B. Carmony, editors. *Aldo Leopold's southwest.* University of New Mexico Press, Albuquerque, New Mexico, USA.

Long, J. N., and F. W. Smith. 2000. Restructuring the forest: goshawks and the restoration of southwestern ponderosa pine. *Journal of Forestry* **98**:25–30.

MacDonald, L. H., and J. D. Stednick. 2003. *Forests and water: a state-of-the-art review for Colorado.* Colorado Water Resources Research Institute Report No. **196**.

Marcot, B. G. 2002. An ecological functional basis for managing decaying wood for wildlife. Pages 895–910 *in* W. F. Laudenslayer, Jr., P. J. Shea, B. E. Valentine, C. P. Weatherspoon, and T. E. Lisle, editors. *Proceedings of the symposium on the ecology and management of dead wood in western forests.* U.S. Forest Service General Technical Report **PSW-GTR-181**.

Metlen, K. L., and C. E. Fiedler. 2006. Restoration treatment effects on understory of ponderosa pine/ Douglas-fir forests in western Montana. *Forest Ecology and Management* **222**:355–369.

Meyer, M. D., M. P. North, and D. A. Kelt. 2005. Short-term effects of fire and forest thinning on truffle abundance and consumption by *Neotamias speciosus* in the Sierra Nevada of California. *Canadian Journal of Forest Research* **35**:1061– 1070.

Mooney, K. A., and Y. B. Linhart. 2006. Contrasting cascades: insectivorous birds increase pine but not parasitic mistletoe growth. *Journal of Animal Ecology* **75**:350–357.

Moore, M. M., C. A. Casey, J. D. Bakker, J. D. Springer, P. Z. Fulé, W. W. Covington, and D. C. Laughlin. 2006. Herbaceous vegetation responses (1992–2004) to restoration treatments in a ponderosa pine forest. *Rangeland Ecology and Management* **59**:135–144.

Moore, M. M., W. W. Covington, and P. Z. Fulé. 1999. Reference conditions and ecological restoration: a southwestern ponderosa pine perspective. *Ecological Applications* **9**(4):1266–1277.

Moore, M. M., D. W. Huffman, P. Z. Fulé, W. W. Covington, and J. E. Crouse. 2004. Comparison of historical and contemporary forest structure and composition of permanent plots in southwestern ponderosa pine forests. *Forest Science* **50**:162–176.

Morgan, T. A., C. E. Fiedler, and C. W. Woodall. 2002. Characteristics of dry site old-growth ponderosa pine in the Bull Mountains of Montana, USA. *Natural Areas Journal* **22**(1):11–19.

Nilsson, C., and G. Grelsson. 1995. The fragility of ecosystems: a review. *Journal of Applied Ecology* **32**: 677–692.

Pattinson, G. S., K. A. Hammill, B. G. Sutton, and P. A. McGee. 1999. Simulated fire reduces the density of arbuscular mycorrhizal fungi at the soil surface. *Mycological Research* **103**(4):491–496.

Reynolds, R. T., T. G. Russel, M. H. Reiser, R. L. Bassett, P. L. Kennedy, D. A. Boyce, Jr., G. Goodwin, R. Smith, and E. L. Fisher. 1992. *Management recommendations for the northern goshawk in the southwestern United States.* U.S. Forest Service General Technical Report **RM-217**.

Romme, W. H., D. W. Jamieson, J. S. Redder, G. Bigsby, J. P. Lindsey, D. Kendall, R. Cowen, T. Kreykes, A. W. Spencer, and J. C. Ortega. 1992. Old-growth forests of the San Juan National Forest in southwestern Colorado. Pages 154–165 *in* M. R. Kaufmann, W. H. Moir, and R. L. Bassett, editors. *Old-growth forests in the southwest and Rocky Mountain regions: Proceedings of a workshop.* U. S. Forest Service General Technical Report **RM-213**.

Saab, V., L. Bate, J. Lehmkuhl, B. Dickson, S. Story, S. Jentsch, and W. Block. 2006. Changes in downed wood and forest structure after prescribed fire in ponderosa pine forests. U.S. Forest Service Proceedings **RMRS-P-41**.

Skov, K. R., T. E. Kolb, and K. F. Wallin. 2004. Tree size and drought affect ponderosa pine physiological response to thinning and burning treatments. *Forest Science* **50**(1):81–91.

Smith, J. E., D. McKay, G. Brenner, J. McIvers, and J. W. Spatafora. 2005. Early impacts of forest restoration treatments on the ectomycorrhizal fungal community and fine root biomass in a mixed conifer forest. *Journal of Applied Ecology* **42**:526– 535.

Smith, J. E., D. McKay, C. G. Niwa, W. G. Thies, G. Brenner, and J. W. Spatafora. 2004. Short-term effects of seasonal prescribed burning on the ectomycorrhizal fungal community and fine root biomass in ponderosa pine stands in the Blue Mountains of Oregon. *Canadian Journal of Forest Research* **34**:2477–2491.

Snyder, M. A. 1992. Selective herbivory by Abert's squirrel mediated by chemical variability in ponderosa pine. *Ecology* **73**:1730–1741.

———. 1993. Interactions between Abert's squirrel and ponderosa pine: the relationship between selective herbivory and host plant fitness. *American Naturalist* **141**:866–879.

Snyder, M. A., and Y. B. Linhart. 1994. Nest-site selection by Abert's squirrel: chemical characteristics of nest trees. *Journal of Mammalogy* **75**:136–141.

Stephenson, N. L. 1999. Reference conditions for giant sequoia forest restoration: structure, process, and precision. *Ecological Applications* **9**:1253–1265.

Swetnam, T. W, C. D. Allen, and J. L. Betancourt. 1999. Applied historical ecology: using the past to manage for the future. *Ecological Applications* **9** (4):1189–1206.

Szaro, R. C., and R. P. Balda. 1979. Bird community dynamics in a ponderosa pine forest. *Studies in Avian Biology* **3.**

van Mantgem, P., and M. Schwartz. 2003. Bark heat resistance of small trees in Californian mixed conifer forests: testing some model assumptions. *Forest Ecology and Management* **178**: 341–352.

Veblen, T. T., T. Kitzberger, and J. Donnegan. 2000. Climatic and human influences on fire regimes in ponderosa pine forests in the Colorado Front Range. *Ecological Applications* **10**(4):1178– 1195.

Vireday, C. C. 1982. *Mycophagy in tassel-eared squirrels (*Sciurus aberti aberti *and* S. a. kaibabensis*) in northern Arizona.* Thesis. Northern Arizona University, Flagstaff, Arizona, USA.

Wallin, K. F., T. E. Kolb, K. R. Skov, and M. R. Wagner. 2004. Seven-year results of thinning and burning restoration treatments on old growth ponderosa pines at the Gus Pearson Natural Area. *Restoration Ecology* **12**:239–247.

Ward, J. P., Jr. 2001. *Ecological responses by Mexican spotted owls to environmental variation in the Sacramento Mountains, New Mexico.* Dissertation. Colorado State University, Fort Collins, Colorado, USA.

Waskiewicz, J.D. 2003. *Snags and partial snags in managed, relict, and restored ponderosa pine forests of the Southwest.* Thesis. Northern Arizona University, Flagstaff, Arizona, USA .

Youngblood, A., T. Max, and K. Coe. 2004. Stand structure in eastside old-growth ponderosa pine forests of Oregon and northern California. *Forest Ecology and Management* **228**:191–217.

Zausen, G. L, T. E. Kolb, J. D. Bailey, and M. R. Wagner. 2005. Long-term impacts of stand management on ponderosa pine physiology and bark beetle abundance in northern Arizona: a replicated landscape study. *Forest Ecology and Management* **218**:291–305.

Zier, J. L., and W. L. Baker. 2006. A century of vegetation change in the San Juan Mountains, Colorado: an analysis using repeat photography. *Forest Ecology and Management* **228**:251–262.

EXHIBIT C

Mixed-severity wildfire and habitat of an old-forest obligate

Damon B. Lesmeister,[1,2,]! Stan G. Sovern,[2] Raymond J. Davis,[3] David M. Bell,[1]
Matthew J. Gregory,[4] and Jody C. Vogeler[4,5]

[1]USDA Forest Service, Pacific Northwest Research Station, Corvallis, Oregon 97331 USA
[2]Department of Fisheries and Wildlife, Oregon State University, Corvallis, Oregon 97331 USA
[3]USDA Forest Service, Pacific Northwest Region, Corvallis, Oregon 97331 USA
[4]Department of Forest Ecosystems and Society, Oregon State University, Corvallis, Oregon 97331 USA
[5]Natural Resources Ecology Lab, Colorado State University, Fort Collins, Colorado 80523 USA

Citation: Lesmeister, D. B., S. G. Sovern, R. J. Davis, D. M. Bell, M. J. Gregory, and J. C. Vogeler. 2019. Mixed-severity wildfire and habitat of an old-forest obligate. Ecosphere 10(4):e02696. 10.1002/ecs2.2696

Abstract. The frequency, extent, and severity of wildfire strongly influence the structure and function of ecosystems. Mixed-severity fire regimes are the most complex and least understood fire regimes, and variability of fire severity can occur at fine spatial and temporal scales, depending on previous disturbance history, topography, fuel continuity, vegetation type, and weather. During high fire weather in 2013, a complex of mixed-severity wildfires burned across multiple ownerships within the Klamath-Siskiyou ecoregion of southwestern Oregon where northern spotted owl (Strix occidentalis caurina) demographics were studied since 1990. A year prior to these wildfires, high-resolution, remotely sensed forest structural information derived from light detection and ranging (lidar) data was acquired for an area that fully covered the extent of these fires. To quantify wildfire impact on northern spotted owl nesting/roosting habitat, we fit a relative habitat suitability model based on pre-fire locations used for nesting and roosting, and forest structure variables developed from 2012 lidar data. Our pre-fire habitat suitability model predicted nesting/roosting locations well, and variable response functions followed known resource selection patterns. These forests had typical characteristics of old-growth forest, with high density of large live trees, high canopy cover, and complex structure in canopy height. We projected the pre-fire model onto lidar data collected two months post-fire to produce a post-fire suitability map, which indicated that >93% of pre-fire habitat that burned at high severity was no longer suitable forest for nesting and roosting. We also quantified the probability that pre-fire nesting/roosting habitat would burn at each severity class (unburned/low, low, moderate, high). Pre-fire nesting/roosting habitat had lower probability of burning at moderate or high severity compared to other forest types under high burning conditions. Our results indicate that northern spotted owl habitat can buffer the negative effects of climate change by enhancing biodiversity and resistance to high-severity fires, which are predicted to increase in frequency and extent with climate change. Within this region, protecting large blocks of old forests could be an integral component of management plans that successfully maintain variability of forests in this mixed-ownership and mixed severity fire regime landscape and enhance conservation of many species.

Key words: forest structure; habitat; lidar; mixed-severity fire regime; northern spotted owl; old forest; pre-fire vegetation condition; Strix occidentalis caurina.

Received 20 September 2018; revised 6 December 2018; accepted 12 March 2019. Corresponding Editor: Joseph A. LaManna.

E-mail: dlesmeister@fs.fed.us

INTRODUCTION

Climate and land-use patterns are strong predictors of disturbance regimes that ultimately influence the structure and function of an ecosystem (Sousa 1984). Globally, forest ecosystems are at risk of large disturbance regime shifts (frequency and severity) and ultimately a range of possible alternative stable states due to climate change-induced drought and heat stress, and associated interactions with insect disease outbreaks and wildfire (Dale et al. 2001, Allen et al. 2010, Kitzberger et al. 2012). In the case of fire regimes, their frequency and severity are typically negatively correlated, such that frequent fires are of lower severity, and strongly influence community dynamics and successional pathways (Agee 2005). Fire regimes play a key role in species adaptations as well as community structure and distribution of ecosystems, including the availability of several key components of wildlife habitat (Bunnell 1995, Noss et al. 2006, Pausas and Keeley 2009). Persistence of native wildlife species that are adapted to historical fire regimes may be at risk given climate change and land management practices that alter patterns in fire frequency and intensity relative to historical patterns. For example, in many dry forests the extent of areas impacted by high-severity fire is increasing, with concern for sensitive wildlife species that rely on forest types altered by fire (Westerling et al. 2006, Miller et al. 2008, Miller and Safford 2012, Reilly et al. 2017, Rockweit et al. 2017).

The fire regime of an ecosystem is defined as the natural patterns of wildfire in a given area including fire frequency, seasonality, extent, severity, and synergistic effects with other disturbances (Agee 1993, Halofsky et al. 2011). Forest successional theory suggests that in most areas, the interval length between disturbances should influence outcomes of succession, such that early-seral stands, low stature, and open micro climates are common in ecosystems with short interval fires, whereas those with long-interval fires generally are dominated by mature forests with relatively closed canopies (Donato et al. 2009, Halofsky et al. 2011). Low-severity regimes are most often associated with dry forest types which experience frequent and predominantly low-severity fires where loss of biomass due to fire is low, and <30% mortality of trees is typical (Agee 1993). This disturbance regime results in stands with open canopies and an understory dominated by sprouting and rhizomatous shrubs and herbaceous plants, which are described in historical accounts as open, parklike forests (Agee 2013). The extent of these forest types was often overrepresented in historical records due to the ease of traveling through them and the opportunities for pleasing photographs (Van Pelt 2008). In truth, these open, parklike forest conditions do not represent many forests in western North America (Odion et al. 2014). Forests in high-severity fire regimes experience infrequent (>200-yr return intervals) but high-severity fires. Large patches of total mortality occur within the fire events and overall mortality is high (>70%), though areas of low- and moderate-severity fire are also common (Agee 1993, Turner and Romme 1994). In western North America, these forest types associated with high-severity fire regimes are characteristic of high-elevation, lodgepole pine (Pinus contorta)-dominated stands, some spruce (Picea spp.)-dominated forests, and moist Douglas-fir (Pseudotsuga menziesii)/western hemlock (Tsuga heterophylla) forests of the Pacific Northwest (Agee 1993).

Within mixed-severity fires, 30–70% tree mortality is common; however, the mixed-severity regime is not simply intermediate between low and high-severity fire regimes (Agee 1993, Perry et al. 2011). The resulting pattern of low-, moderate-, and high-severity fire patches within a given area is highly variable and difficult to predict (Agee 2005), although at a large enough spatial scale (e.g., watersheds), nearly all fires are mixed-severity (Turner and Romme 1994, Baker et al. 2007, Halofsky et al. 2011). This variability can occur at fine spatial and temporal scales dependent on previous fire history, topography, fuel continuity, vegetation type, and weather (Heyerdahl et al. 2001, Donato et al. 2009, Thompson and Spies 2009, Krawchuk et al. 2016). Because of the spatiotemporal variability across the landscape, mixed-severity fire regimes are the most complex and least understood fire regimes, unique in terms of patch metrics and the life history attributes of native species (Schoennagel et al. 2004, Agee 2005, Halofsky et al. 2011). Fire histories in mixed-severity regimes, in particular, are difficult to determine because most fire history techniques have been developed to study either the low- or high severity extremes in fire regimes (Agee 2005). Short-interval severe fires are an important characteristic of mixed-severity fire regimes and are typically considered extreme events and expected to be deleterious to forest succession and diversity (Donato et al. 2009). However, many native plants within these forests possess functional traits (e.g., persistent seed banks, vegetative sprouting, rapid maturation) lending to resilience to short-interval severe fires that result in distinct vegetation assemblages that enhance landscape heterogeneity inherent to mixed-severity fire regimes (Donato et al. 2009). Furthermore, high diversity of vegetation types, driven by short interval repeat fires in a mixed-severity fire regime landscapes, plays an important role in conservation and the structure of avian communities (Fontaine et al. 2009).

Fire behavior is most strongly influenced by weather, topography, and fuels (i.e., above ground vegetation biomass) interacting through multiple pathways and at multiple spatial scales (Agee 1993). Weather is perhaps the most important factor controlling fire behavior and severity, especially in mixed-severity regimes (Bessie and Johnson 1995, Collins et al. 2007, Thompson and Spies 2009, Bradstock et al. 2010). In moderate fire weather, topographical complexity and position (east- and south-facing, upper- and mid slopes) have been shown to strongly influence fire intensity, with pre-fire vegetation condition and fire history also important predictors of severity (Estes et al. 2017). Under these conditions, shrubs and younger forests were more likely to burn at higher intensity than mature forests. In very high and severe fire weather, the amount (fuel loads), type (e.g., younger vs. older forest), and vertical and horizontal spatial arrangement of fuels (contiguous vs. unconnected) can be the primary driver of spatial patterns in mixed-severity fire (Zald and Dunn 2018). Furthermore, previous fires and post-fire management can set up the landscape for patterns of self-perpetuating high-severity fire in mixed-severity regimes (Donato et al. 2009, Thompson and Spies 2010). Even in drier forest types with high frequency of fire, certain topographic settings have lower fire frequencies where patches of dense, old forest can develop and persist as islands in a matrix of open, older forests (Camp et al. 1997, Krawchuk et al. 2016). With changing climates and land management practices, the size of patches of high-severity fire is increasing relative to historical patterns, with concern for sensitive species that rely on forests dramatically altered by fire (Westerling et al. 2006, Miller et al. 2008, Miller and Safford 2012, Reilly et al. 2017, Rockweit et al. 2017).

Northern spotted owls (Strix occidentalis caurina) are an obligate species of old forests in the Pacific Northwest of the United States and southwest Canada and typically nest in large old conifer trees (Wilk et al. 2018). The subspecies was listed as threatened under the U.S. Endangered Species Act because populations declined primarily as result of habitat loss due to large-scale harvest of late-successional forests (USFWS 1990). A variety of forest types are used by northern spotted owls for foraging, but nesting and roosting primarily occur in forests older than 125 yr of age. These older forests have average tree diameters above 50 cm and many trees exceed 75 cm diameter, canopy cover is usually >60%, and the forest has multiple canopy layers (Davis et al. 2016). The Northwest Forest Plan (NWFP) was designed to protect most remaining old forest and, after several decades, provide enough habitat on federal lands for viable populations of several old-forest species, primarily through a network of late-successional forest reserves (USDA and USDI 1994). On federal lands, loss of northern spotted owl habitat due to timber harvest has declined, but losses due to wildfires have increased in recent decades (Davis et al. 2016). Studies focused on the subspecies of northern spotted owls suggest that occupancy and survival generally decline after fire, especially if post-fire logging occurs (Clark et al. 2011, 2013, Rockweit et al. 2017). The effects of fire on individual northern spotted owls and habitat quality are complex and not fully understood (Lesmeister et al. 2018), but clearly suitability of forests for nesting and roosting decreases if canopy cover is reduced and with spatial aggregation of high-severity fire (Davis et al. 2016, Rockweit et al. 2017, Sovern et al. 2019).

Fire regimes within the range of northern spotted owls range from infrequent/high severity in the northern and coastal regions to frequent/low severity in the eastern and southern regions (Spies et al. 2018). In between these two extremes is a broad area of mixed-severity regimes, including the Oregon Klamath, where recent wildfires have caused high rates of loss of old forests and threaten species associated with them (Spies et al. 2006, 2018). Wildfires within this regime are comprised of a mix of burn severities, with low-severity ranging from 45% to 54% of the burned area, moderate-severity from 24% to 36%, and high-severity fire from 23% to 26% (Reilly et al. 2017). While the frequency and extent of high-severity fire have been increasing due to a general increase in large wildfires within the owls range, there is no strong evidence that high-severity wildfire comprises a higher proportion of burned areas than it did historically (Miller and Safford 2012, Reilly et al. 2017).

Within the Klamath-Siskiyou ecoregion of southwestern Oregon, an area characterized as moderate-frequency, mixed-severity fire regime (Spies et al. 2018), northern spotted owl demographics have been studied on the Klamath demographic study area since 1990 (Dugger et al. 2016). In and near the study area, lightning from a thunderstorm on 26 July 2013 started 54 fires that burned under very high fire weather conditions and were managed as the Douglas Complex and Big Windy Fires (Zald and Dunn 2018). Most of the fires joined into several large fires that burned with mixed severity over an area of about 38,000 ha. Within the fire perimeter were large patches of high-severity fire and subsequent salvage logging, primarily on private lands and along roads on federal lands. The non overlapping—but nearby—large mixed-severity wildfires burning simultaneously in a mixed ownership and management landscape presented a unique landscape experiment to evaluate interactions between severity classes (unburned/ low, low, moderate, and high) and vegetation condition (e.g., suitable or unsuitable forest for nesting and roosting by northern spotted owls). Further, the study area provided an exceptional opportunity to study responses of vegetation to fire because high-resolution remote sensing data of vegetation height provided by aerial light detection and ranging (lidar) were available pre and post-fire, which provided an unprecedented ability to measure forest attributes before and immediately following the fires.

Our objectives were to (1) quantify the immediate impact of various wildfire severities on northern spotted owl nesting/roosting habitat, which has typical characteristics of old-growth forests in the Pacific Northwest; and (2) analyze the relative susceptibility of northern spotted owl nesting/ roosting habitat to higher or lower severity fire. We hypothesized that northern spotted owl nesting/roosting habitat would be degraded as severity increased, but the relationship would be non-linear where habitat would not be degraded at low severity, only slightly degraded with moderate severity, and highly degraded with high severity. Because the area was in drought and fire weather was very high to severe, we expected the high fuel loading of northern spotted owl nesting/ roosting habitat may cause these stands to burn at higher or equal severity than other forest types with less fuel (Weatherspoon et al. 1992). However, several lines of evidence suggest older forests with dense, multi-storied canopies are more resistant to high-severity wildfire during severe fire weather (e.g., Countryman 1955).

METHODS

Study site

The study was conducted in the Klamath-Siskiyou ecoregion, which extends from northwestern California into southwestern Oregon (Fig. 1). The Douglas Complex and Big Windy Fires burned mostly within the boundary of the Klamath northern spotted owl demography study area (1422 km^2; Fig. 1) with elevations ranging from 610 to 1680 m. Annual precipitation ranged from 1500 to 3000 mm over the study area (http://prism.oregonstate.edu/), with <15% falling from May to September. The region is among the top global hotspots of species rarity and richness, identified as a global center of biodiversity, a World Wildlife Fund globally outstanding ecoregion (www.worldwildlife.org/publications/ global-200), and an IUCN area of global botanical significance (Olson and Dinerstein 1998, Noss 2000). The complexities of climate, topography, biogeographic patterns, geology, and mixed severity fire regime in the Klamath and Siskiyou Mountains create one of the four richest temperate coniferous forests in the world with high endemism, species richness, and unique community assemblages (Noss et al. 1999, Vance-Borland

1999). Forests were dominated by Douglas fir, ponderosa pine (P. ponderosa), sugar pine (P. lambertiana), and incense cedar (Calocedrus decurrens) and mixed with a variety of other conifers (Pinus spp. and grand fir Abies grandis) and hardwoods (e.g., Pacific madrone Arbutus menziesii, golden chinquapin Castanopsis chryso phylla, and oak Quercus spp.).

Within the Klamath-Siskiyou ecoregion, a complex and variable fire regime prevails, dominated by frequent mixed-severity and very frequent mixed-severity fires (Fig. 1; Spies et al. 2018). Historical fire severity varied in spatial scale, patchiness, and fire-return intervals (c. 5–75 yr), but overall exhibiting mixed severity over time and space (Agee 1993, Taylor and Skinner 1998, Perry et al. 2011). When a stand-replacing fire occurs, rapid recovery of vegetation and fuel continuity, coupled with dry summers and frequent lightning, create the potential for recurrent high-severity fires over decadal timescales (Thompson et al. 2007). Thus, short-interval severe fires have likely been a component of the complex fire regime and a factor structuring vegetation in the region (Agee 1993, Donato et al. 2009).

Fire data

We used daily fire perimeter map data for the Douglas Complex Fires that burned with mixed

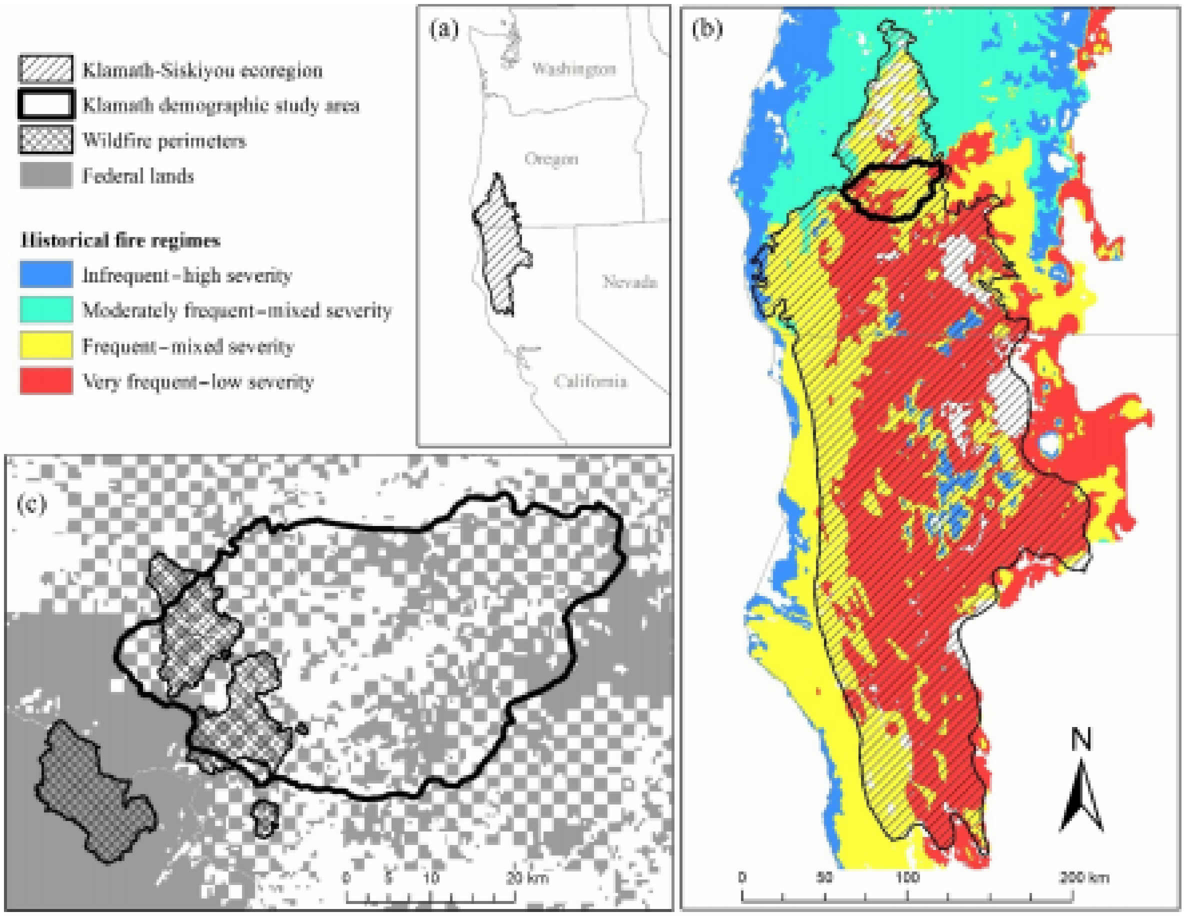

Fig. 1. Maps showing (a) the Klamath-Siskiyou ecoregion of California and Oregon, USA (hatched area); (b) historical fire regimes in the Klamath-Siskiyou ecoregion (Spies et al. 2018), Klamath northern spotted owl demography study area (1422 km^2; center = 123.315° W, 42.782° N, heavy black border); and (c) landownership (federal land, gray; private land, white) and the 2013 Douglas Complex and Big Windy Fires (cross-hatched area).

severity: Dads Creek (final perimeter = 9890 ha), Rabbit Mountain (9706 ha), and Brimstone (928 ha); and for the Big Windy Fire (10,799 ha; Fig. 2). Low precipitation in 2013 resulted in moderate-to-severe drought conditions in southern Oregon (NDMC 2018) and contributed to active fire behavior in the early burning period of these fires. Zald and Dunn (2018; and unpublished data) summarized weather data for the first 4 d of the Douglas and Big Windy Complexes (see Fig. 2 for fourth-day fire perimeters) from three Remote Automatic Weather Stations near fires and found maximum temperature was 25–32°C, minimum relative humidity was 17–30%, and maximum wind speed was 19–29 kmh. After the fourth day of the fire, a temperature inversion developed—a common occurrence in this region (Estes et al. 2017)—which dramatically changed fire behavior and greatly improved the effectiveness of suppression efforts. Mean daily burning index (BI) for the first 4 d of the fire was 52–76, which was above the historic (1991–2017 1 June–30 September) 90th percentile for this period (Zald and Dunn 2018). Mean daily energy release component (ERC) values ranged from 49 to 67, also above the 90th percentile for this area (Dalton et al. 2015) for 3 of 4 d. Burning index is a fire behavior index proportional to flame length that incorporates

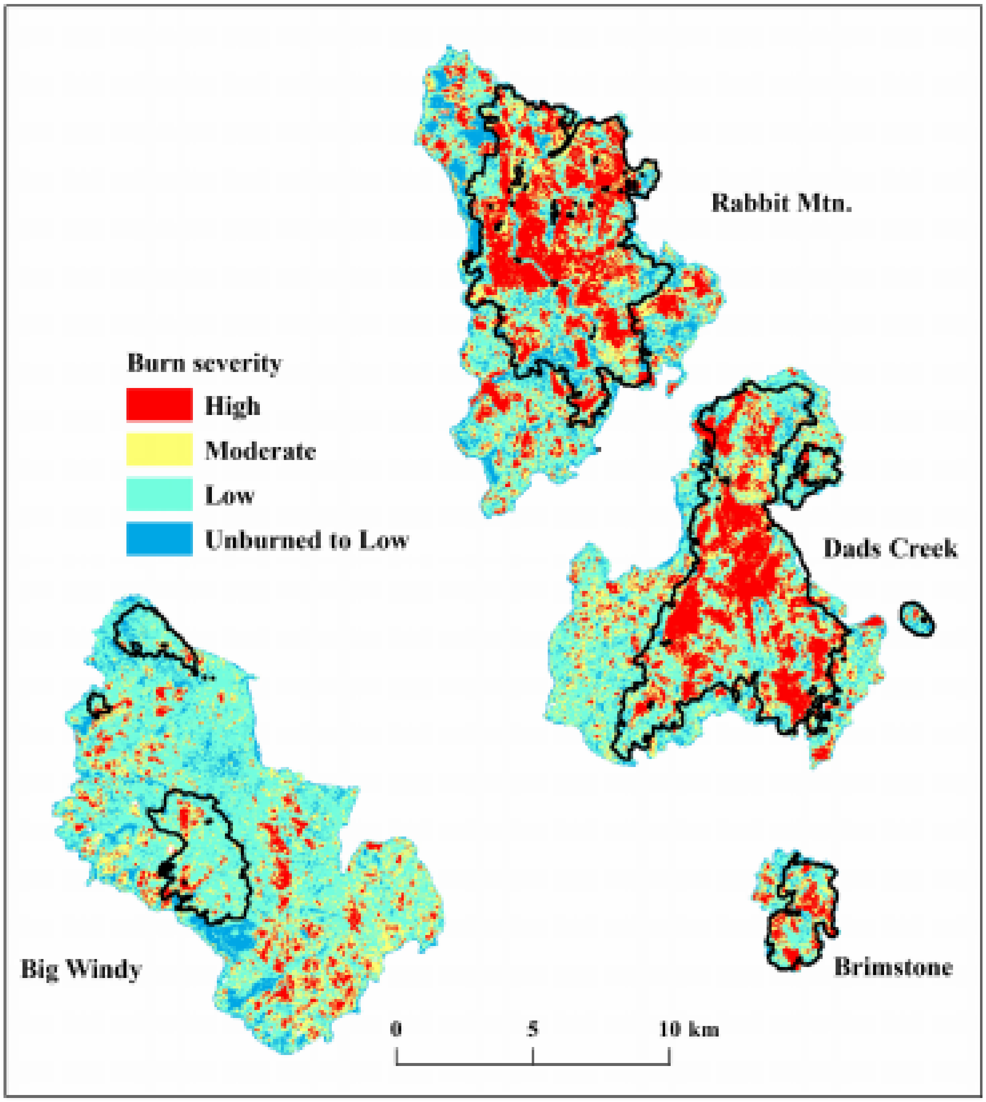

Fig. 2. Map of monitoring trends in burn severity (Eidenshink et al. 2007) data for the Big Windy and Douglas Complex Fires in southwest Oregon, USA, 2013. Severity is based on change in normalized burn ratio (dNBR) from Landsat-8 images from pre- and post-fire. The perimeter of the fires after the fourth day is outlined in black.

wind speed estimates, and ERC is an index of fire energy that includes the cumulative drying effect of weather in the days prior to the estimate and measures live and dead fuel moisture (Bradshaw et al. 1983, Cohen and Deeming 1985). Post-fire logging occurred over much of the high-severity portions of the private lands, but most federal land was unlogged post-fire because the area was designated as a late-successional reserve under the NWFP. The areas of the Douglas Complex Fires were primarily composed of Oregon and California Railroad Lands with federal lands, managed by the U.S. Bureau of Land Management, in a checkerboard pattern with private lands (Fig. 1; Zald and Dunn 2018). The Big Windy Fire burned within an intact landscape of federally managed forest lands (Fig. 1).

Pre- and post-fire habitat suitability

We used program MaxEnt version 3.3.3k (Phillips et al. 2006) to produce a pre-fire relative nesting/roosting habitat suitability model of forests used by northern spotted owls and applied the model algorithm to post-fire forest conditions to map post-fire suitability. MaxEnt is based on the maximum information entropy theory and is widely used to develop resource selection functions through the use of machine learning applied to known species locations (i.e., model training data) and relevant environmental predictor variables (Harte and Newman 2014). Previous efforts also used machine learning to develop nesting/roosting cover type models in several northern spotted owl studies and monitoring reports (Davis et al. 2011, 2016, Glenn et al. 2017). We followed Ackers et al. (2015) by using lidar-derived forest structure variables to develop a model of suitable forest for northern spotted owl nesting and roosting.

We used site locations where northern spotted owls nested and roosted within the demographic study area as training and testing data for relative habitat suitability models. These location data were collected during long-term research of northern spotted owl demography, including survival rates, reproductive rates, and annual rate of population change. The protocol used to determine site occupancy, nesting, and reproductive status for this study followed the guidelines specified by monitoring effectiveness of the NWFP (Franklin et al. 1996, Dugger et al. 2016).

We derived our pre- and post-fire model predictor variables from multiple-return discrete lidar data acquired in 2012 (1 yr pre-fire) and 2013 (2 months post-fire) by Quantum Spatial (previously Watershed Sciences, Corvallis, Oregon, USA) using aircraft-mounted Leica ALS 50 and/or Leica ALS 60 sensors with an average point density of ≥10 points per square meter. The 2012 data were collected as part of the Oregon Lidar Consortium (OLC) Rogue River lidar acquisition, covering an area of ~567,000 ha. Within this OLC Rogue River collection area, ~50,000 ha of lidar data were acquired again in 2013 post-wildfire, encompassing the Douglas complex and Big Windy Fires. We processed all lidar metrics from delivered point clouds, creating 1-m-resolution models of highest (i.e., first) return and bare earth digital elevation models (DEMs) with FUSION/LDV software (McGaughey 2015).

Following Ackers et al. (2015), we derived four metrics from the lidar data known to be important drivers in northern spotted owl nesting and roosting ecology: percentage overstory canopy cover (CANOPY), mean overstory canopy height (HEIGHT), density of large live trees (LARGE TREES), and rumple index (RUMPLE; Parker et al. 2004). We calculated the percent CANOPY taller than 2 m and the mean vegetation height using only first returns at 30 m resolution. We calculated RUMPLE, a measure of stand structure diversity where higher values represent stands with more horizontal and vertical complexity, using a 3 9 3 window focal mean of the 1-m canopy height model (CHM; Ackers et al. 2015). We matched the resolution of the HEIGHT and CANOPY metrics using a cell multiplier of 30 and then derived RUMPLE from the surface area ratio output. We calculated LARGE TREES from point files representing large live tree (≥31 m tall) locations from the 1-m CHM and CanopyMaxima in FUSION/LDV (McGaughey 2015). The tree height threshold of 31 m was the average height of 80-yr-old trees based on a height–age relationship of trees in forest inventory plots from the study area. To minimize the chance of having multiple points for the same tree, we created 10 m radius buffers around all points in ArcGIS 10.1 (ESRI, Redlands, California, USA), dissolved overlapping buffers, and then created a new point layer from the centers of the dissolved buffers. Any trees that were mapped only in the post-fire LARGE TREES map were added to the pre-fire model (with the assumption that large trees present after the fire were present prior to fires).

Northern spotted owl presence data for model training and testing were based on 107 nesting or roosting locations from 27 territories. Given that presence data originated from a long-term northern spotted owl study area, we were confident that we met sampling assumptions of minimal sampling bias and high probability of detecting owls when they were present. We followed standard procedures for presence-only modeling to avoid multi-collinearity between model variables by restricting modeling response functions that were overly complex, using stepwise calibration, and testing of bootstrapped model replicates (O'Brien 2007, Phillips and Elith 2013, Merow et al. 2014). We followed the model selection method used by Ackers et al. (2015) by using a random subset of our owl location data (75%) and 10,000 random modeling region locations to develop bootstrapped replicate models that related location data to random environmental conditions. We used the held-out 25% of northern spotted owl locations to test model predictions. We made stepwise adjustments to the model regularization multipliers that serve as a penalty parameter in machine learning by eliminating model coefficients and keeping only those that increase model gain, which relates to the likelihood ratio of an average species location to average background environmental conditions. Higher gains produce better differentiation of species locations from background conditions. The best model was based on balancing two criteria: (1) minimizing the difference between regularized training gain and test gain to avoid over-fitting the models, while (2) maximizing model test statistics (area under the curve [AUC] and Spearman rank correlation [Rs]). Once the best model was selected, we used the predicted vs. expected (P/E) curve to classify the model into a binary map of suitable and unsuitable nesting/roosting habitat (Hirzel et al. 2006).

Burn severity and change in suitability

We assumed most of the negative effects of wildfire on northern spotted owl nesting/roosting habitat would result from loss of canopy cover and mortality of large trees. To capture changes in the large, live tree component (LARGE TREES), we needed to estimate the proportion of LARGE TREES that suffered mortality by fire severity to adjust our post-fire LARGE TREES variable for the post-fire nesting/roosting habitat model. However, initial examination of the lidar data indicated that the post-fire lidar data could not differentiate live vs. dead trees ≥31 m height, leading to a bias in the lidar-based LARGE TREES variable. Previous research has indicated that lidar variables are better predictors for live and total basal area while multispectral imagery variables (e.g., Landsat data) are better predictors for dead and percent dead basal area (Bright et al. 2014). For example, changes in normalized burn ratio (NBR) are commonly used for mapping forest disturbance, especially timber harvest and wildfire (Miller and Thode 2007, Kennedy et al. 2010, 2012, Schroeder et al. 2011). In particular, changes in NBR have been widely used to assess fire severity (Miller et al. 2009, 2012, Cansler and McKenzie 2012, Lydersen et al. 2016). Furthermore, changes in NBR have been effectively related to changes in canopy cover (Miller et al. 2009) and basal area (Reilly et al. 2017). In this study, we used changes in satellite-based NBR from Landsat-8 to assess changes in canopy cover, and thus tree mortality, in live trees ≥31 m height to avoid biases produced by directly calculating changes in LARGE TREES from pre- and post-fire lidar data.

To assess canopy cover losses, and thus large live tree mortality associated with the fire, we acquired two spatial datasets to be used for mapping vegetation change within the fire perimeters: (1) We used Google Earth Engine (Google Earth Engine Team 2015, Gorelick et al. 2017) to collect 30-m-resolution Landsat-8 LaSRC imagery for the study area from 1 May to 1 August of 2013 and 2014 to generate pre- and post-fire NBR maps; and (2) we used post-fire high-resolution (7.62 cm) imagery acquired concurrently with lidar acquisition to estimate tree canopy

cover. For all 30 9 30 m (900 m^2) pixels in the study area, we calculated NBR in 2013 (pre-fire) and 2014 (post-fire) as the normalized differences between near-infrared and shortwave-infrared bands (bands 5 and 7, respectively; Li et al. 2013) for each Landsat-8 image. For our study area, no single image was optimal (e.g., cloud cover over part of the area on a given date), so we created a median composite image of NBR for each growing season (May–August; Kennedy et al. 2012). Large, live trees represented by LARGE TREES were only located in older forests; therefore, we measured live tree canopy cover visible in the high-resolution aerial photographs at 200 randomly generated 30 9 30 m (900 m^2) plots within older forests (95th percentile lidar return height ≥30.8 m) inside the study area snapped to the 2014 Landsat-8 pixel boundaries. Within each plot, 36 systematically distributed sampling points were established and tree canopy cover was measured as the proportion of sampling points where we observed live tree crowns in the high-resolution imagery. Plots co-located with roads, timber salvage, young plantations, or lacking clear imagery (e.g., steep slope in shadow) were excluded from our analysis, resulting in a final sample size of n = 181 that included post-fire canopy cover in forests experiencing a variety of fire severity conditions. Note that canopy cover measurements collected at these sample locations represent only live tree canopy cover and were independent from lidar-based canopy cover estimates that include both live and dead trees.

Statistical models relating NBR change and forest change (e.g., basal area mortality; Reilly et al. 2017) are available, but we did not have reliable measurements of canopy cover change based on both pre- and post-fire aerial photographs upon which we could parameterize a model. Pre-fire aerial imagery could not be used in conjunction with post-fire aerial imagery to calculate change in canopy cover directly because of the lower resolution images and differing parallax (i.e., an apparent shift in the position of objects as viewed from differing vantage points) between pre- and post-fire images. Therefore, an accurate assessment of cover change between photographs was unreliable. Additionally, published models were not parameterized for our landscape, but rather broad regional datasets for California (Miller et al. 2009) or Oregon and Washington (Reilly et al. 2017). Because only post-fire reference data for canopy cover (high-resolution aerial photographs) were available, we developed a mortality algorithm based on changes in forest canopy cover predicted from NBR data. The algorithm (1) predicted live canopy cover based on post-fire NBR and canopy cover measurements from aerial photography, (2) calculated the change in predicted canopy cover from the pre-fire to post-fire conditions, and (3) assigned mortality to LARGE TREES with probability proportional to the change in Landsat-based canopy cover.

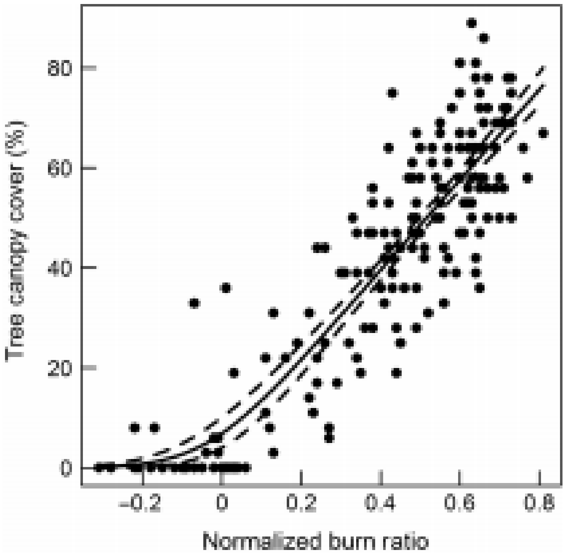

Fig. 3. Mean (solid line) and 95% confidence intervals (dashed lines) for predicted live tree canopy cover as a function of normalized burn ratio within the Douglas Complex and Big Windy Fires in southwest Oregon, USA, in 2013 based on the zero-truncated regression model.

Because tree canopy cover data were nonnegative, we modeled tree canopy cover as a function of NBR with a zero-truncated regression model (Fig. 3). The model was fit to the 2014 NBR (post-fire) and tree canopy cover data in the R statistical environment version 3.3.1 (R Core Team 2016) with the function tobit (AER package; Kleiber and Zeileis 2009). For each 30-m Landsat pixel, tree canopy cover predictions for pre- and post-fire were generated by applying the fitted model to 2013 (before fire ignition) and

2014 NBR data, respectively. To minimize differences between 2013 and 2014 canopy cover maps, we normalized the 2013 NBR data so that the differences between 2013 and 2014 NBR outside the fire perimeter were minimized. We transformed the 2013 NBR image by creating a mask of high NBR (stable forest, both 2013 and 2014 NBR were >0.75) outside the fire boundaries, and within the study area, which served as the population for creating a normalization between the two image dates. We then created a simple least-squares linear fit between NBR 2013 and NBR 2014 based on all pixels in the mask population, with a slope of 0.845 and intercept of 0.119 based on estimated coefficients. We created the transformed NBR 2013 by applying slope/intercept from linear fit, thereby transforming the 2013 image calibrated to the values in the 2014 image and quantified differences.

Pre- and post-fire predictions of canopy cover were differenced and divided by the predicted pre-fire canopy cover to calculate the proportional change in canopy cover (DC). The probability of mortality for a given 30-m pixel on the landscape was taken to be 1 – DC (i.e., canopy cover-weighted tree mortality). Areas with canopy cover increases (i.e., DC > 0) were assumed to have no tree mortality. We assessed the performance of the canopy cover-weighted mortality by comparing our predictions for each pixel with a large live tree with an independent basal area-weighted mortality prediction generated using existing models (Appendix S1; Reilly et al. 2017). We use these data for validation because the models produced by Reilly et al. (2017) predict basal area-weighted tree mortality from a regional forest inventory network based on RdNBR (r^2 = 0.68) and perform particularly well in identifying patches of forest experiencing basal area-weighted mortality >75% (classification accuracy = 82.8%).

Large tree mortality within each pixel was assigned proportional to 1 – DC. For a given pixel with n canopy dominant trees identified based on lidar imagery, a sample n 9 (1 – DC) trees, rounded to the nearest integer, was taken and recorded as having died during the fire, with the remaining n 9 DC trees surviving. This assumes that the number of trees dying during the fire was proportional to the canopy cover losses and that the identity of trees dying does not matter. For canopy dominant trees examined in this paper, such an assumption seems reasonable. We, therefore, used the mortality algorithm to modify our post-fire point file of tree stems to estimate which trees mapped by lidar suffered mortality. We then used the post-fire live tree point file to generate our post-fire LARGE TREES density variable for nesting/roosting habitat modeling.

We recognize that by leveraging multiple data sets and modeling techniques—lidar-based LARGE TREES and satellite-based canopy cover weighted mortality—there is the opportunity to propagation of error from one step to another. For example, errors in estimating forest carbon stocks may arise from field data collection, allometric equations, and modeling errors (Clough et al. 2016). In the case of this study, errors associated with canopy cover modeling, the calculation of canopy cover-weighted mortality, and the application of that mortality to attribute tree death to individual trees all contribute to overall errors.

Pre-fire vegetation vs. fire severity analysis

Our main interest was to examine the relationship between fire severity and nesting/roosting habitat with limited confounding effects of fire suppression activities and differences in fire weather during the time the fire burned. Though it is difficult to separate the confounding effects of suppression efforts when analyzing almost all fires, we reasoned we could minimize this effect by examining the early days of the fire before more extensive backfiring occurred and suppression activities had limited effect. Thus, we used the spatial extent of daily fire growth (as mapped using aerial IR technology each night) throughout the first 4 d after ignition. Starting at approximately day 5 of the fire, changes in atmospheric temperature altered fire weather conditions and suppression efforts included igniting backfires in some areas (K. Kosel, personal communication; Fig. 2). Additionally, by focusing on these rapid fire growth days we believe there is little to no alteration of natural fire behavior or severity across the spectrum of northern spotted owl nesting/roosting habitat suitability. To quantify the odds of forest types burning in 1 of 4 severity types, we evaluated the ratios of the proportion of suitable and unsuitable nesting/roosting

habitat that burned (B) at each fire severity to what was available to burn (A). Fire severity types were taken from Monitoring Trends in Burn Severity (MTBS 2017) data, a map product based on changes in NBR commonly used by forest management agencies. The types include high severity, moderate severity, low severity, and unburned to low severity. By using the same fire severity classifications commonly used by land managers, communication and application of results from this research will be more straightforward. A value of B/A < 1 indicates that the forest type burned less than would have been expected by chance, and a ratio B/A > 1 indicates it burned more than would be expected by chance (Moreira et al. 2001, 2009, Manly et al. 2010). While the canopy cover-weighted mortality modeling we used to attribute large tree mortality depends on NBR and is thus likely related to the MTBS fire severity classes, we use the MTBS classes for summarizing across severity classes because of their widely accepted use in forest planning.

Results

Pre- and post-fire habitat suitability

Our best model of nesting/roosting habitat suitability predicted nesting/roosting locations well with an AUC statistic of 0.89 and a P/E curve Spearman rank correlation of 0.92. The binary classification of the habitat model into suitable and unsuitable was based on P/E = 1 (0.32). Model variable response functions (Fig. 4) followed known resource selection patterns by owls (Ackers et al. 2015, Glenn et al. 2017).

Burn severity and change in suitability

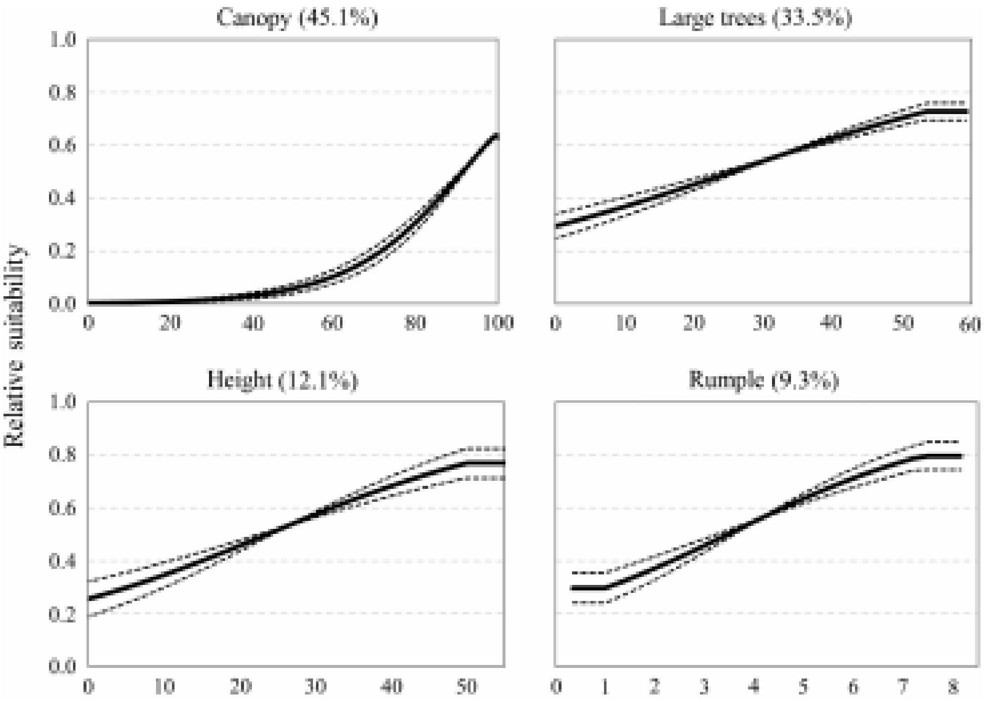

Fig. 4. Variable response functions with percent contribution (%) to pre-fire nesting/roosting habitat suitability model for northern spotted owls in the Klamath demographic study area in southwest Oregon, USA, where the Douglas Complex and Big Windy Fires burned in 2013. The solid line represents the mean, and the dashed lines represent 95% confidence intervals. Variables were derived from lidar data, and the variables included were CANOPY (percent canopy cover), LARGE TREES (large live trees per hectare), RUMPLE (rumple index), and HEIGHT (mean tree height [m]).

Table 1. Metrics within areas burned at four severity classes based on Monitoring Trends in Burn Severity (MTBS) measurements.

Fire severity	Pre-fire live trees	Trees killed	% Mort	Mean pre-fire NBR	Mean post-fire NBR	∆ Mean NBR (%)	Mean pre-fire suitability	Mean post-fire suitability	% Loss suitable habitat
Unburned to low	66,015	2830	4	0.75	0.68	!9.2	0.22	0.20	4.5
Low	251,356	49,413	20	0.74	0.56	!24.6	0.22	0.21	25.5
Moderate	71,826	40,038	56	0.72	0.30	!58.3	0.10	0.08	63.9
High	67,897	62,348	92	0.75	!0.04	!104.9	0.12	0.03	93.7

Notes: Reported are estimated number of large live trees pre-fire, estimated number large live trees killed during fire, percentage of large live trees killed, mean normalized burn ratio (NBR) pre (2013)- and post-fire (2014), percent change in NBR, pre (2012)- and post-fire (2013) mean nesting/roosting habitat suitability, and percent loss of suitable nesting/roosting habitat for northern spotted owls in the Douglas Complex and Big Windy wildfires in southwest Oregon during 2013.

Post-fire nesting/roosting habitat suitability decreased with increasing fire severity (Table 1), mainly owing to fire-caused decreases in LARGE TREES and CANOPY. Low-severity fire had little effect on nesting/roosting habitat suitability. High-severity fire resulted in 75% decrease in mean suitability and >93% loss of suitable nesting/roosting habitat (Table 1) and commonly converted pre-fire suitable forests to conditions that were unsuitable for nesting and roosting (Fig. 5). Overall, most pre-fire habitat was lost if it burned at moderate severity (Table 1), but depending on the pre-fire suitability, moderate severity fire produced mixed effects on nesting/ roosting habitat suitability and did not consistently result in a loss of suitability. The forests that burned at unburned to low severities had pre-fire suitability values approximately two times higher than suitability of forests that burned at moderate or high severity (Table 1); thus, moderate- to high-severity fire had the greatest effect on pre-fire areas with low habitat suitability for northern spotted owls (Fig. 6).

Tree mortality and pre-fire vegetation vs fire severity

Canopy cover-weighted mortality (Appendix S1: Fig. S1) generated as the basis of attributing post fire tree mortality for large trees exhibited a slight positive bias (mean error = 2.42% mortality) and root mean square deviation of 5.82% compared to an existing basal area-weighted mortality model based on regional forest inventory datasets co-located with large wildfires (Reilly et al. 2017). Despite these errors, our canopy cover-weighted mortality predictions were highly correlated with the existing basal area-weighted mortality predictions (Pearson correlation = 0.99).

Based on lidar tree mapping and the post-fire NBR analysis, we estimated the fires directly killed a total of 154,629 large live trees (51.1% of total pre-fire estimate). Tree mortality increased with fire severity and percent change in NBR (Table 1). There were 2.27 times more large live trees in areas that experienced unburned to low severity fire compared to those areas that burned at moderate and high severity (Table 1). The susceptibility of forests to moderate- and high-severity fire was lower in suitable nesting/roosting habitat and higher in unsuitable forest than would be expected by chance (Fig. 6). The differences between low and moderate/high severity were more pronounced in suitable nesting/roosting habitat than unsuitable forest. The odds that suitable nesting/roosting habitat would burn at lower severity was 2–3 times higher than the odds it would burn at moderate-to-high severity. There were significant differences (based on nonoverlapping 95% confidence intervals) between odds of burning at low severity and burning at moderate/high severity among forest types. There was no evidence for a difference between the odds (i.e., B/A index) of burning at moderate or high severity within suitable nesting/roosting habitat or unsuitable forest types, but there were differences between suitable and unsuitable forest types (Fig. 6). The odds that unsuitable forest burned at moderate-to-high severity was about twice that of suitable nesting/roosting habitat.

DISCUSSION

Here, we used newly developed tools and lidar data to examine the interaction between mixed-severity fires and northern spotted owl

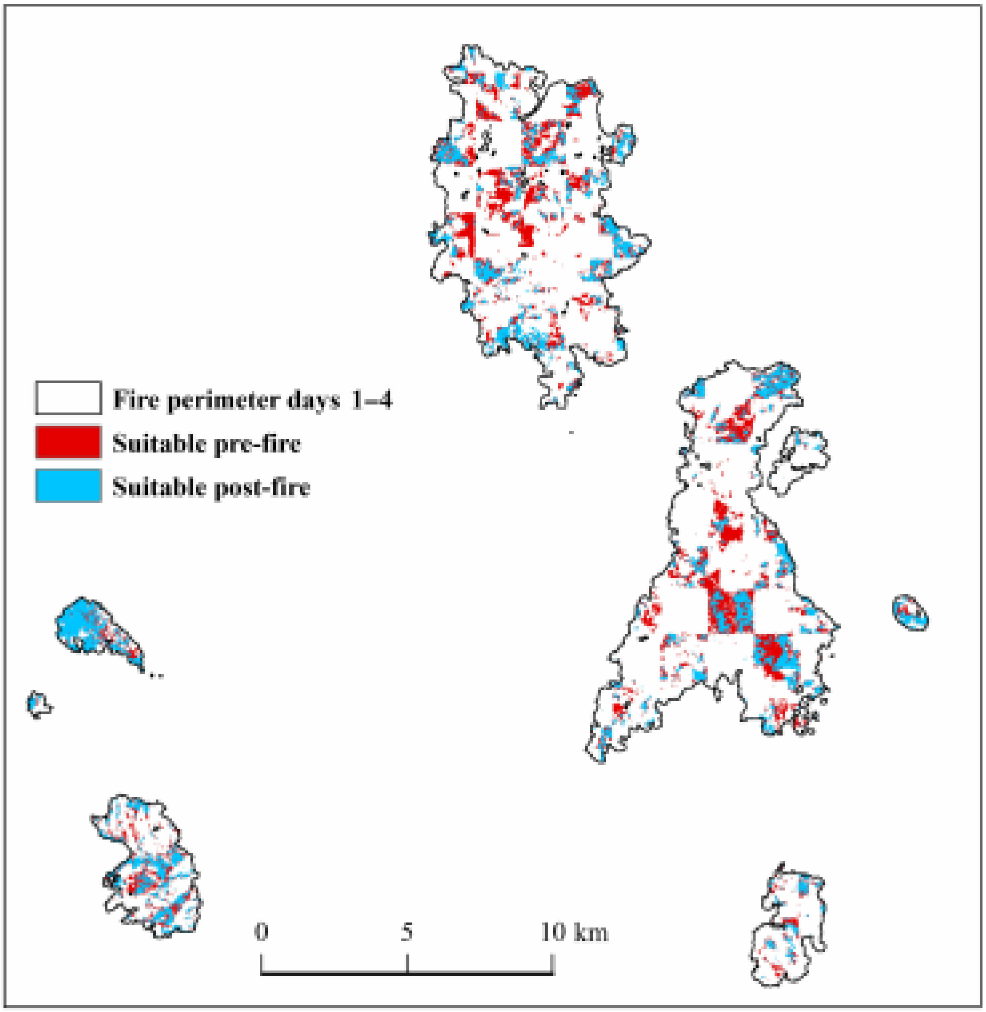

Fig. 5. Patterns of conversion from suitable habitat to unsuitable conditions for northern spotted owl nesting and roosting in the Douglas Complex and Big Windy Fires that burned in southwestern Oregon, USA. Binary classification of nesting/roosting habitat was based on predicted vs. expected ratio threshold of 0.32, and lidar metrics of live vegetation height, canopy cover, stand complexity (rumple index), and large tree density. Area shown is the perimeter of the fires 4 d after the fire ignited on 26 July 2013.

nesting/roosting habitat under high fire weather conditions in a landscape characterized by the interactions between land-use patterns and a mixed-severity fire regime. Because of high site fidelity, northern spotted owls may continue to use areas if suitable nesting/roosting cover remains and prey are available. However, survival decreases through time in areas with a high proportion of high-severity fire likely because post-fire habitat quality decreases to the point that territories are only marginally capable of supporting northern spotted owls (Rockweit et al. 2017). Within a few years post-fire, areas opened up by tree mortality change structurally (i.e., standing dead trees transitioning to fallen logs) and prey may be less accessible with high density of shrubs and herbaceous understory in high-severity burn areas. As expected, in our study the suitability of northern spotted owl nesting/roosting habitat decreased with increasing fire severity, to the degree that much of the pre-fire habitat that burned at high severity was no longer suitable cover for nesting or roosting. The greatest impacts from moderate- and high-severity fire

due to shade, lower temperatures, lower wind speeds, and more compact litter layers (Countryman 1955, Chen et al. 1996, Kitzberger et al. 2012, Frey et al. 2016, Spies et al. 2018). In addi

Fig. 6. Ratio of proportion of suitable and unsuitable nesting/roosting habitat that burned (B) at each fire severity to what was available (A) to burn (B/A index) with 95% confidence intervals, Douglas Complex and Big Windy Fires, southwestern Oregon, USA, 2013. We used Monitoring Trends in Burn Severity (MTBS 2017) to determine fire severity types (UB LOW, unburned to low severity; LOW, low severity; MOD, moderate severity; HIGH, high severity) and separated into suitable nesting/roosting habitat for northern spotted owls or unsuitable forest types based on lidar metrics. B/A index < 1 indicates that the forest type (suitable or unsuitable) burned at the severity class less than would have been expected by chance, and B/A index > 1 indicates forest type burned at the class more than by chance alone.

were observed in those forests exhibiting low habitat suitability for northern spotted owl nesting and roosting before the fire.

We found that the old-forest conditions associated with northern spotted owl habitat burned at lower severity despite having higher fuel loading than other forest types on the landscape. The microclimate and forest structure likely played a key role in lower fire severity in nesting/roosting habitat compared to other forest types. As succession progresses and canopy cover of shade tolerant tree species increases, forests eventually gain old-growth characteristics and become less likely to burn because of higher relative humidity in soil and air, less heating of the forest floor

tion, as the herbaceous and shrub layer is reduced by shading from lower to mid-layer canopy trees, the connection between surface fuels and the canopy declines, despite possible increases in canopy layering (Halofsky et al. 2011, Odion et al. 2014). Alexander et al. (2006) found that in the Klamath-Siskiyou ecoregion, southern aspects tended to burn with greater severity, but exogenous factors also played an important role because areas with large trees burned less and had less fire damage than areas dominated by smaller trees. On the 2002 Biscuit Fire that burned near our study area, Thompson and Spies (2009) concluded that weather and pre-fire vegetation conditions were the primary determinants of crown damage. They found that forests with small-stature vegetation and areas of open tree canopies and dense shrubs experienced the highest levels of tree crown damage, while older, closed-canopy forests with high levels of large conifer cover were associated with the lowest levels of tree crown damage. The moisture content of air and soil in a forest affects the amount of fuel moisture, and thus the probability of ignition and burning temperature (Heyerdahl et al. 2001). In addition to the potential to mitigate negative effects of climate warming at local scales by creating refugia and enhancing biodiversity (Frey et al. 2016), we suggest that northern spotted owl nesting/roosting habitat also has the potential to function as fire refugia (i.e., areas with higher probability of escaping high-severity fire compared to other areas on landscape) in areas with mixed-severity fire regimes under most weather conditions. Thus, in these landscapes, management strategies to conserve old-growth characteristics may also reduce risk of high-severity wildfire (Bradley et al. 2016) and serve as buffer to negative effects of climate change (Betts et al. 2018).

Although it has long been recognized that older forests have lower flammability than other forest types (Countryman 1955), federal agencies are often criticized for not extensively managing old forests to reduce risk of high-severity fire (OFRI 2010). The perception is that forest succession leads to increased flammability with age

(Kitzberger et al. 2012, Duff et al. 2017). Where this view may be correct is in dry forests with historically very frequent fire-return intervals (<10 yr), and contemporary increased fuel continuity has resulted from fire exclusion and led to increased sizes of high-severity patches when fires burn under extreme weather (Reilly et al. 2017). In the driest forest types, fire exclusion converts open forests with grassy understories to dense forests with high fuel loads, and the increased fuel continuity can result in larger patches of high severity fire than would have occurred historically. In other forest types, succession likely decreases risk of high-severity fire. Compared to older forest, younger forests have lower canopies and thinner barked trees that reduce resistance to fire, and thinned young forests can be susceptible to high mortality from fire unless surface fuels are treated with prescribed fire (Raymond and Peterson 2005). Thinned forests have more open conditions, which are associated with higher temperatures, lower relative humidity, higher wind speeds, and increasing fire intensity. Furthermore, live and dead fuels in young forest or thinned stands with dense saplings or shrub understory will be drier, making ignition and high heat more likely, and the rate of spread higher because of the relative lack of wind breaks provided by closed canopies with large trees.

Primarily as inputs to fire models that estimate likely fire behavior, fuel models involve typing forested stands according to fuel loading and are often used to explore or inform management directions because fuels are under the purview of forest managers (Deeming and Brown 1975, Anderson 1982, Bradshaw et al. 1983, Finney 2004, Scott and Burgan 2005, Andrews 2009). Suitable nesting/roosting habitat often falls in classes rated as highly burnable, with fast rates of fire spread, high flame lengths, and intense fire behavior (Anderson 1982). Thus, fire model results can show nesting/roosting habitat has higher burn probabilities and higher crown fire potential than adjacent areas (Ager et al. 2007, 2012). The results of this study as well as other recent studies show that these older forests in mixed-conifer forest environments are less susceptible to high-severity fire than other successional stages, even under high fire weather conditions and with short return intervals <15 yr (Donato et al. 2009). Running fire models for our study area based on conditions during the Douglas Complex and Big Windy Fires would be a worthwhile exercise to evaluate model predictions relative to the actual behavior of those fires. However, based on the findings of this study and many others (see review by Duff et al. 2017), we contend that fire models that continue to use fuel models that rate older forests with higher relative fire behavior will likely overestimate fire severity and inflate estimated loss of old forests in the Pacific Northwest. An alternative is to consider forest fuels in a more holistic manner and alter native age–flammability models (Kitzberger et al. 2012, Duff et al. 2017).

Intensive management (especially on timber industry lands) that results in reduced fuel loading does not always equate to less frequent or severe fire. Results by Charnley et al. (2017) in southcentral Oregon showed that private industry lands had more than three times the percentage area of open-canopy forest compared to U.S. Forest Service-managed lands that included thinning trees <53.3 cm diameter, prescribed fire, and no active management. Federal land management practices resulted in forests with more resilience to high-severity wildfire as opposed to management on private lands (Charnley et al. 2017). Furthermore, Zald and Dunn (2018) found that ownership patterns were the best predictor for high-severity fire in the Douglas Complex Fires, where federal lands, with primarily older forests in late-successional reserves, burned at lower severity than non-federal forests that were primarily private timber industry lands.

Gradual changes in temperature or precipitation patterns may have little effect until a disturbance driven threshold is reached at which a large shift occurs that might be difficult or impossible to reverse (Scheffer and Carpenter 2003). Peterson (2002) described "ecological memory" and how previous patterns of disturbance can predispose an area to follow a certain disturbance pathway. For example, a landscape that experiences severe disturbance (e.g., high-severity fire, clear-cut logging, post-fire salvage logging) can be predisposed to high-severity fire in a mixed-severity fire regime (Thompson et al. 2007, Donato et al. 2009, Thompson and Spies 2009, Zald and Dunn 2018). High-severity wildfire can alter soil and successional pathways and potentially shift the system into an alternative stable state (Peterson 2002). A key component of overall ecosystem function and sustainability occurs belowground, and with high severity fire, changes in the soil physical, chemical, and biological functions can be deleterious to the entire ecosystem caused by changes in successional rates and species composition (Neary et al. 1999). Conversely, low-severity fire effects on soil can promote herbaceous flora, increase plant diversity, increase available nutrients, and thin over-crowded forests, all of which can enhance healthy forest ecosystems (Neary et al. 1999). The time for recovery of belowground systems is a key driver of ecosystem processes and depends on burning intensity and on previous land-use practices. Soils are greatly altered and degraded in young intensively managed forest and post salvage logged sites, which are more susceptible to repeat and short-interval high-severity wildfire, and these forests that experience multiple rapid successions of natural and human-derived disturbances may cross thresholds and be changed catastrophically (Lindenmayer and Noss 2006).

The Klamath-Siskiyou ecoregion is currently dominated by biodiverse temperate coniferous forest and may be near a tipping point toward an alternative stable state (shrub/hardwood chaparral) with extensive loss of conifer forest, dominance by deciduous trees and shrubs, and recurring early-seral and young forest conditions (Tepley et al. 2017, Serra-Diaz et al. 2018). The region has experienced short intervals between recent high-severity fires coupled with intensive timber management in this mixed-severity fire regime area, and the likelihood of further shortening of fire-return intervals with climate change (Davis et al. 2017). Even where climate is suitable to sustain dense mature forests, early-seral and non-forest conditions may perpetuate because of a cycle of short-interval repeat burning and timber harvest and have dramatic impacts on biodiversity and wildlife habitats (Lindenmayer et al. 2011, Tepley et al. 2017). Under this scenario, the persistence of old-forest associated species, including northern spotted owls, within the Klamath-Siskiyou ecoregion would be further threatened.

It was recognized early in the history of northern spotted owl conservation that fire would play a major role in determining the success of management plans (Agee and Edmunds 1992). The 2011 federal northern spotted owl recovery plan calls for increasing fire resiliency in dry forests with focus on active management outside of northern spotted owl core areas to meet project goals (USFWS 2011). For many dry forests in the western United States that historically experienced frequent, low- to moderate-severity fire regimes, prescribed fire and mechanical treatments have been effective at reducing surface fuel loads, forest structure, and potential fire severity (Stephens et al. 2009). In mixed-severity landscapes, the fire severity mosaic is highly variable and the effects of topography and climate are strong predictors for this regime, but forest conditions also are important and much less predictable and stable (Beaty and Taylor 2001), further complicating management decisions aimed at increasing fire resiliency of forests. Management actions employed in dry forest types to reduce wildfire risk may not work equivalently in mixed-severity regimes. Active management actions that include mechanical treatments degrade suitability of forests for nesting and roosting by northern spotted owls (Lesmeister et al. 2018) and may not always decrease risk of high-severity fire. Further, considering trends and forecasts for earlier spring snowmelt and longer fire seasons, climate change may exacerbate the effects of wildfire (Dale et al. 2001, Westerling et al. 2006), and thus the framed conundrum between northern spotted owl habitat and fire management in mixed-severity regimes. Our results indicate that older forest in late-successional reserves (i.e., northern spotted owl nesting/roosting habitat) with no active management can serve as a buffer to the effects of climate change and associated increase in wildfire occurrence. These multi-storied old forests in these environments enhance biodiversity and have the highest probability to persist through fire even in weather conditions associated with high fire activity.

Fuel-reduction treatments such as mechanical thinning can effectively reduce fire severity in the short term, but these treatments, by themselves, may not effectively mitigate long-term dynamics of fire behavior under severe weather conditions and may not restore the natural complexity of historical stand and landscape structure (Schoennagel et al. 2004). On the other hand, prescribed fire that mimics severity and return intervals of natural fire regimes in forests that historically

experienced fire can result in landscapes that are both self-regulating and resilient to fire (Parks et al. 2015). Prescribed fire is generally considered to be the most effective way to reduce the likelihood of high-severity fire in combination with mechanical treatments (Stephens et al. 2009). The 2013 Rim Fire in the Sierra Nevada, California, USA, burned with low severity in areas previously treated with prescribed fires, suggesting that prescribed burning was an effective management tool to reduce fire severity (Harris and Taylor 2017). Many fire-prone forests will require active management to restore ecosystem function, but no single prescription will be appropriate for all areas and, in some portions of the forests, minimal maintenance may be more sustainable in the long term (Noss et al. 2006). Within the Klamath Siskiyou ecoregion, flexible and multi-scale land management approaches that promote diversity of forest types will likely enhance conservation of a range of species requiring different forest conditions for long-term persistence. An integral component of these approaches could include resistance strategies (i.e., no active management) to protect high-value older forest (Millar et al. 2007) and prescribed fire to promote and maintain a mix of forest conditions in this landscape characterized by mixed-ownership and mixed-severity fire regime. Ultimately, spatial heterogeneity that includes the buffering effects of northern spotted owl nesting/roosting habitat may serve as a stabilizing mechanism to climate change and reduce tendency toward large-scale catastrophic regime shifts.

ACKNOWLEDGMENTS

We are deeply indebted to R. Horn and many other field biologists for the long-term collection of northern spotted owl data presented here. We are grateful to G. McFadden and B. Hollen for support and facilitating primary funding from USDI Bureau of Land Management. Additional support was provided by USDA Forest Service Region 6 and Pacific Northwest Research Station. K. Kosel provided background information on fire suppression efforts for the fires. We thank T. Spies and two anonymous reviewers, whose suggested edits and comments on an earlier version greatly improved the manuscript. This publication represents the views of the authors, and any use of trade, firm, or product names is for descriptive purposes only and does not imply endorsement by the U.S. Government.

LITERATURE CITED

Ackers, S. H., R. J. Davis, K. A. Olsen, and K. M. Dugger. 2015. The evolution of mapping habitat for northern spotted owls (Strix occidentalis caurina): a comparison of photo-interpreted, Landsat-based, and lidar-based habitat maps. Remote Sensing of Environment 156:361–373.

Agee, J. K. 1993. Fire ecology of Pacific Northwest Forests. Island Press, Washington, D.C., USA. Agee, J. K. 2005. The complex nature of mixed severity fire regimes. In L. Taylor, J. Zelnik, S. Cadwallader, and B. Hughes, editors. Mixed severity fire regimes: ecology and management. Association for Fire Ecology, Spokane, Washington, USA. Agee, J. K. 2013. Historical range of variability in eastern Cascades forests, Washington, USA. Landscape Ecology 18:725–740.

Agee, J. K., and R. L. Edmunds. 1992. Forest protection guidelines for the northern spotted owl, vol. 2. Pages 181–244 in USDI, editor. Recovery plan for the northern spotted owl-final draft. Volume 2. US Government Printing Office, Washington, D.C., USA.

Ager, A. A., M. A. Finney, B. K. Kerns, and H. Maffei. 2007. Modeling wildfire risk to northern spotted owl (Strix occidentalis caurina) habitat in Central Oregon, USA. Forest Ecology and Management 246:45–56.

Ager, A. A., N. M. Vaillant, M. A. Finney, and H. K. Preisler. 2012. Analyzing wildfire exposure and source–sink relationships on a fire prone forest landscape. Forest Ecology and Management 267:271–283.

Alexander, J. D., N. E. Seavy, C. J. Ralph, and B. Hogoboom. 2006. Vegetation and topographical correlates of fire severity from two fires in the Klamath-Siskiyou region of Oregon and California. International Journal of Wildland Fire 15:237–245.

Allen, C. D., et al. 2010. A global overview of drought and heat-induced tree mortality reveals emerging climate change risks for forests. Forest Ecology and Management 259:660–684.

Anderson, H. E. 1982. Aids to determining fuel models for estimating fire behavior. INT-GTR-122. USDA Forest Service, Intermountain Forest and Range Experiment Station, Ogden, Utah, USA.

Andrews, P. L. 2009. BehavePlus fire modeling system, version 5.0. Variables. RMRS-GTR-213. USDA Forest Service, Rocky Mountain Research Station, Fort Collins, Colorado, USA.

Baker, W. L., T. T. Veblen, and R. L. Sherriff. 2007. Fire, fuels and restoration of ponderosa pine-Douglas fir forests in the Rocky Mountains, USA. Journal of Biogeography 34:251–269.

Beaty, R. M., and A. H. Taylor. 2001. Spatial and temporal variation of fire regimes in a mixed conifer forest landscape, Southern Cascades, California, USA. Journal of Biogeography 28:955–966.

Bessie, W. C., and E. A. Johnson. 1995. The relative importance of fuels and weather on fire behavior in subalpine forests. Ecology 76:747–762.

Betts, M. G., B. Phalan, S. J. K. Frey, J. S. Rousseau, Z. Yang, and T. Albright. 2018. Old-growth forests buffer climate-sensitive bird populations from warming. Diversity and Distributions 24:439–447.

Bradley, C. M., C. T. Hanson, and D. A. DellaSala. 2016. Does increased forest protection correspond to higher fire severity in frequent-fire forests of the western United States? Ecosphere 7:e01492.

Bradshaw, L. S., J. E. Deeming, R. E. Burgan, and J. D. Cohen. 1983. The 1978 National Fire-Danger Rating System: technical Documentation. General Technical Report INT-169. USDA Forest Service, Intermountain Forest and Range Experiment Station, Ogden, Utah, USA.

Bradstock, R. A., K. A. Hammill, L. Collins, and O. Price. 2010. Effects of weather, fuel and terrain on fire severity in topographically diverse landscapes of south-eastern Australia. Landscape Ecology 25:607–619.

Bright, B. C., A. T. Hudak, R. E. Kennedy, and A. J. H. Meddens. 2014. Landsat time series and lidar as predictors of live and dead basal area across five bark beetle-affected forests. IEEE Journal of Selected Topics in Applied Earth Observations and Remote Sensing 7:3440–3452.

Bunnell, F. L. 1995. Forest-dwelling vertebrate faunas and natural fire regimes in British Columbia: pat terns and implications for conservation. Conservation Biology 9:636–644.

Camp, A., C. Oliver, P. Hessburg, and R. Everett. 1997. Predicting late-successional fire refugia pre-dating European settlement in the Wenatchee Mountains. Forest Ecology and Management 95:63–77.

Cansler, C. A., and D. McKenzie. 2012. How robust are burn severity indices when applied in a new region? Evaluation of alternate field-based and remote-sensing methods. Remote Sensing 4:456–483.

Charnley, S., T. A. Spies, A. M. G. Barros, E. M. White, and K. A. Olsen. 2017. Diversity in forest management to reduce wildfire losses: implications for resilience. Ecology and Society 22:22.

Chen, J., J. F. Franklin, and T. A. Spies. 1996. Growing season microclimate gradients from clearcut edges into old-growth Douglas-fir forests. Ecological Applications 5:74–86.

Clark, D. A., R. G. Anthony, and L. S. Andrews. 2011. Survival rates of northern spotted owls in post-fire landscapes of southwest Oregon. Journal of Raptor Research 45:38–47.

Clark, D. A., R. G. Anthony, and L. S. Andrews. 2013. Relationship between wildfire, salvage logging, and occupancy of nesting territories by northern spotted owls. Journal of Wildlife Management 77:672–688.

Clough, B. J., M. B. Russel, G. M. Domke, and C. W. Woodall. 2016. Quantifying allometric model uncertainty for plot-level live tree biomass stocks with a data-driven, hierarchical framework. Forest Ecology and Management 372:176–188.

Cohen, J. D., and J. E. Deeming. 1985. The National Fire-Danger Rating System: basic equations. Pacific Southwest Forest and Range Experiment Station, Berkeley, California, USA.

Collins, B. M., M. Kelly, J. W. van Wagtendonk, and S. L. Stephens. 2007. Spatial patterns of large natural fires in Sierra Nevada wilderness areas. Landscape Ecology 22:545–557.

Countryman, C. M. 1955. Old-growth conversion also converts fire climate. USDA Forest Service Fire Control Notes 17:15–19.

Dale, V. H., et al. 2001. Climate change and forest disturbances. BioScience 51:723.

Dalton, M. M., J. T. Abatzoglou, L. Evers, and K. Hegewisch. 2015. Projected changes in the energy release component under climate change in northwest predictive services areas. The Oregon Climate Change Research Institute (OCCRI), Corvallis, Oregon, USA.

Davis, R. J., K. M. Dugger, S. Mohoric, L. Evers, and W. C. Aney. 2011. Northwest Forest Plan—the first 15 years (1994–2008): status and trends of northern spotted owl populations and habitat. General Technical Report PNW-GTR-850, USDA Forest Service, Pacific Northwest Research Station, Portland, Oregon, USA.

Davis, R. J., B. Hollen, J. Hobson, J. E. Gower, and D. Keenum. 2016. Northwest Forest Plan—the first 20 years (1994–2013): status and trends of northern spotted owl habitats. PNW-GTR-929. USDA Forest Service, Pacific Northwest Research Station, Portland, Oregon, USA.

Davis, R., Z. Yang, A. Yost, C. Belongie, and W. Cohen. 2017. The normal fire environment—Modeling environmental suitability for large forest wildfires using past, present, and future climate normals. Forest Ecology and Management 390:173–186.

Deeming, J. E., and J. K. Brown. 1975. Fuel models in the national fire-danger rating system. Journal of Forestry 73:347–350.

Donato, D. C., J. B. Fontaine, W. D. Robinson, J. B. Kauffman, and B. E. Law. 2009. Vegetation response to a short interval between high-severity

wildfires in a mixed-evergreen forest. Journal of Ecology 97:142–154.

Duff, T., R. Keane, T. Penman, and K. Tolhurst. 2017. Revisiting wildland fire fuel quantification methods: the challenge of understanding a dynamic, biotic entity. Forests 8:351.

Dugger, K. M., et al. 2016. The effects of habitat, climate and Barred Owls on the long-term population demographics of Northern Spotted Owls. Condor 118:57–116.

Eidenshink, J., B. Schwind, K. Brewer, Z. Ahu, B. Quayle, and S. Howard. 2007. A project for monitoring trends in burn severity. Fire Ecology Special Issue 3:3–21.

Estes, B. L., E. E. Knapp, C. N. Skinner, J. D. Miller, and H. K. Preisler. 2017. Factors influencing fire severity under moderate burning conditions in the Klamath Mountains, northern California, USA. Ecosphere 8:e01794.

Finney, M. A. 2004. FARSITE: fire area simulator—model development and evaluation. RMRS-RP-4 revised. USDA Forest Service, Rocky Mountain Research Station, Fort Collins, Colorado, USA.

Fontaine, J. B., D. C. Donato, W. D. Robinson, B. E. Law, and J. B. Kauffman. 2009. Bird communities following high-severity fire: response to single and repeat fires in a mixed-evergreen forest, Oregon, USA. Forest Ecology and Management 257:1496–1504.

Franklin, A. B., D. R. Anderson, E. D. Forsman, K. P. Burnham, and F. W. Wagner. 1996. Methods for collecting and analyzing demographic data on the Northern Spotted Owl. Studies in Avian Biology 17:12–20.

Frey, S. J. K., A. S. Hadley, S. L. Johnson, M. Schulze, J. A. Jones, and M. G. Betts. 2016. Spatial models reveal the microclimatic buffering capacity of old growth forests. Science Advances 2:e1501392.

Glenn, E. M., D. B. Lesmeister, R. J. Davis, B. Hollen, and A. Poopatanapong. 2017. Estimating density of a territorial species in a dynamic landscape. Landscape Ecology 32:563–579.

Google Earth Engine Team. 2015. Google Earth Engine: a planetary-scale geospatial analysis platform. https://earthengine.google.com/

Gorelick, N., M. Hancher, M. Dixon, S. Ilyushchenko, D. Thau, and R. Moore. 2017. Google Earth Engine: planetary-scale geospatial analysis for everyone. Remote Sensing of Environment 202:18–27.

Halofsky, J. E., et al. 2011. Mixed-severity fire regimes: lessons and hypotheses from the Klamath-Siskiyou Ecoregion. Ecosphere 2:art40.

Harris, L., and A. H. Taylor. 2017. Previous burns and topography limit and reinforce fire severity in a large wildfire. Ecosphere 8:e02019.

Harte, J., and E. A. Newman. 2014. Maximum information entropy: a foundation for ecological theory. Trends in Ecology and Evolution 29:384–389.

Heyerdahl, E. K., L. B. Brubaker, and J. K. Agee. 2001. Spatial controls of historical fire regimes: a multi scale example from the interior west, USA. Ecology 82:660–678.

Hirzel, A. H., G. Le Lay, V. Helfer, C. Randin, and A. Guisan. 2006. Evaluating the ability of habitat suitability models to predict species presences. Ecological Modelling 199:142–152.

Kennedy, R. E., Z. Yang, and W. B. Cohen. 2010. Detecting trends in forest disturbance and recovery using yearly Landsat time series: 1. LandTrendr— Temporal segmentation algorithms. Remote Sensing of Environment 114:2897–2910.

Kennedy, R. E., Z. Yang, W. B. Cohen, E. Pfaff, J. Braaten, and P. Nelson. 2012. Spatial and temporal patterns of forest disturbance and regrowth within the area of the Northwest Forest Plan. Remote Sensing of Environment 122:117–133.

Kitzberger, T., E. Araoz, J. H. Gowda, M. Mermoz, and J. M. Morales. 2012. Decreases in fire spread probability with forest age promotes alternative community states, reduced resilience to climate variability and large fire regime shifts. Ecosystems 15:97–112.

Kleiber, C., and A. Zeileis. 2009. AER: applied Econometrics with R. R package version 1.1.

Krawchuk, M. A., L. Haire, J. Coop, M.-A. Parisien, E. Whitman, G. Chong, and C. Miller. 2016. Topographic and fire weather controls of fire refugia in forested ecosystems of northwestern North America. Ecosphere 7:e01632.

Lesmeister, D. B., R. J. Davis, P. H. Singleton, and J. D. Wiens. 2018. Northern spotted owl habitat and populations: status and threats. In T. Spies, P. Stine, R. Gravenmier, J. Long, and M. Reilly, editors. Synthesis of science to inform land management within the northwest forest plan area. PNW-GTR 966. USDA Forest Service, Pacific Northwest Research Station, Portland, Oregon, USA.

Li, P., L. Jiang, and Z. Feng. 2013. Cross-comparison of vegetation indices derived from Landsat-7 enhanced thematic mapper plus (ETM+) and Landsat-8 operational land imager (OLI) sensors. Remote Sensing 6:310–329.

Lindenmayer, D. B., R. J. Hobbs, G. E. Likens, C. J. Krebs, and S. C. Banks. 2011. Newly discovered landscape traps produce regime shifts in wet forests. Proceedings of the National Academy of Sciences 108:15887–15891.

Lindenmayer, D. B., and R. F. Noss. 2006. Salvage logging, ecosystem processes, and biodiversity conservation. Conservation Biology 20:949–958.

Lydersen, J. M., B. M. Collins, J. D. Miller, D. L. Fry, and S. L. Stephens. 2016. Relating fire-caused change in forest structure to remotely sensed estimates of fire severity. Fire Ecology 12:99–116.

Manly, B. F. J., L. L. McDonald, D. L. Thomas, T. L. McDonald, and W. P. Erickson. 2010. Resource selection by animals: statistical design and analysis for field studies, 2nd edition.. Kluwer Academic Publishers, Dordrecht, The Netherlands.

McGaughey, R. J. 2015. FUSION/LDV: providing fast, efficient, and flexible access to LiDAR, IFSAR and terrain datasets. U.S. Department of Agriculture, Forest Service, Pacific Northwest Research Station, Portland, Oregon, USA.

Merow, C., M. J. Smith, T. C. Edwards, A. Guisan, S. M. McMahon, S. Normand, W. Thuiller, R. O. Wuest, N. € E. Zimmermann, and J. Elith. 2014. What do we gain from simplicity versus complexity in species distribution models? Ecography 37:1267–1281.

Millar, C. I., N. L. Stephenson, and S. L. Stephens. 2007. Climate change and forests of the future: managing in the face of uncertainty. Ecological Applications 17:2145–2151.

Miller, J. D., E. E. Knapp, C. H. Key, C. N. Skinner, C. J. Isbell, R. M. Creasy, and J. W. Sherlock. 2009. Calibration and validation of the relative differenced Normalized Burn Ratio (RdNBR) to three measures of fire severity in the Sierra Nevada and Klamath Mountains, California, USA. Remote Sensing of Environment 113:645–656.

Miller, J. D., and H. Safford. 2012. Trends in wildfire severity: 1984 to 2010 in the Sierra Nevada, Modoc Plateau, and Southern Cascades, California, USA. Fire Ecology 8:41–57.

Miller, J. D., H. D. Safford, M. Crimmins, and A. E. Thode. 2008. Quantitative evidence for increasing forest fire severity in the Sierra Nevada and southern Cascade Mountains, California and Nevada, USA. Ecosystems 12:16–32.

Miller, J. D., C. N. Skinner, H. D. Safford, E. E. Knapp, and C. M. Ramirez. 2012. Trends and causes of severity, size, and number of fires in northwestern

California, USA. Ecological Applications 22:184–203.

Miller, J. D., and A. E. Thode. 2007. Quantifying burn severity in a heterogeneous landscape with a relative version of the delta Normalized Burn Ratio (dNBR). Remote Sensing of Environment 109:66–80.

Moreira, F., F. C. Rego, and P. G. Ferreira. 2001. Temporal (1958–1995) pattern of change in a cultural landscape of northwestern Portugal: implications for fire occurrence. Landscape Ecology 16:557–567.

Moreira, F., P. Vaz, F. Catry, and J. S. Silva. 2009. Regional variations in wildfire susceptibility of land cover types in Portugal: implications for landscape management to minimize fire hazard. International Journal of Wildland Fire 18:563–574.

MTBS. 2017. MTBS Data Access: fire Level Geospatial Data. USDA Forest Service and USDI Geological Survey.

NDMC. 2018. National Drought Mitigation Center, Drought Impact Summary. https://droughtmonitor.unl.edu/DroughtSummary.aspx

Neary, D. G., C. C. Klopatek, L. F. DeBano, and P. F. Ffolliott. 1999. Fire effects on belowground sustainability: a review and synthesis. Forest Ecology and Management 122:51–71.

Noss, R. F. 2000. High-risk ecosystems as foci for considering biodiversity and ecological integrity in ecological risk assessments. Environmental Science & Policy 3:321–332.

Noss, R. F., J. F. Franklin, W. L. Baker, T. Schoennagel, and P. B. Moyle. 2006. Managing fire-prone forests in the western United States. Frontiers in Ecology and the Environment 4:481–487.

Noss, R. F., J. R. Strittholt, P. Frost, K. Vance-Borland, and C. Carroll. 1999. A conservation plan for the Klamath-Siskiyou Ecoregion. Natural Areas Journal 19:392–411.

O'Brien, R. M. 2007. A caution regarding rules of thumb for variance inflation factors. Quality & Quantity 41:673–690.

Odion, D. C., et al. 2014. Examining historical and current mixed-severity fire regimes in ponderosa pine and mixed-conifer forests of western North America. PLoS ONE 9:e87852.

OFRI. 2010. Federal Forestland in Oregon: coming to terms with active forest management of federal forestland. A Special Report of the Oregon Forest Resources Institute, Portland, Oregon, USA.

Olson, D. M., and E. Dinerstein. 1998. The global 200: a representation approach to conserving the earth's most biologically valuable ecoregions. Conservation Biology 12:502–515.

Parker, G. G., M. E. Harmon, M. A. Lefsky, J. Chen, R. V. Pelt, S. B. Weis, S. C. Thomas, W. E. Winner, D. C. Shaw, and J. F. Franklin. 2004. Three-dimensional structure of an old-growth Pseudotsuga Tsuga canopy and its implications for radiation balance, microclimate, and gas exchange. Ecosystems 7:440–453.

Parks, S. A., L. M. Holsinger, C. Miller, and C. R. Nelson. 2015. Wildland fire as a self-regulating mechanism: the role of previous burns and weather in limiting fire progression. Ecological Applications 25:1478–1492.

Pausas, J. G., and J. E. Keeley. 2009. A burning story: the role of fire in the history of life. BioScience 59:593–601.

Perry, D. A., P. F. Hessburg, C. N. Skinner, T. A. Spies, S. L. Stephens, A. H. Taylor, J. F. Franklin, B. McComb, and G. Riegel. 2011. The ecology of mixed severity fire regimes in Washington, Oregon, and Northern California. Forest Ecology and Management 262:703–717.

Peterson, G. D. 2002. Contagious disturbance, ecological memory, and the emergence of landscape pattern. Ecosystems 5:329–338.

Phillips, S. J., R. P. Anderson, and R. E. Schapire. 2006. Maximum entropy modeling of species geographic distributions. Ecological Modelling 190:231–259.

Phillips, S. J., and J. Elith. 2013. On estimating probability of presence from use–availability or presence–background data. Ecology 94:1409–1419.

R Core Team. 2016. R: a language and environment for statistical computing. R Foundation for Statistical Computing, Vienna, Austria.

Raymond, C. L., and D. L. Peterson. 2005. Fuel treatments alter the effects of wildfire in a mixed-evergreen forest, Oregon, USA. Canadian Journal of Forest Research 35:2981–2995.

Reilly, M. J., C. J. Dunn, G. W. Meigs, T. S. Spies, R. E. Kennedy, J. D. Bailey, and K. Briggs. 2017. Contemporary patterns of fire extent and severity in forests of the Pacific Northwest, USA (1985–2010). Ecosphere 8:e01695.

Rockweit, J. T., A. B. Franklin, and P. C. Carlson. 2017. Differential impacts of wildfire on the population dynamics of an old-forest species. Ecology 98:1574–1582.

Scheffer, M., and S. R. Carpenter. 2003. Catastrophic regime shifts in ecosystems: linking theory to observation. Trends in Ecology & Evolution 18:648–656.

Schoennagel, T., T. T. Veblen, and W. H. Romme. 2004. The interaction of fire, fuels, and climate across Rocky Mountain forests. BioScience 54:661–676.

Schroeder, T. A., M. A. Wulder, S. P. Healey, and G. G. Moisen. 2011. Mapping wildfire and clearcut harvest disturbances in boreal forests with Landsat time series data. Remote Sensing of Environment 115:1421–1433.

Scott, J. H., and R. E. Burgan. 2005. Standard fire behavior fuel models: a comprehensive set for use with Rothermel's surface fire spread model. RMRS GTR-153. USDA Forest Service, Rocky Mountain Research Station, Fort Collins, Colorado, USA.

Serra-Diaz, J. M., C. Maxwell, M. S. Lucash, R. M. Scheller, D. M. Laflower, A. D. Miller, A. J. Tepley, H. E. Epstein, K. J. Anderson-Teixeira, and J. R. Thompson. 2018. Disequilibrium of fire-prone forests sets the stage for a rapid decline in conifer dominance during the 21st century. Scientific Reports 8:6749.

Sousa, W. P. 1984. The role of disturbance in natural communities. Annual Review of Ecology and Systematics 15:353–359.

Sovern, S. G., D. B. Lesmeister, K. M. Dugger, M. S. Pruett, R. J. Davis, and J. M. Jenkins. 2019. Activity center selection by northern spotted owls. Journal of Wildlife Management Early View. https://doi. org/10.1002/jwmg/21632

Spies, T. A., M. A. Hemstrom, A. Youngblood, and S. Hummel. 2006. Conserving old-growth forest diversity in disturbance-prone landscapes. Conservation Biology 20:351–362.

Spies, T. A., P. F. Hessburg, C. N. Skinner, K. J. Puettmann, M. J. Reilly, R. J. Davis, J. A. Kertis, J. W. Long, and D. C. Shaw. 2018. Old growth, disturbance, forest succession, and management in the area of the Northwest Forest Plan. In T. A. Spies, P. Stine, R. Gravenmier, J. W. Long, and M. J. Reilly, editors. Synthesis of Science to inform land management within the northwest forest plan area. PNW-GTR-966. USDA Forest Service, Pacific Northwest Research Station, Portland, Oregon, USA.

Stephens, S. L., et al. 2009. Fire treatment effects on vegetation structure, fuels, and potential fire severity in western U.S. forests. Ecological Applications 19:305–320.

Taylor, A. H., and C. N. Skinner. 1998. Fire history and landscape dynamics in a late-successional reserve, Klamath Mountains, California, USA. Forest Ecology and Management 111:285–301.

Tepley, A. J., J. R. Thompson, H. E. Epstein, and K. J. Anderson-Teixeira. 2017. Vulnerability to forest loss through altered postfire recovery dynamics in a warming climate in the Klamath Mountains. Global Change Biology 23:4117–4132.

Thompson, J. R., and T. A. Spies. 2009. Vegetation and weather explain variation in crown damage within a large mixed-severity wildfire. Forest Ecology and Management 258:1684–1694.

Thompson, J. R., and T. A. Spies. 2010. Factors associated with crown damage following recurring mixed-severity wildfires and post-fire management in southwestern Oregon. Landscape Ecology 25:775–789.

Thompson, J. R., T. A. Spies, and L. M. Ganio. 2007. Reburn severity in managed and unmanaged vegetation in a large wildfire. Proceedings of the National Academy of Sciences 104:10743–10748.

Turner, M. G., and W. H. Romme. 1994. Landscape dynamics in crow fire ecosystems. Landscape Ecology 9:59–77.

USDA and USDI. 1994. Final supplemental environmental impact statement on management of habitat for late-successional and old-growth forest related species within the range of the northern spotted owl. USFS, Portland, Oregon, USA.

USFWS. 1990. Endangered and threatened wildlife and plants: determination of threatened status for the northern spotted owl. Federal Register 55:26114–26194.

USFWS. 2011. Revised recovery plan for the northern spotted owl (Strix occidentalis caurina). USDI Fish and Wildlife Service, Portland, Oregon, USA.

Van Pelt, R. 2008. Identifying old trees and forest in Eastern Washington. Washington State Department of Natural Resources, Olympia, Washington, USA.

Vance-Borland, K. W. 1999. Physical habitat classification for conservation planning in the Klamath Mountains region. Thesis. Oregon State University, Corvallis, Oregon, USA.

Weatherspoon, C. P., S. J. Husari, and J. W. van Wagtendonk. 1992. Fire and fuels management in relation to owl habitat in forests of the Sierra Nevada and southern California. In J. Verner, K. S. McKelvey, B. R. Noon, R. J. Gutierrez, G. I. Gould Jr., and T. W. Beck, editors. The California spotted owl: a technical assessment of its current status. PSW-GTR-133. USDA Forest Service, Pacific Southwest Research Station, Albany, California, USA.

Westerling, A. L., H. G. Hidalgo, D. R. Cayan, and T. W. Swetnam. 2006. Warming and earlier spring increase western U.S. forest wildfire activity. Science 313:940–943.

Wilk, R. J., D. B. Lesmeister, and E. D. Forsman. 2018. Nest trees of northern spotted owls (Strix occidentalis caurina) in Washington and Oregon, USA. PLoS ONE 13:e0197887.

Zald, H. S. J., and C. J. Dunn. 2018. Severe fire weather and intensive forest management increase fire severity in a multi-ownership landscape. Ecological Applications 28:1068–1080.

SUPPORTING INFORMATION

Additional Supporting Information may be found online at: http://onlinelibrary.wiley.com/doi/10.1002/ecs2.

EXHIBIT D

Ecological Importance of Large-Diameter Trees in a Temperate Mixed-Conifer Forest

James A. Lutz[1]*, Andrew J. Larson[2], Mark E. Swanson[3], James A. Freund[4]

1 College of the Environment, University of Washington, Seattle, Washington, United States of America, 2Department of Forest Management, University of Montana, Missoula, Montana, United States of America, 3 School of the Environment, Washington State University, Pullman, Washington, United States of America, 4 School of Environmental and Forest Sciences, University of Washington, Seattle, Washington, United States of America

Abstract

Large-diameter trees dominate the structure, dynamics and function of many temperate and tropical forests. Although both scaling theory and competition theory make predictions about the relative composition and spatial patterns of large diameter trees compared to smaller diameter trees, these predictions are rarely tested. We established a 25.6 ha permanent plot within which we tagged and mapped all trees $1 cm dbh, all snags $10 cm dbh, and all shrub patches $2 m^2. We sampled downed woody debris, litter, and duff with line intercept transects. Aboveground live biomass of the 23 woody species was 507.9 Mg/ha, of which 503.8 Mg/ha was trees (SD = 114.3 Mg/ha) and 4.1 Mg/ha was shrubs. Aboveground live and dead biomass was 652.0 Mg/ha. Large-diameter trees comprised 1.4% of individuals but 49.4% of biomass, with biomass dominated by Abies concolor and Pinus lambertiana (93.0% of tree biomass). The large-diameter component dominated the biomass of snags (59.5%) and contributed significantly to that of woody debris (36.6%). Traditional scaling theory was not a good model for either the relationship between tree radii and tree abundance or tree biomass. Spatial patterning of large-diameter trees of the three most abundant species differed from that of small-diameter conspecifics. For A. concolor and P. lambertiana, as well as all trees pooled, large-diameter and small-diameter trees were spatially segregated through inter-tree distances ,10 m. Competition alone was insufficient to explain the spatial patterns of large-diameter trees and spatial relationships between large-diameter and small-diameter trees. Long-term observations may reveal regulation of forest biomass and spatial structure by fire, wind, pathogens, and insects in Sierra Nevada mixed-conifer forests. Sustaining ecosystem functions such as carbon storage or provision of specialist species habitat will likely require different management strategies when the functions are performed primarily by a few large trees as opposed to many smaller trees.

Citation: Lutz JA, Larson AJ, Swanson ME, Freund JA (2012) Ecological Importance of Large-Diameter Trees in a Temperate Mixed-Conifer Forest. PLoS ONE 7(5): e36131. doi:10.1371/journal.pone.0036131

Editor: Ben Bond-Lamberty, DOE Pacific Northwest National Laboratory, United States of America

Received February 14, 2012; Accepted March 28, 2012; Published May 2, 2012

Funding: Funding was received from the Smithsonian Institution Center for Tropical Forest Science (http://www.ctfs.si.edu/) and the University of Washington College of the Environment (http://coenv.washington.edu/). In-kind support was received from the University of Washington, the University of Montana, Washington State University, the US Geological Survey, and Yosemite National Park. The funders had no role in study design, data collection and analysis, decision to publish, or preparation of the manuscript.

Competing Interests: The authors have declared that no competing interests exist.

* E-mail: jlutz@uw.edu

Introduction

Large-diameter trees dominate the structure, dynamics, and function of many temperate and tropical forest ecosystems and are of considerable scientific and social interest. They comprise a large fraction of forest wood volume, biomass and carbon stocks [1,2], and modulate stand-level leaf area, transpiration, and microclimates [3,4]. Large-diameter trees contribute disproportionately to reproduction [5], influence the rate and pattern of tree regeneration and forest succession [6], and originate further disturbance by crushing or injuring neighboring trees when they fall to the ground [7,8]. Arboreal wildlife species preferentially occupy large trees as habitat (e.g. [9]), and the greater structural complexity of large tree crowns [10] supports habitat for obligate wildlife species (e.g. [11]), unique epiphyte communities [12], and soil development and water storage within the forest canopy [13].

Large-diameter trees continue to contribute disproportionately to forest ecosystem structure and function after they die. Dead large-diameter trees persist as standing snags for many years, providing additional wildlife habitat. In temperate forests large diameter logs may persist on the forest floor for centuries, where they continue to provide habitat for diverse assemblages of vertebrates and invertebrates and microorganisms, store carbon and other nutrients, serve as substrates for tree regeneration, and play numerous other functional roles [14,15].

Human societies derive many non-timber values from large diameter trees. Tree ring chronologies from large trees provide long records of past forest development and disturbance [16], as well as proxy records of annual climatic variation [17]: they are an important source of the data required to test and refine ecological theories and models. Large trees are culturally [18] and spiritually important [19] in many societies; individuals and organizations maintain large tree registries (e.g., [20]), and government agencies manage parks and preserves dedicated to the conservation of exceptionally large trees, such as Redwood and Sequoia & Kings Canyon National Parks in California, USA.

Populations of large-diameter trees can be intractable study subjects. Large-diameter trees occur at low densities and estimates of their abundance, spatial patterns, and contributions to ecosystem function (e.g. biomass) are subject to high rates of sampling error [21,22]. Consequently, descriptive statistics and hypothesis tests for large-diameter trees require very large sample plots [22]. The combination of low abundance and low mortality rates [8,23,24] make detecting changes in demographic rates or spatial patterns of large-diameter trees even more difficult, further underscoring the requirement for large sample plots. Conventional studies based on small (1 ha to 4 ha) plots often do not contain enough large-diameter trees to conduct even community-level (i.e., pooled across species) analyses (e.g., [24]). Consequently, despite their ecological and cultural significance, relatively less is known – and with greater uncertainty – about the abundance, distribution, and dynamics of large-diameter trees.

Predictions for large-diameter trees

Scaling theory and competition theory both provide frameworks for predictions about the relative contributions of large-diameter structures to aboveground biomass, the spatial distribution of large-diameter trees, and the spatial relationships between large diameter and small-diameter trees. Scaling theory predicts that a relatively few trees in the largest diameter classes will dominate stand-level aboveground biomass [25,26], and that there are continuous relationships between tree diameter and density, and total forest biomass. However, scaling theory has been repeatedly shown to underpredict large tree densities and mortality rates [27,28]. This discrepancy likely arises because trees rarely die from competition once they reach large sizes but rather succumb to biological agents, physical disturbances, and combinations thereof [8,29]. Although scaling theory predicts dominance of biomass pools by a few large individuals, the simplifying assumptions about tree mortality embedded in the theory may render it inadequate to predict accurately either the aggregate large tree contributions to stand biomass or the local-scale variation. We were interested in quantifying the actual contribution of large-diameter pieces to aboveground biomass pools—which should be substantial [14]— because predictions from scaling theory alone may not be accurate enough to serve as inputs into ecosystem models or to support sound natural resource policies and management.

Tree spatial patterns integrate past tree-tree interactions. Competition theory predicts that distance and density-dependent growth and mortality during forest development will lead to increasingly uniform spatial patterns in larger diameter classes [30,31]. Therefore, the arrangement of large-diameter trees should be more uniform than small-diameter trees, and the largest trees should exhibit spatial regularity at the tree neighborhood scale. Competition theory also predicts spatial relationships between large and small-diameter trees. When large trees compete asymmetrically with small trees their respective spatial locations become segregated because seedlings preferentially survive and grow into understory trees where they are not suppressed by larger competitors [30,32,33].

Our study was motivated by three purposes: (1) determine the degree to which predictions from ecological theory hold for contemporary populations of large-diameter trees; (2) establish a permanent forest research plot of sufficient size to detect and attribute forest ecosystem change, including for the large-diameter component, in order to test future predictions against longitudinal data; and (3) support current management efforts to restore large diameter tree populations in Sierra Nevada mixed-conifer forest, which were dramatically reduced by widespread logging through out the range of this important forest type during the 19th and 20th centuries [34,35]. We established the Yosemite Forest Dynamics Plot (YFDP) in an old-growth Sierra Nevada mixed-conifer forest and within the plot quantified the relative contribution of large diameter trees, snags, and down woody debris to the aboveground biomass pools, the comparative spatial patterns of large-diameter and small-diameter trees, and spatial relationships between them.

Results

Species composition

In the 25.6 ha of the Yosemite Forest Dynamics Plot (YFDP), there were 34,458 live stems $1 cm dbh of 11 tree species (Table 1) and 3.87 ha (15.1%) of continuous shrub cover comprising 12 shrub species that reach 1 cm in diameter at 1.37 m height (Table 2). Eleven plant families were represented. All woody stems were native plants. Live tree basal area was 64.3 m^2/ha and biomass was 503.8 Mg/ha (SD = 114.3 Mg/ha) (Table 3). Of the three principal species by biomass (Pinus lambertiana, Abies concolor, and Calocedrus decurrens), P. lambertiana had a much higher average biomass (Fig. 1) and exhibited a rotated sigmoid diameter distribution, possibly reflecting lower mortality of middle-aged individuals (Fig. 2). Diameter distributions of A. concolor and C. decurrens followed negative exponential distributions (Fig. 2). Relative dominance of Abies concolor declines at diameters above ,90 cm (Fig. 2). Calocedrus decurrens exhibits almost an order of magnitude less biomass than either P. lambertiana or A. concolor (Fig. 2). However, some individuals do persist into large diameter classes (Fig. 2). Live shrub biomass was 4.1 Mg/ha (Table 2). There were 2,697 snags (19.9% of living trees of this diameter). Biomass of snags $10 cm dbh was 43.0 Mg/ha (Table 3). Biomass of the forest floor components (Table 3, Fig. 3) was 53.1 Mg/ha for down woody debris (SD = 102.9 Mg/ha) and 48.0 Mg/ha (SD = 22.5) for fine fuels (Table 3). Litter and duff averaged 1.05 cm (SD = 0.38) and 1.20 cm (SD = 0.68) in depth, respec tively. A correlogram analysis of woody debris volumes as estimated by the 20 m line intercept segments showed no spatial correlation in fuel loads at any distance. Total above-ground biomass of living and dead components was 652.0 Mg/ha.

Large-diameter composition

The large diameter component dominated most biomass pools (Table 3). For living trees, 1.4% of individuals had dbh $100 cm dbh (19.1 large-diameter trees ha^{21}), but these individuals comprised 49.4% of tree biomass. For snags, 12.4% were large diameter, comprising 59.5% of snag biomass. Snags $100 cm dbh were about half as numerous (42.9%) as live trees $100 cm dbh. There were 10 pieces of woody debris $100 cm (3.8%) measured on the line intercepts, and the large debris component comprised 36.6% of down woody debris biomass. There is, by definition, no large-diameter component to shrubs, fine fuels, litter or duff. Overall, large-diameter structures constituted 44.9% of above ground live and dead biomass.

Scaling theory was informative for the relationship between tree density and diameter class (r^2= 0.84); the theoretical relationship under-predicted the density of medium and large trees, but over predicted the density of trees $170 cm dbh (Fig. 2). Although informative, the relationship between tree density and diameter class was better explained by a negative exponential distribution (r^2= 0.99). The theoretical relationship between tree radii and biomass was not informative (r^2= 0.00) (Fig. 2).

Spatial patterns

Small-diameter subpopulations of A. concolor, C. decurrens, P. lambertiana, as well as all tree species combined, exhibited significant aggregation relative to the null model of complete spatial randomness (CSR) from 0–9 m (Monte Carlo goodness-of

Table 1. Tree species within the Yosemite Forest Dynamics Plot in 2010.

Tree species	Family	Trees $1 cm dbh Density (stems/ha)	Basal area (m^2/ha)	Stems $ 1 cm dbh	Stems $ 10 cm dbh	Stems $ 100 cm dbh	Large diameter prop. (%)
Abies concolor	Pinaceae	956.3	29.28	24,481	9,634	103	0.4
Pinus lambertiana	Pinaceae	185.5	28.75	4,748	2,166	339	7.1
Cornus nuttallii	Cornaceae	92.5	0.26	2,368	287	-	-
Calocedrus decurrens	Cupressaceae	62.2	4.78	1,592	685	45	2.8
Quercus kelloggii	Fagaceae	43.3	1.12	1,109	735	-	-
Prunus spp.	Rosaceae	5.0	t	128	-	-	-
Abies magnifica	Pinaceae	0.4	0.06	11	5	1	9.1
Salix scouleriana	Salicaceae	0.4	t	11	-	-	-
Pseudotsuga menziesii	Pinaceae	0.2	0.03	6	3	1	16.7
Pinus ponderosa	Pinaceae	t	0.01	2	1	-	-
Rhamnus californica	Rhamnaceae	t	t	1	-	-	-
Live tree total		1,346.0	64.32	34,458	13,516	489	1.4
Snags $10 cm dbh							
Abies concolor					1,971	64	3.2
Pinus lambertiana					530	133	25.1
Quercus kelloggii					127	-	-
Calocedrus decurrens					46	5	10.9
Pseudotsuga menziesii					1	1	100.0
Cornus nuttallii					1	--	
Unknown					21	7	33.3
Dead tree total					2,697	210	7.8

t – trace; less than one tree per 10 ha; less than 0.01 m^2/ha.

doi:10.1371/journal.pone.0036131.t001

Table 2. Shrub species occurring in patches of continuous cover $2 m^2 within the Yosemite Forest Dynamics Plot in 2010.

Species	Family	Cover (m^2)	Demography plot data		YFDP extrapolation	
			Density[a] (stems/m^2)	Biomass (kg/m^2)	Density (stems/ha)	Biomass (Mg/ha)
Arctostaphylos patula	Ericaceae	2,524	5.333	14.747	526	1.454
Ceanothus cordulatus	Rhamnaceae	1,220	1.667	1.189	79	0.057
Ceanothus integerrimus	Rhamnaceae	194	7.875	10.427	60	0.079
Ceanothus parvifolius	Rhamnaceae	187	3.250	1.527	24	0.011
Chrysolepis sempervirens	Fagaceae	13,082	3.167	1.464	1,618	0.748
Corylus cornuta var. californica	Betulaceae	13,310	1.000	1.565	520	0.814
Cornus serecia	Cornaceae	2,320	8.667	6.087	785	0.552
Leucothoe davisiae	Ericaceae	2,151	0.250	2.430	21	0.204
Vaccinium uliginosum	Ericaceae	2,937	0.083	1.069	10	0.123
Sambucus racemosa[b]	Adoxaceae	13	1.000	1.565	t	0.001
Rhododendron occidentale[c]	Ericaceae	687	0.083	1.069	2	0.029
Ribes nevadense[c]	Grossulariaceae	7	0.083	1.069	t	t
Ribes roezlii[d]	Grossulariaceae	66	0	0.534	0	0.001
Total		38,698			3,645	4.103

Baseline density and biomass equations were generated from 25, 2 m62 m shrub demography plots, and allometric equations from [90].

[a] Stems $1 cm dbh.

[b] Substituted biomass and density for Corylus cornuta var. californica.

[c] Substituted biomass and density for Vaccinium uliginosum.

[d] Substituted one half the biomass of Vaccinium uliginosum. No stems reach 1 cm dbh.

t – trace; ,1 stem/ha; ,1 kg/ha.

doi:10.1371/journal.pone.0036131.t002

Table 3. Biomass within the Yosemite Forest Dynamics Plot in 2010.

Large-diameter prop.
Tree species Biomass $1 cm (Mg/ha) Biomass $10 cm (Mg/ha) Biomass $100 cm (Mg/ha) (%)

Trees $1 cm

Abies concolor 214.703 (37.505) 210.533 (36.916) 47.983 (8.950) 22.3 Pinus lambertiana 254.039 (66.623) 253.380 (66.508) 187.345 (47.594) 73.7 Cornus nuttallii 1.411 (0.301) 0.765 (0.199) - - - Calocedrus decurrens 24.978 (7.911) 24.764 (7.845) 12.964 (4.076) 51.9 Quercus kelloggii 7.849 (1.935) 7.736 (1.907) - - - Prunus spp. 0.005 (0.002) - - - - - Abies magnifica 0.609 (0.110) 0.609 (0.110) 0.469 (0.078) 77.0 Salix scouleriana tt - - -- - Pseudotsuga menziesii 0.146 (0.033) 0.144 (0.032) 0.134 (0.030) 91.8 Pinus ponderosa 0.064 (0.003) 0.064 (0.003) - - - Rhamnus californica tt - - -- -

Live tree total 503.804 (114.346) 497.994 (113.444) 248.896 (60.651) 49.4 Snags $10 cm

Abies concolor 20.276 6.708 33.1 Pinus lambertiana 21.167 17.959 84.8 Quercus kelloggii 0.244 - - Calocedrus decurrens 0.893 0.551 61.7 Pseudotsuga menziesii 0.196 0.196 100.0 Cornus nuttallii t--

Unknown 0.181 0.147 81.2 Dead tree total 42.958 25.562 59.5 Forest floor woody debris $10 cm 53.099 (102.897) 19.444 (78.977) 36.6

Shrubs total 4.103 - - -

Forest floor fine fuels{

100-hour fuels 4.562 (4.820) - - - 10-hour fuels 5.176 (3.487) - - - 1-hour fuels 1.129 (0.834) - - - Litter 13.150 (6.244) - - - Duff 24.017 (16.517) - - - Total fine fuels 48.034 (22.495) - - -

Biomass is shown to three significant figures (corresponding to 1 kg/ha) to facilitate comparison between less abundant, small-diameter species and more abundant species (standard deviation shown in parentheses). Standard deviation of tree biomass was based on the root mean squared error of the underlying allometric equations, and standard deviation of down woody debris biomass was based on Brown's method [89]. Biomass of shrubs and snags are derived from cover (m^2) or measured dimensions and fixed wood density values [see Methods]. Total of living and dead biomass pools was 652.0 Mg/ha. t – trace; less than 1 kg/ha.

{Fine litter measured by fuel classifications [88]. 100-hour fuels are defined as twigs and fragments with diameter 10 to 30 (2.5 cm to 7.6 cm); 10-hour fuels have diameter 0.250 to 10 (0.6 cm to 2.5 cm); 1-hour fuels have diameter 00 to 0.250 (0 cm to 0.6 cm). Litter and duff are measured by depth.

doi:10.1371/journal.pone.0036131.t003

fit tests; A. concolor: P = 0.004; C. decurrens: P = 0.001; P. lambertiana: P = 0.001, all trees: P = 0.004). In other words, when averaged across all points in a given pattern, small-diameter trees of these species have more neighbors of the same type located within a circle with a radius of 9 m than would be expected if tree locations were completely independent of each other. $\hat{L}(r)$ values for small diameter stems of both P. lambertiana and A. concolor rose steeply at small scales (Fig. 4), reaching a plateau at about 20 m, indicating that the strong spatial aggregation in these respective subpopulations primarily manifests at scales ,20 m. The $\hat{L}(r)$ curves for small-diameter C. decurrens stems rose steadily from 0–80 m, indicating moderate but consistent clustering across the entire range of scales analyzed (Fig. 4).

The spatial arrangement of large-diameter A. concolor, C. decurrens and P. lambertiana individually, and for all species combined, were not different from complete spatial randomness from 0–9 m (Monte Carlo goodness-of-fit tests; A. concolor: P = 0.012; C. decurrens: P = 0.074; P. lambertiana: P = 0.132; all trees: P = 0.057). However, the behavior of the individual $\hat{L}(r)$ curves from 0–80 m reveals spatial structure within large-diameter A. concolor and P. lambertiana subpopulations at other interpoint distances (Fig. 4). The empirical $\hat{L}(r)$ curve (Fig. 4) for large-diameter P. lambertiana was negative and steadily decreased from 0–2 m, tracking the lower boundary of the simulation envelope, indicating spatial inhibition at these scales. From 2–4 m the large-diameter P. lambertiana $\hat{L}(r)$ curve sharply increased, providing evidence of

Figure 1. Heterogeneity in biomass and density of the principal tree species of the Yosemite Forest Dynamics Plot. Each boxplot represents

values from the 640, 20 m620 m quadrats of the plot.
doi:10.1371/journal.pone.0036131.g001

Figure 2. Diameter distribution of the number of trees and the biomass of trees in the Yosemite Forest Dynamics Plot. Each point represents a 5 cm diameter class (first bin; 1 cm#dbh,5 cm) of the trees from the entire 25.6 ha plot (34,458 live stems $1 cm dbh totaling 12,897 Mg); identical data are shown with linear diameter bins (left) and log diameter (right). Solid lines represent the best fitting equation of the form specified by scaling theory, tree density~Ar$^{\{2}$ (r^{2} = 0.84) and biomass~Br$^{2=3}$ (r^{2} = 0.00), where r is tree radius.
doi:10.1371/journal.pone.0036131.g002

Discussion

The relative proportion of large trees varies in old-growth forests worldwide [28], and at 49.4%, the contribution that large diameter trees make to the total biomass of the YFDP is higher than in most other forests. Although some forests have almost all of their biomass concentrated in large-diameter trees (most notably Sequoia sempervirens; [13,36]), the biomass of most forest types is concentrated in trees ,100 cm dbh. In a 1 ha plot in tropical moist forests of Rondoˆnia, Brazil, Brown et al. [1] found that three trees $100 cm dbh had biomass of 64.3 Mg compared to a total aboveground biomass of 285 Mg (22.6%). In 5.15 ha of neotropical lowland rain forest in Costa Rica, Clark & Clark [2] found that trees $70 cm dbh comprised 27% of the biomass of 241 Mg/ha (,18% for trees $100 cm dbh; [2], Fig. 1). In semi-evergreen forests of northeast India, Baishya et al. [37] found ,12% of biomass in trees $100 cm dbh, and plantation forests or forests that are recovering from disturbance may have few or no large

Figure 3. Biomass of forest floor components of the Yosemite Forest Dynamics Plot. Each boxplot represents values from 112 transects of 20 m (2.24 km of line transects). Outliers represent intercepted pieces of large-diameter debris.
doi:10.1371/journal.pone.0036131.g003

spatial clustering at these scales, with continued evidence for clustering occurring out to 22 m, where the empirical value reached the upper bound of the simulation envelope. Large diameter A. concolor also exhibited rapid changes in spatial pattern at small scales, with steadily decreasing $\hat{L}(r)$ values from 0–3 m (evidence of spatial inhibition) then increasing sharply from 3– 5.5 m, indicating strong spatial clustering over this short range of scales. A sustained increase in the $\hat{L}(r)$ curve for large-diameter A. concolor from 13–38 m provided further evidence for spatial aggregation at larger scales. The $\hat{L}(r)$ curves for large-diameter C. decurrens stems rose steadily from 0–80 m, reaching the upper bound of the simulation envelope at 30 m, indicating moderate but consistent clustering across these scales.

The relative spatial patterns of large- and small-diameter trees differed for all species combined, as well as for P. lambertiana and A. concolor, but not for C. decurrens. Small-diameter P. lambertiana were always more aggregated than large conspecifics at the same scale. Large-diameter A. concolor were less aggregated than conspecific small-diameter trees at scales of 0–3 m, then rapidly became more aggregated than small trees from 3–6 m, and remained so up to 80 m (Fig. 4). The spatial pattern of large and small C. decurrens subpopulations was similar from 0–80 m (Fig. 4).

We found evidence for negative associations between large diameter and small-diameter P. lambertiana and A. concolor, and for all tree species combined, relative to the population independence hypothesis when evaluated from 0–9 m (Monte Carlo goodness-of fit tests; A. concolor: P = 0.001; P. lambertiana: P = 0.001; all trees: P = 0.001). Spatial locations of large-diameter and small-diameter C. decurrens were independent at the 9 m neighborhood scale (Monte Carlo goodness-of-fit test; P = 0.378). The $\hat{L}_{1,2}(r)$ curve for P. lambertiana (Fig. 5) indicates spatial repulsion between large and small from 0–10 m, and modest attraction from 10–40 m. The $\hat{L}_{1,2}(r)$ curve for A. concolor decreased steadily from 0–80 m, but was only outside the simulation envelope at scales less than 10 m. Large and small stems of C. decurrens were spatially attracted from 15–80 m, with the empirical $\hat{L}_{1,2}(r)$ curve at or beyond the upper boundary of the simulation envelope (Fig. 5).

diameter trees, even when stem density and diversity are high [37,38].

Within the Smithsonian Center for Tropical Forest Science network (http://www.ctfs.si.edu/plots/), only the Gilbertiodendron dewevrei (mbau) forest of the Congo has a higher live biomass, with the dipterocarp forests of Malaysia having equivalent live biomass (Table 4, [39,40]). Other old-growth forest types have a biomass of ,60% of the YFDP [39]. When the live and dead biomass are considered together, the biomass of the YFDP is 652.0 Mg/ha, currently the highest in the CTFS network. Unlike either of the high-biomass tropical plots, live biomass in the YFDP is dominated by two tree species (both Pinaceae), Pinus lambertiana (50.4% biomass) and Abies concolor (42.6% biomass), while down woody debris biomass is similarly dominated by these two species (57% and 32%, respectively). Scaling theory did not describe the distribution of biomass in this system (Fig. 2). Differences between theory and this forest are likely driven by the reoccurrence of fire throughout the period of stand development, and because of mortality rates that vary with diameter class. However, the very high levels of heterogeneity in density and biomass at 20 m scales (Fig. 1) would make scaling theory even less informative in study areas smaller than the YFDP.

Although the YFDP has high biomass, the diversity of woody plants $1 cm dbh is the lowest among the CTFS plots $25 ha. The combination of summer drought and winter snow may reduce the species pool. Other temperate plots (Changbaishan, Wabikon, and the Smithsonian Ecological Research Center, SERC) have higher species diversity [41,42]. However, those plots either receive precipitation evenly distributed throughout the year (Wabikon and SERC), or the wet season coincides with the growing season (Changbaishan).

One almost ubiquitous difficulty in biomass analyses of large diameter trees is the uncertainty of allometric equations. The use of previously published equations to predict biomass of large trees from ground-level measurement of DBH assumes that these equations were based on adequate sampling of large trees. However, most allometric equations for tree biomass have been developed from dissection of 10–50 trees [43], and the number of large trees used in formulating equations is very low. Some of the large-diameter P. lambertiana, A. concolor, and C. decurrens exceeded the maximum diameter of any that have been dissected, and for these individual trees, substitute species were used [see Appendix S1]. Moreover, DBH is often a poor predictor of whole-tree biomass as large tree DBH is a poor reflection of tree size [10]. Nonetheless, many comparative studies of primary forest biomass use allometric equations that probably predict large-diameter tree

Figure 4. Univariate tree spatial patterns in the Yosemite Forest Dynamics Plot. Solid black lines show the $\hat{L}(r)$ statistic for the actual patterns, where r is the intertree distance; thin gray lines show $\hat{L}(r)$ curves for 999 simulations of complete spatial randomness. Positive values indicate spatial clumping and negative values indicate spatial regularity. Large-diameter trees are $100 cm dbh; small-diameter trees are ,100 cm dbh.

doi:10.1371/journal.pone.0036131.g004

biomass poorly (i.e. [39,40]). Our calculations (Table 3) have been presented to a level of 1 kg/ha to enable comparison of forest dominants with less common and smaller tree species and likely represent an underestimation of whole tree biomass. However, the SD of biomass for principal species in the YFDP is 17% to 32% of the calculated value (Table 3), so the uncertainty of the large diameter biomass could be larger than the smaller biomass pools.

Biomass calculations for shrubs, snags, and woody debris also embody several simplifying assumptions (i.e. uniform stem density per unit area, single measures of diameter, simple geometry, no hollows in snags) that could lead to imprecise biomass totals.

Unlike the tropical forests where decomposition of snags and woody debris is rapid, the YFDP features considerable biomass of standing and down woody debris, also a characteristic of

Figure 5. Spatial interactions between large-diameter and small-diameter trees. Solid black lines show the $\hat{L}_{1,2}(r)$ statistic for the actual pattern, where r is the intertree distance; thin gray lines show $\hat{L}(r)$ curves for 999 patterns simulated by synchronous random torodial shifts of large and small tree subpopulations. Positive values indicate spatial attraction and negative values indicate spatial repulsion. Large-diameter trees are $100 cm dbh; small-diameter trees are ,100 cm dbh.
doi:10.1371/journal.pone.0036131.g005

temperate broadleaf forests [44]. The combination of snowy winters and dry summers contributes to slow decomposition, and even the fastest decomposing tree species (A. concolor) has a half-life of 14 years [14]. Large-diameter snags account for a relatively high proportion of total snag biomass, while large-diameter down woody debris accounted for a lower proportion of the woody debris. This may be due to low-severity fires in the historical period that might have consumed large-diameter woody debris via glowing combustion, decreasing the proportion relative to snag representation [45], or because small snags tend to fall over relatively quickly, thus being better represented in the woody debris pool. The lack of spatial correlation of the woody debris at any scale suggests that, while mortality may be non-random, tree and snag-fall events may result in loss of spatial pattern between standing individuals and the patterns of down wood they produce.

The observed univariate spatial patterns of large and small trees provide modest support for the inference that past competition contributed to the present spatial distribution of large-diameter trees. In particular, the increasing spatial uniformity from small to large size classes is consistent with competition theory [30,31]. However, the observed random arrangement of large trees at neighborhood scales differs from spatial uniformity expected when competition is the dominant process affecting tree spatial patterns. Previous studies of large-diameter tree spatial patterns in Sierra Nevada mixed-conifer forests agree with our findings (N.B., with large-diameter thresholds differing somewhat from 100 cm). Van Pelt and Franklin [32] found that main canopy trees at Giant Forest in Sequoia National Park were not different from spatial randomness at scales ,9 m. In addition, their empirical $\hat{L}(r)$ curve [32] was similar to those for P. lambertiana and A. concolor in the YFDP: inhibited from 0–1.5 m. The observed small-scale (0– 3 m) inhibition is most likely due to physical requirements for minimum hard core spacing due to the large size of the boles and limits to crown plasticity, although resource competition may

Table 4. Comparison of the Yosemite Forest Dynamics Plot with other Smithsonian CTFS-affiliated forest plots.

Location	Latitude	Forest type	Live biomass (Mg/ha)	Live and dead biomass (Mg/ ha)	Woody species	Citation
Changbaishan, China	42.2uN	Korean pine mixed forest	318.9		52	Hao et al. [41]
Yosemite, USA	37.8uN	Mixed-conifer forest	507.9	652.0	23	This study
BCI, Panama	9.2uN	Lowland tropical moist forest	306.5		299	Chave et al. [39]
Lambir, Malaysia	4.2uN	Mixed dipterocarp forest	497.2		1,182	Chave et al. [39]
Lenda, Congo	1.3uN	Mbau forest	549.7		423	Makena et al. [40]

Live biomass includes woody stems $1 cm dbh. Live and dead biomass includes snags $10 cm dbh and forest floor components as well as live biomass (also see [38] for basal area comparisons among additional large forest plots.
doi:10.1371/journal.pone.0036131.t004

contribute as well. At Teakettle Experimental Forest (an old growth, mixed-conifer forest 100 km south of the YFDP), stems $76 cm dbh were randomly arranged from 0–60 m [46]. However, Bonnicksen and Stone [47] found that main canopy P. lambertiana and A. concolor trees were uniformly spaced in a giant sequoia mixed-conifer forest in Kings Canyon National Park. Past competition and competitive mortality undoubtedly influenced the development of spatial patterning in large-diameter tree popula tions in some Sierra Nevada mixed-conifer forests [48,49]. However, it appears that the cumulative effects of any past self thinning in the YFDP were not sufficient to completely override the effects of clustered or random tree regeneration [50], non random mortality or other potential sources of heterogeneity in the distribution of large-diameter trees.

We must thus consider processes other than competition to explain spatial patterns of large-diameter trees in the YFDP. For the fire-tolerant and modestly shade-tolerant P. lambertiana, meso scale aggregation (2–22 m) in the large-diameter subpopulation is most readily explained by clustered establishment, consistent with a disturbance-centric model of forest dynamics and spatial pattern formation in low and mixed severity fire regimes [51]. For A. concolor (fire intolerant when small) the strong clustering of large diameter trees at local (3–5.5 m) and intermediate (13–38 m) scales may originate from fire refugia that allowed groups of A. concolor to survive and reach large diameters. Clustered establish ment alone (e.g., in gaps or in moisture-receiving microtopo graphic features) could explain the aggregation of large A. concolor stems, but given the historical regime of frequent fire [51] it is likely that heterogeneous fire effects leading to patchy A. concolor survival also contributed.

The observed spatial segregation of large and small trees is consistent with inference that competitive interactions between these size classes influence their spatial relationships and overall forest structure. Spatial segregation of large and small trees has been documented in many other forest types (i.e. [33] and the studies reviewed therein), including Sierra Nevada mixed-conifer forests [32]. Spatial segregation between large and small trees may arise from asymmetrical competition for light and gap-phase regeneration [33]. However, we acknowledge that other mecha nisms acting at the tree neighborhood scale potentially contribute to the observed spatial segregation between large and small A. concolor and P. lambertiana, including crushing mortality by falling limbs and bole fragments from live large-diameter trees [8,52], and the spatially heterogeneous buildup and subsequent burning of surface fuels. Additionally, in the absence of fire large-diameter P. lambertiana accumulate a deep mound of debris (bark and needles) at their base [53], a substrate not suitable for seedling establishment, which would also give rise to repulsion between large and small stems. Prior to fire exclusion, Sierra Nevada mixed-conifer forests had low densities of small-diameter trees [35,51]; the observed repulsion between tree diameter classes may also be due to preferential tree establishment in fire-maintained openings following disruption of the historical fire regime [54].

Conclusions

We assessed the degree to which scaling theory and competition theory explain variation of accumulated biomass and spatial patterns across the tree size spectrum. These respective bodies of theory were not sufficient to explain our empirical results. However, our results do not indicate the rejection of these theories. Scaling theory is clearly a powerful framework for developing novel ecological insights, but our results and those of others [21,27,28] show that the requisite simplifying assumptions render predictions from scaling theory inappropriate as inputs in to ecosystem models or as a basis for natural resource decision making. A vast body of accumulated scientific literature details mechanisms and outcomes of plant competition; our results do not contradict this theory. Rather, competition theory alone was insufficient to explain our empirical measurements of tree spatial patterns, strengthening the conclusion that competition is not the dominant control of tree population dynamics and forest development in old-growth Sierra Nevada mixed-conifer forests [24].

We predict that long-term observations at our study site and other sites throughout the range of Sierra Nevada mixed-conifer forests will reveal strong top-down regulation of forest biomass and spatial structure by pathogens, insects and physical disturbances, especially in old-growth forests. We also suggest that, in forests with high functional inequality across the tree size spectrum, ecosystem function may be more sensitive to natural perturbations, environmental change or management actions – at least those affecting the large-diameter trees – than in forests where ecosystem function is distributed more equitably across the tree size spectrum. Sustaining ecological functions and services, such as carbon storage or provision of habitat for specialist species, will likely require different forest management strategies when the ecosystem services are provided primarily by a few large trees as opposed to many smaller trees.

Materials and Methods

Study area

The Yosemite Forest Dynamics Plot (YFDP) is located in the mixed-conifer forest of the western portion of Yosemite National Park (Fig. 6). The plot is approximately oriented to the cardinal directions with dimensions of 800 m east to west and 320 m north to south (25.6 ha) centered at 37.77uN, 119.82uW. Elevation ranges between 1774.1 m and 1911.3 m for a vertical relief of 137.2 m (Fig. S1). The YFDP is comprised of vegetation types within the Abies concolor – Pinus lambertiana Forest Alliance [55], including Abies concolor-Pinus lambertiana/Ceanothus cordulatus Forest, Abies concolor-Pinus lambertiana/Maianthemum racemosum (Smilacina racemosa, Hickman [56])-Disporum hookeri Forest, Abies concolor Calocedrus decurrens-Pinus lambertiana/Cornus nuttallii/Corylus cornuta var. californica Forest, Abies concolor-Calocedrus decurrens-Pinus lambertiana/Adenocaulon bicolor Forest, and Abies concolor-Pinus lambertiana Calocedrus decurrens/Chrysolepis sempervirens Forest, classified accord ing to the U.S. National Vegetation Classification [57](Fig. 7). Overall demographic rates in Sierra Nevada conifer forests between 1500 m and 2000 m elevation are approximately 1.5% [58,59]. Canopy emergents, principally P. lambertiana and A. concolor, reach 60 m to 67 m in height. The soils of the YFDP are derived from metamorphic parent material. Approximately 85% of the soils of the YFDP are metasedimentary soils of the Clarksdodge-Ultic Palexeralfs complex with a water-holding capacity of 160 mm in the top 150 cm of the soil profile [60]. The soils of the northwest 15% of the YFDP are Humic Dystroxerepts-Typic Haploxerults-Inceptic soils of the Haploxer alfs complex with a water-holding capacity of 70 mm in the top 150 cm of the soil profile [60]. Plant nomenclature follows Hickman [56].

The climate at the YFDP is Mediterranean, with cool moist winters and long dry summers. Between 1971 and 2000, the modeled mean temperature range at the YFDP was from 12.2uC to 26.1uC in July and 22.7uC to 9.4uC in February; annual precipitation was 1061 mm, with most precipitation falling in the winter months as snow [61,62]. Snow depth on April 1st is generally 100 cm to 150 cm. The seasonality of precipitation yields a summer drought with a mean annual climatic water deficit of 200 mm [63] (Fig. S2).

Figure 6. Location of the Yosemite Forest Dynamics Plot (YFDP). The YFDP is located near the western boundary of Yosemite National Park (left, green) in the lower montane, mixed-conifer zone of the Sierra Nevada, California, USA. The plot is located in relatively uniform, late-successional forest near Crane Flat (right). The area immediately north of the YFDP was logged in the early 1930s, as was the area comprising the western 1/3 of the image.
doi:10.1371/journal.pone.0036131.g006

Disturbance processes: fire, wind, insects, pathogens, vertebrates, and human use

Fire is the dominant natural disturbance process in Sierra Nevada mixed-conifer forests [64]. The fire regime is of mixed severity with fires burning in a mosaic of high, moderate, and low severities. The pre-Euro-American fire return interval for the YFDP was 10–13 years [51]. The combination of repeated fire and other disturbances gives rise to a fine-grained mosaic structure [50,65]. During the Landsat TM period of record (1984–2011), most fires in this forest type have been either low severity management-ignited prescribed fires or moderate and high severity wildfires [66–68]. The YFDP has not burned since comprehensive park fire records were initiated in 1930. Mechan

Figure 7. Structure and composition of the Yosemite Forest Dynamics Plot (YFDP). Four images from different parts of the YFDP illustrate defining characteristics of the ecosystem. Most precipitation falls in the winter as snow yielding a spring snowpack of approximately 1 m (upper left image, April 11, 2011). The forest is composed of an overstory of large-diameter trees with abundant but heterogeneous shrub

and herbaceous layers (upper right image, June 22, 2009). Shrubs can be locally dense enough to reduce tree recruitment (lower left image, June 22, 2009). Although most trees and shrubs are evergreen, the presence of the deciduous species Cornus nuttallii and Quercus kelloggii results in seasonal openings in the canopy (lower right image, November 11, 2010). All photos by J. A. Lutz.
doi:10.1371/journal.pone.0036131.g007

ical damage, whether from wind, snow, or crushing of smaller individuals by falling trees or tree parts contributes to stand structural development [8,69]. Many of the larger trees in the YFDP have broken tops, or reiterated tops that have regrown following damage.

Insects are important agents of mortality, with most common conifer tree species having coevolved bark beetles (family Scolytidae) that are always present at low levels [70,71]. In particular, Dendroctonous ponderosa (mountain pine beetle) attacks Pinus lambertiana and P. ponderosa and Scolytus ventralis attacks Abies concolor and A. magnifica. Other bark beetles such as S. subscaber, D. valens (red turpentine beetle) and Ips spp. have been less abundant in the recent past but contribute to tree mortality. Quercus kelloggii (California black oak) also has associated bark beetles (Pseudopityophthorus spp.). Conophthorus ponderosae (ponderosa pine cone beetle) is present and can reduce the reproductive output of P. lambertiana.

Pathogens include the structural root rots Armillaria spp. [72], Heterobasidion annosum [73] and Phaeolus schweinitzii [71]. The root rots spread through roots and root contacts at rates of approximately 30 cm per year, and hence tend to occur in patches. Armillaria spp. are somewhat generalist pathogens and attack Abies spp., Prunus spp., and Cornus nuttallii. Phaeolus schweinitzii infects Pinus lambertiana and Abies spp., but tends to progress much more slowly than Heterobasidion and Armillaria. Pinus lambertiana is also affected by the introduced pathogen Cronartium ribicola [74]. Calocedrus decurrens, Abies concolor, and Quercus kelloggii are hosts to mistletoes: Phoradendron libocedri on C. decurrens, Phoradendron pauciflorum and Arceuthobium abietinum on A. concolor, and Phoradendron villosum on Q. kelloggii [75]. These mistletoes are distributed both by birds, and in the case of Arceuthobium abietinum, also by explosive discharge that can carry seeds up to 16 m (typically 10 m; [75]).

The YFDP has a rich fauna, with most species of herbivores and their predators present since prior to Euro-American settlement. Large mammals include Ursus americanus (black bear), Felis concolor (mountain lion), Canis latrans (coyote), and Odocoileus hemionus (mule deer). Altogether, vertebrate species observed within similar forest types within 5 km of the YFDP include 16 rodent species, 12 bat species, 7 carnivore species, one hooved mammal, 7 raptor species, 38 passerine species, 5 amphibian species, and 7 reptile species Table S1, [76–79]).

Yosemite has been inhabited at least since 100 AD [80]. Immediately prior to Euro-American discovery of the region in 1833 [81] and the subsequent entry of Euro-Americans into Yosemite Valley in 1851 [82], the area was occupied by the Central Sierra Miwok and the Southern Sierra Miwok [83]. Because the YFDP contains only intermittent streams and seeps, Native American use of the site was probably low, and modification of the fire regime at this site by Native Americans appears unlikely [84]. The YFDP is near the transit route from Hazel Green to Crane Flat used by sheepherders in the late 19th century. John Muir may have passed through or near the YFDP on July 9th, 1869 – the topography and vegetation are consistent with his journal entry [85].

The original Yosemite Grant (1864) placed Yosemite Valley and the Mariposa Grove of giant sequoia in protected status. The YFDP lies within what was a single parcel of land prior to its inclusion into Yosemite National Park in 1930. The parcel of land immediately to the north of the YFDP (,20 m from the plot boundary) was in different ownership and was logged in the early 1930s. The northwest corner of the YFDP contains four large stumps that appear to be associated with the logging of the parcel to the north. Logging outside the YFDP continued throughout the 1920s until the area was purchased by the National Park Service and John D. Rockefeller. The area of unlogged sugar pine containing the YFDP is today termed the Rockefeller Grove in honor of J.D. Rockefeller's role in protecting this part of the park.

Surveying

We established a sampling grid using Total Stations with accuracies of at least 5 seconds of arc (Leica models 1100, Builder R200M Power, Builder 505, and TC 2003). We set permanent markers on nominal 20 m centers, offset for tree boles, coarse woody debris, or large rocks. Survey closure across the plot was 0.18 m northing, 0.05 m easting, and 0.03 m elevation (,1/ 5000). In addition to the sampling grid, we established control points in open areas near the plot where marginal Global Positioning System (GPS) reception was possible. Three survey grade GPS receivers (Magellan Z-Extremes) were used to establish control to and across the plot, using a reference station approximately 2 km from the plot (MGROVE, PID DF8617 on the California State Plane Coordinate System and being described in the National Geodetic Survey Datasheets). The GPS receivers collected data at 10 second intervals for 2–6 hours. The static GPS measurements were post-processed with GNSS Solutions software (Magellan Navigation, Inc., pro.magellangps.com), with final accuracies in the range of 0.01 m horizontally and 0.02 m vertically. We transformed the plot grid to Universal Transverse Mercator coordinates with Lewis and Lewis Coordinated Geometry software (Lewis and Lewis Land Surveying Equipment, Inc., www.lewis-lewis.net). We augmented the ground survey with LiDAR-derived elevation data at 1 m horizontal resolution. Aerial LiDAR data were acquired on 22 July 2010 by Watershed Sciences Inc., Corvallis, Oregon with a density of 40 returns per square meter. Ground survey data and the LiDAR-derived ground model coincided with a root-mean-squared error of 0.15 m.

Field sampling of trees, shrubs, snags, and woody debris

In the summers of 2009 and 2010 we tagged and mapped all live trees $1 cm at breast height (1.37 m; dbh), following the methods of Condit [86], with some alterations. We measured tree diameter at 1.37 m (instead of 1.30 m), and trees large enough to accept a nail were nailed at the point of measurement, both in keeping with research methods of the western United States. We used stainless steel tags, nails and wire to increase tag longevity in this fire-dominated ecosystem. We measured tree locations from the surveyed grid points with a combination of hand-held lasers (Laser Technologies Impulse 200 LR), mirror compasses, and tapes. Tapes were laid south to north between adjacent grid points, and a perpendicular angle determined by sighting a target bole with a mirror compass. The distance from the tape to each tree was then measured with the hand-held lasers. We calculated the location of the tree center from the horizontal and perpendicular references to the surveyed grid points and dbh with the assumptions of cylindrical boles and linear interpolation of elevation between adjacent grid points. All measurements were slope corrected.

We mapped continuous patches of shrub cover $2 m^2 relative to the 20 m sampling grid with a combination of tapes, mirror compasses, and lasers. For each shrub patch we recorded the shape of the patch as a polygon, as well as average and maximum shrub heights. To convert between shrub cover and the number of stems and biomass in the YFDP, we established 25 shrub demography plots for nine species (Arctostaphylos patula, Ceanothus cordulatus, Ceanothus integerrimus, Ceanothus parvifolius, Chrysolepis sempervirens, Corylus cornuta var. californica, Cornus sericia, Leucothoe davisiae, and Vaccinium uliginosum). We tagged every woody stem in each of these 2 m62 m plots. We measured basal diameter for

every woody stem. If stems were 1.37 m tall (or long), we made an additional measurement at 1.37 m.

We tagged and mapped dead trees $10 cm dbh and $1.8 m in height. For each snag, we collected height, top diameter (with a laser), and snag decomposition class data (following [87]; class 1 = least decayed, class 5 = most decayed). We did not collect data on trees ,10 cm dbh at the original census because of the difficulty in finding small stems a few years after they die.

To measure down woody debris, litter, and duff, we established four interior fuel transects totaling 2.24 km (112 transects of 20 m). We used the National Park Service fuel monitoring protocols [88], in turn based on Brown transects [89]. Litter included freshly fallen leaves, needles, bark, flakes, acorns, cones, cone scales, and miscellaneous vegetative parts [88]. Duff included the fermentation and humus layers, not the fresh material of the litter layer. Down woody material included branches, trunks of trees, and shrubs that had fallen on or within 2 m above the ground [88]. Intercept diameter and decay class were recorded for all intercepted woody debris $10 cm in intercept diameter (measured perpendicular to the orientation of the piece of debris). To sample fine woody debris we used portions of the 112 line intercept transects 22 m for material 0 cm–2.5 cm in diameter (1- hour and 10-hour fuels), and 4 m for material 2.5 cm–7.6 cm (100-hour fuels). We calculated biomass according to Brown's method [89].

Biomass calculations

We reviewed all allometric equations from the two compendia of equations for North America [43,90] and selected those that best matched the species, geographic location, diameter ranges, and tree densities of the YFDP [44,90–93]. Where no allometric equation existed, we substituted a species (or diameter class within a species) that was a close match for morphology and wood density (see Appendix S1 for details). Because no whole tree biomass equations exist for the largest individuals of the species in the YFDP, we used proxy species. For the largest Abies concolor (n = 112) we used bole equations for A. procera. For Pinus lambertiana, we used branch and foliage equations for Pseudotsuga menziesii, and for the Pinus lambertiana .179.6 cm dbh (n = 7), we used a bole equation for Pseudotsuga menziesii. Additionally, no biomass equations exist for branches and foliage of Abies .110 cm dbh or Pseudotsuga .162 cm dbh. For those trees we capped the branch and foliage biomass at the values associated with trees of diameter 110 cm and 162 cm, respectively. All biomass calculations were made within the data ranges of the selected allometric equations (See Appendix S1 for full details of allometric equations). We calculated an error term for tree biomass from the underlying allometric equations. The root mean square error (standard error of estimate) of the allometric equations was transformed from log units to arithmetic units of standard deviation (i.e. Mg/ha) [92]. We defined large diameter structures as pieces $100 cm in diameter to facilitate comparisons with earlier studies of large diameter trees in old-growth conifer forests on the Pacific Slope of western North America.

We calculated the biomass of the stems within each 4 m^2 shrub demography plot based on allometric equations using basal diameter [90]. We used the biomass of the stems within the demography plots and the total area of shrub patches $2 m^2 within the YFDP to calculate total shrub biomass. We used the demography plot data for sampled species as proxies for the four species without demography plots (Corylus cornuta var. californica for Sambucus racemosa, Vaccinium uliginosum for Rhododendron occidentale and Ribes nevadense, and one-half the value of Vaccinium uliginosum for Ribes roezlii). To calculate a stem density equivalent to the standard Smithsonian CTFS protocol [86], we tallied the number of stems that were $1 cm dbh in each shrub demography plot and multiplied by the area of each shrub patch $2 m^2. Details of allometric equations are in Appendix S1.

We calculated snag biomass using the wood density values of Harmon et al. [15] and a bole volume calculated as a frustum of a cone. We calculated the biomass of litter and duff using the methods of Stephens et al. [94]. For down woody debris larger than 1000-hour fuels (4 inches; ,10 cm), we used the large transect protocols of Harmon et al. [15], and we calculated the mass of woody debris using the methods of Harmon and Sexton [87].

To compare actual density and biomass values with the predictions of scaling theory, we used the equations from West et al. [26]. Specifically, we compared the actual diameter (radius) distribution with their predicted distribution, (r) ! $^{1}r^{2}$, where r is tree radius at breast height. We then reconfigured their radius mass relationship, r ! $m^{3=8}$, to m ! $r^{8=3}$, where r is tree radius and m is tree biomass, and combined the mass and frequency equations to develop a relationship for total biomass in terms of tree radius: (m!$r^{8=3}$)(n!$r^{\{2}$) or biomass!$r^{2=3}$. We used 5 cm diameter bins (2.5 cm radius bins) to regress curves of these forms to the data.

Quantifying spatial pattern

We quantified global spatial patterns with the univariate and bivariate forms of Ripley's K function, using the square root (L function) transformation in all cases. For a given fully mapped pattern, an estimate of the L(r) function, the statistic

$\hat{L}(r)$, is based on the count of neighboring points occurring within a circle of radius r centered on the ith point, summed over all points in the pattern [95,96]. The bivariate form $\hat{L}_{1,2}(r)$ is a straightforward extension of the univariate case: it is the count of type 2 points occurring within a circle of radius r of the ith type 1 point, summed over all type 1 points in the pattern. We characterized patterns at interpoint distances from 0 m to 80 m (one quarter the minimum plot dimension) and used isotropic edge correction to account for points located closer than r to a plot edge [96]. Our study area included enough large-diameter trees to analyze spatial patterns of three tree species: Abies concolor, Calocedrus decurrens and Pinus lambertiana.

Inferential framework for spatial analyses

Univariate tree patterns were compared against a null distribution generated by a completely spatially random (CSR) process. Under CSR the location of each point in the pattern is completely independent of the locations of other points in the pattern. Positive values of $\hat{L}(r)$ indicate spatial clustering (trees have more neighbors than expected under CSR) while negative values of $\hat{L}(r)$ indicate spatial inhibition or uniformity (trees have fewer neighbors than expected under CSR).

Bivariate tree patterns were evaluated against the hypothesis of no interaction between the large-diameter and small-diameter subpopulations. We evaluated this hypothesis using the null model of population independence based on the guidelines of Goreaud & Pe´lissier [97]. Population independence is evaluated by holding the relative intratype spatial configuration constant (i.e., the relative tree locations within a diameter class are fixed) while subjecting the populations to random toroidal shifts. Under population independence significantly positive values of $\hat{L}_{1,2}(r)$ indicate a spatial attraction between the two types (e.g., originating from a parent-offspring relationship or facilitation) while significantly negative values indicate spatial repulsion between the two

types (e.g., Janzen-Connell effects or intraspecific competition). Large-diameter trees were $100 cm dbh; small-diameter trees were ,100 cm dbh.

We used the 9 m radius neighborhood size estimated by Das et al. [24,98] for Sierra Nevada mixed-conifer forests and tested the respective empirical patterns against the corresponding null models over 0 m#r#9 m using the goodness-of-fit test developed by Loosmore and Ford [99]. We set a = 0.05 and used n = 999 simulated patterns in each test (n = 250 simulated patterns were used for univariate analyses of small-diameter A. concolor and all species pooled, respectively, to mitigate excessively long computation times). To control for multiple tests (n = 12) we used the Bonferroni correction, resulting in a threshold P-value of 0.004. Because we had no a priori hypotheses about tree patterns at spatial scales .9 m we investigated patterns at larger scales in an exploratory framework by comparing the empirical $\hat{L}(r)$ curves to the full distribution of $\hat{L}(r)$ curves calculated for the simulated patterns. All analyses were implemented in the statistical program R version 2.14.1 [100]. Spatial analyses were conducted using the spatstat package version 1.25-1 [101].

Supporting Information

Figure S1 Topography of the Yosemite Forest Dynamics Plot. LiDAR-derived ground model at 1 m resolution (5 m contours; 137.2 m vertical relief). Dots indicate corners of each 20 m620 m quadrat of the 800 m6320 m plot. Elevation ranges from 1774.1 m in the northeast corner to 1911.3 m along the southern boundary for a vertical relief of 137.2 m. Drainages contain vernal streams.
(TIF)

Figure S2 Climatology and water balance of the Yosemite Forest Dynamics Plot. The combination of temperature and precipitation (A) give rise to a pronounced summer drought (B). Potential evapotranspiration (PET) exceeds available water supply from May through September, decreasing actual evapotranspiration (AET) and producing a climatic water deficit (Deficit) of 197 mm of water.
(TIF)

Table S1 Vertebrate species reported in similar forest types within 5 km of the Yosemite Forest Dynamics Plot between 1980 and 2011.
(PDF)

Appendix S1 Allometric equations for total above ground biomass for trees $1 cm dbh and shrubs in patches of continuous cover $2 m^2 in the Yosemite Forest Dynamics

References

1. Brown IF, Martinelli LA, Thomas WW, Moreira MZ, Ferreira CAC, et al. (1995) Uncertainty in the biomass of Amazonian forests: An example from Rondoˆnia, Brazil. Forest Ecology and Management 75: 175–189.
2. Clark DB, Clark DA (1996) Abundance, growth and mortality of very large trees in Neotropical lowland rain forest. Forest Ecology and Management 80: 235–244.
3. Martin TA, Brown KJ, Kucˇera J, Meinzer FC, Sprugel DG, et al. (2001) Control of transpiration in a 220-year old Abies amabilis forest. Forest Ecology and Management 152: 211–224.
4. Rambo T, North M (2009) Canopy microclimate response to pattern and density of thinning in a Sierra Nevada forest. Forest Ecology and Management 257: 435–442.
5. van Wagtendonk JW, Moore PE (2010) Fuel deposition rates of montane and subalpine conifers in the central Sierra Nevada, California, USA. Forest Ecology and Management 259: 2122–2132.
6. Keeton WS, Franklin JF (2005) Do remnant old-growth trees accelerate rates of succession in mature Douglas-fir forests? Ecological Monographs 75: 103–118.
7. Chao K-J, Phillips OL, Monteagudo A, Torres-Lezama A, Va´squez Martı´nez R (2009) How do trees die? Mode of death in northern Amazonia. Journal of Vegetation Science 20: 260–268.
8. Larson AJ, Franklin JF (2010) The tree mortality regime in temperate old growth coniferous forests: the role of physical damage. Canadian Journal of Forest Research 40: 2091–2103.
9. Meyer MD, Kelt DA, North MP (2005) Nest trees of northern flying squirrels in the Sierra Nevada. Journal of Mammalogy 86: 275–280.
10. Van Pelt R, Sillett SC (2008) Crown development of coastal Pseudotsuga menziesii, including a conceptual model for tall conifers. Ecological Monographs 78: 283–311.
11. Hammer TE, Nelson SK (1995) Characteristics of marbled murrelet nest trees and nesting stands. In: Ralph CJ, Hunt GL, Jr., Raphael MG, Piatt JF, eds. Ecology and conservation of the marbled murrelet. General Technical Report PSW-152. Department of Agriculture, Forest Service, Pacific Southwest Research Station, Albany, California.
12. Nadkarni NM, Matelson TJ (1989) Bird use of epiphyte resources in Neotropical trees. Condor 91: 891–907.

Plot.
(PDF)

Acknowledgments

This research was performed under National Park Service research permits YOSE-2008-SCI-0098, YOSE-2010-SCI-0003, and YOSE-2011-SCI 0015. We thank B. Blake of Blake Land Surveys, Buellton, California, for assistance with surveying, GPS location, and geospatial consulting, and J. Knox, K. Blake, J. Bratt, R. Moore, M. Alvarez, R. McMillan, and G. Rice for surveying assistance. We thank S. Roberts for vertebrate data. We thank J. Meyer and the Yosemite National Park Divisions of Resources and Science, Fire and Aviation, Campground Management, and Law Enforcement for logistical support. We thank two anonymous reviewers who helped improve previous versions of this manuscript. This project was made possible by the 115 students and volunteers listed individually at http://www.yfdp.org.

Author Contributions

Conceived and designed the experiments: JAL AJL MES JAF. Performed the experiments: JAL AJL MES JAF. Analyzed the data: JAL AJL MES JAF. Wrote the paper: JAL AJL MES.

13. Sillett SC, Van Pelt R (2007) Trunk reiteration promotes epiphytes and water storage in an old-growth redwood forest canopy. Ecological Monographs 77: 335–359.
14. Harmon ME, Cromack K, Smith BG (1987) Coarse woody debris in mixed conifer forests, Sequoia National Park, California. Canadian Journal of Forest Research 17: 1265–1272.
15. Harmon ME, Woodall CW, Fasth B, Sexton J (2008) Woody detritus density and density reduction factors for tree species in the United States: a synthesis. USDA Forest Service General Technical Report NRS-29. Northern Research Station, Newtown Square, Pennsylvania.
16. Winter LE, Brubaker LB, Franklin JF, Miller EA, DeWitt DQ (2002) Canopy disturbance over the five-century lifetime of an old-growth Douglas-fir stand in the Pacific Northwest. Canadian Journal of Forest Research 32: 1057–1070.
17. Swetnam TW (1993) Fire history and climate change in giant sequoia groves. Science 262: 885–889.
18. Hall CM, James M, Baird T (2011) Forests and trees as charismatic mega-flora: implications for heritage tourism and conservation. Journal of Heritage Tourism 6: 309–323.
19. Omura H (2004) Trees, forests and religion in Japan. Mountain Research and Development 24: 179–182.
20. Van Pelt R (2001) Forest giants of the Pacific coast. Seattle: University of Washington Press.
21. Enquist BJ, West GB, Brown JH (2009) Extensions and evaluations of a general quantitative theory of forest structure and dynamics. Proc Natl Acad Sci U S A 106: 7046–7051.
22. Knight FR (2003) Stem mapping methodologies and analyses of stem density, plot size, sample size and spatial patterns of large trees in old-growth mixed conifer and pine forests ofthe Sierra Nevada and Oregon. Dissertation. University of Washington, Seattle, Washington.
23. Busing RT (2005) Tree mortality, canopy turnover, and woody detritus in old cove forests of the southern Appalachians. Ecology 86: 73–84.
24. Das A, Battles J, Stephenson NL, van Mantgem PJ (2011) The contribution of competition to tree mortality in old-growth coniferous forests. Forest Ecology and Management 261: 1203–1213.
25. Enquist BJ, Niklas KJ (2001) Invariant scaling relations across tree-dominated communities. Nature 410: 655–660.

26. West GB, Enquist BJ, Brown JH (2009) A general quantitative theory of forest structure and dynamics. Proc Natl Acad Sci U S A 106: 7040–7045.
27. Coomes DA, Duncan RP, Allen RB, Truscott J (2003) Disturbances prevent stem size-density distributions in natural forests from following scaling relationships. Ecology Letters 6: 980–989.
28. Muller-Landau HC, Condit RS, Harms KE, Marks CO, Thomas SC, et al. (2006) Comparing tropical forest tree size distributions with the predictions of metabolic ecology and equilibrium models. Ecology Letters 9: 589–602.
29. Franklin JF, Shugart HH, Harmon ME (1987) Tree death as an ecological process. BioScience 37: 550–556.
30. Pielou EC (1962) The use of plant-to-neighbor distances for the detection of competition. Journal of Ecology 50: 357–367.
31. Getzin S, Dean C, He F, Trofymow JA, Wiegand K, et al. (2006) Spatial patterns and competition of tree species in a Douglas-fir chronosequence on Vancouver Island. Ecography 29: 671–682.
32. Van Pelt R, Franklin JF (2000) Influence of canopy structure on the understory environment in tall, old-growth, conifer forests. Canadian Journal of Forest Research 30: 1231–1245.
33. Larson AJ, Franklin JF (2006) Structural segregation and scales of spatial dependency in Abies amabilis forests. Journal of Vegetation Science 17: 489–498.
34. Taylor AH (2004) Identifying forest reference conditions on early cut-over lands, Lake Tahoe Basin, USA. Ecological Applications 14: 1903–1920. 35. North M, Chen J, Oakley B, Song B, Rudnicki M, et al. (2004) Forest stand structure and pattern of old-growth western hemlock/Douglas-fir and mixed conifer forests. Forest Science 50: 299–311.
36. Busing RT, Fujimori T (2002) Dynamics and composition and structure in an old Sequoia sempervirens forest. Journal of Vegetation Science 13: 785–792. 37. Baishya R, Barik SJ, Upadhaya K (2009) Distribution pattern of aboveground biomass in natural and plantation forests of humid tropics in northeast India. Tropical Ecology 50: 295–304.
38. Gilbert GS, Howard E, Ayala-Orozco B, Bonilla-Moheno M, Cummings J, et al. (2010) Beyond the tropics: forest structure in a temperate forest mapped plot. Journal of Vegetation Science 21: 388–405.
39. Chave J, Condit R, Muller-Landau HC, Thomas SC, Ashton PS, et al. (2008) Assessing evidence for a pervasive alteration in tropical tree communities. PLoS Biology 6: e45.
40. Makana J-R, Ewango CN, McMahon SM, Thomas SC, Hart TB, et al. (2011) Demography and biomass change in monodominant and mixed old-growth forest of the Congo. Journal of Tropical Ecology 27: 447–461.
41. Hao ZQ, Li BH, Zhang J, Wang XG, Ye J, et al. (2008) Broad-leaved Korean pine (Pinus koraiensis) mixed forest plot in Changbaishan (CBS) of China: Community composition and structure. Acta Phytoecologica Sinica 32: 238–250. [In Chinese.].
42. Wang X, Wiegand T, Wolf A, Howe R, Davies SJ, et al. (2011) Spatial patterns of tree species richness in two temperate forests. Journal of Ecology 99: 1382–1393.
43. Jenkins JC, Chojnacky DC, Heath LS, Birdsey RA (2004) Comprehensive database of diameter-based biomass regressions for North American tree species. USDA Forest Service General Technical Report NE-319. Northeast ern Research Station, Newtown Square, Pennsylvania.
44. Keeton WS, Whitman AA, McGee GC, Goodale CL (2011) Late-successional biomass development in northern hardwood-conifer forests of the northeastern United States. Forest Science 57: 489–505.
45. Morrison ML, Raphael MG (1993) Modeling the dynamics of snags. Ecological Applications 3: 322–330.
46. North M, Innes J, Zald H (2007) Comparison of thinning and prescribed fire restoration treatments to Sierran mixed-conifer historic conditions. Canadian Journal of Forest Research 37: 331–342.
47. Bonnicksen TM, Stone EC (1980) The giant sequoia-mixed conifer forest community characterized through pattern analysis as a mosaic of aggregations. Forest Ecology and Management 3: 307–328.
48. Das A, Battles J, van Mantgem PJ, Stephenson NL (2008) Spatial elements of mortality risk in old-growth forests. Ecology 89: 1744–1756.
49. Lutz JA, van Wagtendonk JW, Franklin JF (2009) Twentieth-century decline of large-diameter trees in Yosemite National Park, California, USA. Forest Ecology and Management 257: 2296–2307.
50. Larson AJ, Churchill D (2012) Tree spatial patterns in fire-frequent forests of western North America, including mechanisms of pattern formation and implications for designing fuel reduction and restoration treatments. Forest Ecology and Management 267: 74–92.
51. Scholl AE, Taylor AH (2010) Fire regimes, forest change, and self-organization in an old-growth mixed-conifer forest, Yosemite National Park, USA. Ecological Applications 20: 362–380.
52. Clark DB, Clark DA (1991) The impact of physical damage on canopy tree regeneration in tropical rain forest. Journal of Ecology 72: 447–457. 53. Nesmith JCB, O'Hara KL, van Mantgem PJ, de Valpine P (2010) The effects of raking on sugar pine mortality following prescribed fire in Sequoia and Kings Canyon National Parks, California, USA. Fire Ecology 6(3): 97–116. 54. Sa´nchez Meador AJ, Moore MM, Bakker JD, Parysow PF (2009) 108 years of change in spatial pattern following selective harvest of a Pinus ponderosa stand in northern Arizona, USA. Journal of Vegetation Science 20: 79–90. 55. Keeler-Wolf T, Moore PE, Reyes ET, Menke JM, Johnson DN, et al. (In press) Yosemite National Park Vegetation Classification and Mapping Project Report. Natural Resource Report NPS/XXXX/NRR-20XX/XXX. National Park Service, Fort Collins, Colorado.
56. Hickman JC, ed. The Jepson Manual: Higher Plants of California. Berkeley: University of California Press.
57. Jennings MD, Faber-Langendoen D, Loucks OL, Peet RK, Roberts D (2009) Standards for associations and alliances of the U.S. National

Vegetation Classification. Ecological Monographs 79: 173–199.

58. Stephenson NL, van Mantgem PJ (2005) Forest turnover rates follow global and regional patterns of productivity. Ecology Letters 8: 524–531. 59. Stephenson NL, van Mantgem PJ, Bunn AG, Bruner H, Harmon ME, et al. (2011) Causes and implications of the correlation between forest productivity and tree mortality rates. Ecological Monographs 81: 527–555.

60. Natural Resources Conservation Service (NRCS) (2007) Soil survey geographic (SSURGO) database for Yosemite National Park, California, USA (Soil survey area symbol CA790). http://soildatamart.nrcs.usda.gov USDA Natural Resources Conservation Service, Fort Worth, Texas, USA.

61. PRISM (2004) 800-m Climate Normals (1971–2000). PRISM Climate Group, Oregon State University, Corvallis, Oregon, USA.

62. Daly C, Halbleib M, Smith JI, Gibson WP, Dogett MK, et al. (2008) Physiographically-sensitive mapping of temperature and precipitation across the conterminous United State. International Journal of Climatology 28: 2031–2064.

63. Lutz JA, van Wagtendonk JW, Franklin JF (2010) Climatic water deficit, tree species ranges, and climate change in Yosemite National Park. Journal of Biogeography 37: 936–950.

64. van Wagtendonk JW, Fites-Kaufman J (2006) Sierra Nevada bioregion. 264–294. in Sugihara NG, van Wagtendonk JW, Shaffer KE, Fites-Kaufman J, Thode AE, eds. Fire in California's Ecosystems, University of California Press, Berkeley, California, USA.

65. Tarnay LW, Lutz JA (2011) Sustainable fire: Preserving carbon stocks and protecting air quality as the Sierra Nevada warm. Park Science 28(1): 48–55.

66. van Wagtendonk JW, Lutz JA (2007) Fire regime attributes of wildland fires in Yosemite National Park, USA. Fire Ecology 3(2): 34–52.

67. Lutz JA, Key CH, Kolden CA, Kane JT, van Wagtendonk JW (2011) Fire frequency, area burned, and severity: a quantitative approach to defining a normal fire year. Fire Ecology 7(2): 51–65.

68. Thode AE, van Wagtendonk JW, Miller JD, Quinn JF (2011) Quantifying the fire regime distributions for severity in Yosemite National Park, California, USA. International Journal of Wildland Fire 20: 223–239.

69. Lutz JA, Halpern CB (2006) Tree mortality during early forest development: a long-term study of rates, causes, and consequences. Ecological Monographs 76: 257–275.

70. Furniss RL, Carolin VM (1977) Western Forest Insects. USDA Forest Service Miscellaneous Publication 1339, Washington DC.

71. Edmonds RL, Agee JK, Gara RI (2000) Forest health and protection. Boston: McGraw-Hill.

72. Baumgartner K, Rizzo DM (2001) Distribution of Armillaria species in California. Mycologia 93: 821–830.

73. Rizzo DM, Slaughter GW (2001) Root disease and canopy gaps in developed areas of Yosemite Valley, California. Forest Ecology and Management 146: 159–167.

74. van Mantgem PJ, Stephenson NL, Keifer MB, Keeley J (2004) Effects of an introduced pathogen and fire exclusion on the demography of sugar pine. Ecological Applications 14: 1590–1602.

75. Hawksworth FG, Wiens D (1996) Dwarf mistletoes: biology, pathology, and systematics. USDA Agriculture Handbook 709, USDS Forest Service, Washington DC.

76. Pierson ED, Rainey WE, Chow LS (2006) Bat use of the giant sequoia groves in Yosemite National Park. Yosemite Fund Report, Yosemite National, California.

77. Meyer MD, North MP, Kelt DA (2007) Nest trees of northern flying squirrel in Yosemite National Park, California. Southwestern Naturalist 52: 157–161.

78. Roberts SL, van Wagtendonk JW, Kelt DA, Miles AK, Lutz JA (2008) Modeling the effects of fire severity and spatial complexity on small mammals in Yosemite National Park, California. Fire Ecology 4(2): 83–104. 79. Roberts SL, van Wagtendonk JW, Miles AK, Kelt DA (2011) Effects of fire on California spotted owl occupancy in a late-successional forest. Biological Conservation 144: 610–619.

80. Elsasser AB (1978) Development of regional prehistoric cultures. In:, , Heizer RF, volume editor (1978) Handbook of North American Indians, Volume 8, California. Washington DC: Smithsonian Institution. pp 37–57.

81. Hiskes G, Hiskes J (2009) The discovery of Yosemite 1833: route of the Walker Expedition through the Yosemite region Red Fox Press.

82. Bunnel LH (1880) Discovery of the Yosemite and the Indian War of 1851. Chicago: Flemmin H Revell.

83. Levy R (1978) Eastern Miwok. In, , Heizer RF, volume editor (1978) Handbook of North American Indians, Volume 8, California. Washington DC: Smithsonian Institution. pp 398–413.

84. Parker AJ (2002) Fire in Sierra Nevada forests: evaluating the ecological impact of burning by Native Americans. In Vale TR, ed. Fire, native peoples, and the natural landscape. Washington DC: Island Press. pp 233–267.

85. Muir J (1911) My first summer in the Sierra. In Cronon W, ed. John Muir: nature writings. New York: The Library of America. pp 147–310.

86. Condit R (1998) Tropical forest census plots. Berlin: Springer-Verlag, Georgetown: R.G. Landes Company. 211 p.

87. Harmon ME, Sexton J (1996) Guidelines for measurements of woody detritus in forest ecosystems. U.S. LTER Network Office: University of Washington, Seattle, WA, USA. 73 p.

88. USDI National Park Service (2003) Fire Monitoring Handbook. Fire Management Program Center, National Interagency Fire Center, Boise, Idaho, USA.

89. Brown JK (1974) Handbook for inventorying downed material. USDA Forest Service Gen Tech Report INT-16. Ogden, Utah, USA.

90. Means JE, Hansen HA, Koerper GJ, Alaback PB, Klopsch MW (1994) Software for computing plant biomass – BIOPAK users guide. USDA Forest Service General Technical Report PNW-GTR-340. Pacific Northwest Research Station, Portland, Oregon, USA.

91. Gholz HL, Grier CC, Campbell AG, Brown AT (1979) Equations for estimating biomass and leaf area of plants of the Pacific Northwest. Research Paper 41. Forest Research Lab, Oregon State University. Corvallis.

92. Westman WE (1998) Aboveground biomass, surface area, and production relations of red fir (Abies magnifica) and white fir (A. concolor). Canadian Journal of Forest Research 17: 311–319.

93. Jenkins JC, Chojnacky DC, Heath LS, Birdsey RA (2003) National-scale biomass estimators for United States tree species. Forest Science 49: 12–35.

94. Stephens SL, Finney MA, Schantz H (2004) Bulk density and fuel loads of ponderosa pine and white fir forest floors: impacts of leaf morphology. Northwest Science 78: 93–100.

95. Fortin MJ, Dale M (2005) Spatial analysis: a guide for ecologists. Cambridge University Press, Cambridge, UK.

96. Diggle P (2003) Statistical analysis of spatial point patterns. Arnold, London, UK.

97. Goreaud F, Pe´lissier R (2003) Avoiding misinterpretation of biotic interactions with the intertype K_{12}-function: population independence vs. random labeling hypotheses. Journal of Vegetation Science 14: 681–692.

98. Larson AJ, Churchill D (2008) Spatial patterns of overstory trees in late successional conifer forests. Canadian Journal of Forest Research 38: 2814–2825.

99. Loosmore NL, Ford ED (2006) Statistical inference using the G or K point pattern spatial statistics. Ecology 87: 1925–1931.

100. R Development Core Team (2011) R: A language and environment for statistical computing. R Foundation for Statistical Computing, Vienna, Austria. http://www.R-project.org/.

101. Baddeley A, Turner R (2005) Spatstat: an R package for analyzing spatial point patterns. Journal of Statistical Software 12(6): 1–42.

EXHIBIT E

Project Title: Optimizing Spatial and Temporal Treatments to Maintain Effective Fire and Non-fire Fuels Treatments at Landscape Scales

Final Report: JFSP Project: 06-3-3-14

Project Website:

Principal Investigators:

Dr. J. Greg Jones, Research Forester, Human Dimensions Program,
Rocky Mountain Research Station, PO Box 7669, 200 East
Broadway Missoula, MT 59807; Phone: (406) 329-3396; Fax: (406)
329-3487;
Email: jgjones@fs.fed.us

Dr. Woodam Chung, Associate Professor, College of Forestry and
Conservation, The University of Montana, Missoula, MT 59812;
Phone: (406) 243-6606; Fax: (406) 243-4845;
Email: woodam.chung@umontana.edu

Co-Principal Investigator:

Dr. Carl Seielstad, College of Forestry and Conservation, The University
of Montana, Missoula, MT 59812; Phone: (406) 532-3283;
Email: carl@ntsg.umt.edu

Software Developers:

Janet Sullivan, Human Dimensions Program, Rocky Mountain Research
Station, 200 East Broadway, Missoula, MT 59807; Phone: (406) 329-3414;
Fax: (406) 329-3487; Email: jsullivan@fs.fed.us

Kurt Krueger, Human Dimensions Program, Rocky Mountain Research
Station, 200 East Broadway, Missoula, MT 59807; Phone: (406) 329- 3420;
Fax: (406) 329-3487; Email: kkrueger@fs.fed.us

This research was sponsored in part by the Joint Fire Science Program. For further information go to www.firescience.gov

I. Abstract

There is a recognized need to apply and maintain fuel treatments to reduce catastrophic wildland fires. A number of models and decision support systems have been developed for addressing different aspects of fuel treatments while considering other important resource management issues and constraints. Although these models address diverse aspects of the fuel treatment planning problem, no one model adequately handles the strategic maintenance scheduling of fuel treatments while considering 1) the spatial and temporal changes of fuel treatment effects on a landscape, and 2) the economics of maintenance fuel treatments plus other operational constraints.

The objective of this project was to integrate existing fire behavior, vegetation simulation, and land management planning tools into a system that supports long-term fuel management decisions. The system was to build on the existing land management optimization tool MAGIS, while incorporating the Forest Vegetation Simulator and the Fire and Fuels Extension (FVS FFE) to project vegetation change over planning periods and predict the resulting fuel parameters for fire behavior modeling, and FlamMap to model fire behavior in each planning period. The system was to include automated data transfer interfaces between the models to offer an easier way to use multiple sophisticated models for analyzing alternative fuel management schedules.

The project developed OptFuels, a GIS-based modeling system for spatially scheduling forest fuel treatments over multiple planning periods in the presence of budget and other constraints. OptFuels utilizes FVS-FFE to project stands into the future both with and without fuel treatments and compute the fuel parameters needed for fire behavior modeling in FlamMap, which is conducted for each planning period in each iteration of the OptFuels solver. The OptFuels solver spatially schedules fuel treatments over multiple planning periods (1 – 5 user-defined periods) to minimize the expected loss from potential future wildland fire.

OptFuels has been tested on two fuel treatment planning areas on the Bitterroot National Forest, the 34,000-acre Trapper-Bunkhouse area, and the 103,689-acre Willow-Gird area. Fuel treatment scenarios scheduled over two planning periods were able to substantially reduce the fire arrival time in the wildland urban interface portion of the Trapper-Bunkhouse area, thereby reducing the expected loss from future fires. Smaller reductions in expected loss were found in the Willow-Gird area. Although increases in arrival time were created by the scheduled fuel treatments, these treatments did not increase the arrival times sufficiently in the areas on the landscape having the highest expected loss, such as the wildland urban interface. This occurred primarily because of the relatively close proximity of the ignition points in the wildland urban interface simulating human ignited fires.

II. Background and Purpose

There is a recognized need to apply and maintain fuel treatments to reduce catastrophic wildland fires. The Healthy Forests Restoration Act of 2003 mandates actions to identify and inventory priority areas. Treating all of the 81 million hectares of federal land in the USA considered at risk from fire (Schmidt et al. 2002) would be costly and impractical. Forest managers faced with limited budgets, narrow burning windows, air quality issues, and effects on other critical forest resources must establish priorities for where, when, and how to apply new and maintenance fuel

treatments. Science-based yet field applicable guidelines to strategically maintain fuel treatments on landscapes should be incorporated into treatment design to reduce catastrophic fire and restore ecosystem health over time. Therefore, decision support systems that can predict the outcomes of fuel treatments are valuable information tools for fuel management decisions.

There is a need for the use of such models to be utilized at a national level.

A number of models and decision support systems have been developed for addressing different aspects of fuel treatments while considering other important resource management issues and constraints. These models operate on a variety of geographic scales, varying from an individual stand to an entire landscape comprised of many individual stands. Some models operate only on current conditions, while others span over multiple decades.

A. Fire behavior and fuel hazard modeling

The FARSITE Fire Area Simulator (Finney 1998) was designed to model continuous fire behavior over multiple burning periods at a 30-meter resolution. FARSITE is able to compare the effectiveness of different suppression strategies and treatments for containing fire under varying weather conditions. FARSITE evaluations are based on simulating fires starting at various locations and spreading under varying fuel and weather conditions. There is, however, no temporal component to these analyses that reflects how the effectiveness of treatments changes over time with vegetative growth.

FlamMap (http://fire.org/) is a spatial fire area potential calculator for assessing fuel hazard in terms of fire behavior. The purpose of FlamMap is to generate fire behavior data that are comparable across a landscape for a given set of weather and/or fuel moisture data inputs. The fire behavior models in FlamMap are used to make calculations for all cells of a raster landscape, independently of one another (there is no contagious process that accounts for fire movement across the landscape or among adjacent cells). FlamMap calculates the instantaneous behavior of a fire occurring at each pixel in the analysis area based on the same local weather inputs. In this way FlamMap compares potential fire behavior across a landscape by distinguishing different hazardous fuel and topographic combinations.

FlamMap contains an option called Minimum Travel Time (MTT) (Finney 2002) which is a fire growth simulator that uses minimum travel time methods to simulate how fast one fire or a band of multiple fires are expected to move across a landscape. It is used to identify the routes where fire is expected to travel most quickly. Like the main component of FlamMap, these simulations are based on the current fuels, specific locations for fire starts, and weather conditions. If one accepts that fuel treatments should be prioritized on the basis of juxtaposition of high values to hazardous fuels, this program begins to give us the ability to develop a biophysical definition of wildland urban interface based on the distance fire can travel under specified conditions. It does not include endogenous scheduling of treatments, and like the other fire behavior-based models, works only with the current fuels.

The Treatment Optimization Model (TOM) (Finney 2006) is another option on the FlamMap menu. It uses minimum travel time logic to determine effective locations for fuel treatments on a landscape. The treatment locations are based on the fire behavior expected from the current fuels present on the landscape, specific locations for fire starts, and weather conditions. The solutions suggest location, sizes, and orientations of fuel treatments that are efficient and effective at changing large fire growth by reducing the fire spread rate. The treatment locations are selected

to reduce the rates of fire spread across the landscape, and are not designed to protect specific locations on a landscape, such as designated wildland urban interface. Also, the placement of treatments does not consider feasibility factors associated with location or shape, nor do they address resource effects, or management limitations such as budget. Finally, there is no temporal aspect to TOM, so it cannot analyze alternative timings of fuel maintenance treatments on a landscape.

The Fire and Fuels Extension to the Forest Vegetation Simulator (FVS-FFE) evaluates the effectiveness of proposed fuel treatments in the context of potential fire effects on short- and long-term stand dynamics (Reinhardt and Crookston 2003). In contrast to other fire behavior fuel hazard models, the FVS-FFE has the ability to simulate the dynamics of vegetation, snags, and surface fuels, and the appropriate interactions between these processes at a stand level (Kurz and Beukema 1999). In combination with the Parallel Processing Extension (PPE; Crookston and Stage 1991) the FVS-FFE can be used to simulate the dynamics of landscapes containing several hundred to a few thousand stands. The FVS-FFE does not simulate fire spread between stands, but it has the ability to provide inputs to FARSITE and FlamMap (Hayes and others 2004).

Other fire models include 1) the First Order Fire Effects Model (FOFEM) which models duff and woody fuel consumption, mineral soil exposure, soil heating, smoke production, and tree mortality (Reinhardt and others 1997), 2) FIREHARM which can be used to calculate fire behavior and effects potentials for varying weather percentiles used in fire management planning, and 3) NEXUS (Scott and Reinhardt 2001) which is an Excel(tm) spreadsheet linking surface and crown fire prediction models. All these fire models, however, do not include treatment scheduling or address temporal aspects of fuels management.

B. Landscape simulation and treatment scheduling modeling

SIMPPLLE is a stochastic simulation model for projecting vegetation spatially in the presence of disturbances such as insects, disease, and wildland fire (Chew 1997, Chew and others 2004). Simulations can be made with or without fire suppression, with or without fuel treatments, and under average or extreme fire conditions. Spread logic is included for wildland fire and other disturbance processes. The location and frequencies of disturbance processes quantified from multiple stochastic simulations provide estimates of the location and probabilities of future disturbance processes. These provide a basis for identifying "problem areas," as well as estimating costs and effects associated with disturbances processes.

MAGIS is an optimization model for spatially scheduling treatments that effectively meet resource and management objectives while satisfying user-imposed resource and operational constraints (Zuuring and others 1995). MAGIS accommodates a wide variety of land management treatment types, and associated costs, revenues, and effects. MAGIS also contains a road-network component for analyzing road construction, re-construction, and closure. The combination of the land management and road-network components provides the capability to include the limitations (for example sediment production) and costs associated with vegetation treatments as well as access and roads in spatially analyzing maintenance of fuel treatments.

SIMPPLLE and MAGIS have been used in a process for spatially scheduling treatments and analyzing the effectiveness of those treatments (Jones and Chew 1999, Chew and others 2003, Jones and others 2004). In this process, SIMPPLLE is used first to run stochastic simulations for the "no action" management alternative. From these simulations the frequency of natural

disturbances is recorded for each polygon in the landscape, representing the risk of these natural processes occurring over a period of time. These risks are then incorporated into MAGIS and combined with resource and operational objectives and constraints to develop an alternative spatial treatment schedule. These treatments schedules are then simulated in SIMPPLLE and the results compared with the results of the "no action" simulations to measure the effectiveness of the fuel treatment scenario. Key questions, however, remain in the SIMPPLLE/MAGIS approach involving computation of the risk index and the treatment patterns resulting from it, among others.

A past Joint Fire Science project, A Risk-Based Comparison of Potential Fuel Treatment Trade off Models, compared the SIMPPLLE/MAGIS approach with two non-spatial models FETM

(CH2M Hill 1998) and VDDT (Beukema and Kurz 1998) on eight areas representative of major fuel types. The focus was on modeling fuel treatment trade-offs for use in strategic planning. The comparison found significant differences in how information is assembled and used in the models. SIMPPLLE and MAGIS were sensitive to the spatial arrangement of vegetation and treatments, making the data requirements somewhat more stringent, but they also provide as output the spatial arrangement of proposed treatments. Non-spatial solutions may not be either optimal or even operationally feasible.

C. The need for integrating types of models

Although these models address diverse aspects of the fuel treatment-planning problem, no one model adequately handles the strategic maintenance scheduling of fuel treatments while considering 1) the spatial and temporal changes of fuel treatment effects on a landscape, and 2) the economics of maintenance fuel treatments plus other operational constraints. For example, FARSITE and FlamMap are able to compute fire behavior characteristics at a landscape scale, but neither maintenance scheduling nor temporal effects of treatments are included in either model. FVS-FFE has the ability to model stand-level fuel and vegetation dynamics, but it does not simulate the spread of fires between stands. On the contrary, MAGIS has the ability to spatially schedule fire and non-fire maintenance treatments that effectively meet resource and management objectives, but no fire spread logic exists in the system. Fire managers have to use these multiple systems in order to analyze spatial and temporal effects of maintenance fuel treatments, but lack of time and resources to maintain and operate these sophisticated systems has been a hurdle. Consequently, there is a critical need to merge these systems into one easy-to use decision support system that 1) facilitates automatic linkages among the existing models, 2) streamlines analyses for identifying where, when, and how to treat in order to achieve and maintain desired fuel reduction goals, and 3) bridges the fire sciences and management gap by incorporating given resource and operational constraints (e.g. budgets, treatment acres, and operational feasibility of treatments) into decision-making process.

D. Project objectives

The main objective of this project was to integrate existing fire behavior, vegetation simulation, and land management planning tools into a system that supports long-term fuel management decisions. The system was to build on the existing land management optimization tool MAGIS, while incorporating FVS-FFE to project vegetation change over planning periods and predict the resulting fuel parameters for fire behavior modeling, and FlamMap to model fire behavior in each planning period. The system was to include automated data transfer interfaces between the